A Training School from COST Action TD0905
Epigenetics: bench to bedside

Confocal Microscopy and Living Cell Studies

Eva Bártová
Institute of Biophysics
Academy of Sciences of the
Czech Republic

History of microscopy:

the light microscope (discovered by Robert Hook, 1665): an instrument that enables the human eye, by means of a lens or combinations of lenses, to observe enlarged images of tiny objects. It made visible the fascinating details of naked eye invisible worlds.

1957: Marvin Minsky patented the fist confocal microscope

Types of light microscopes

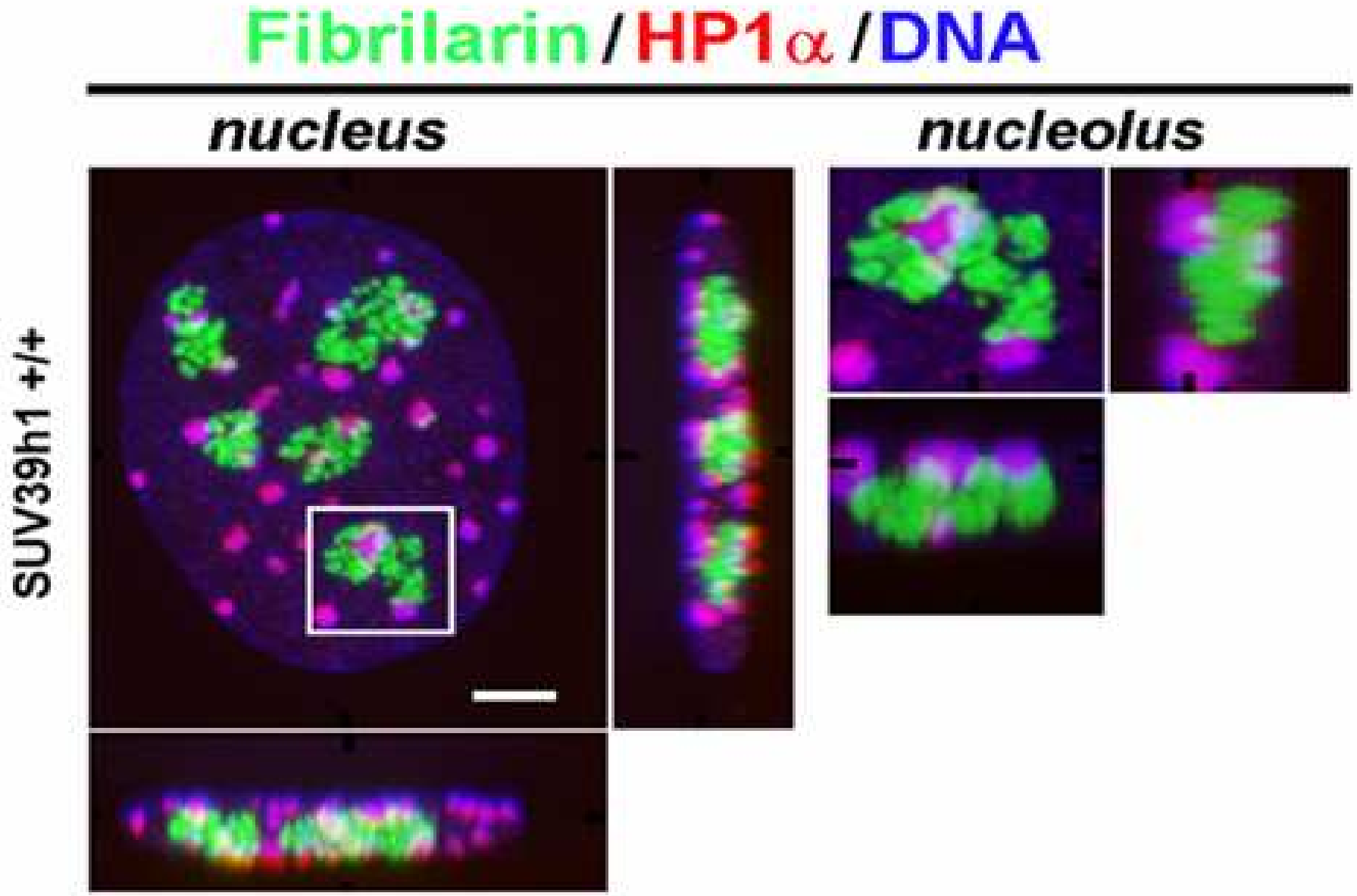

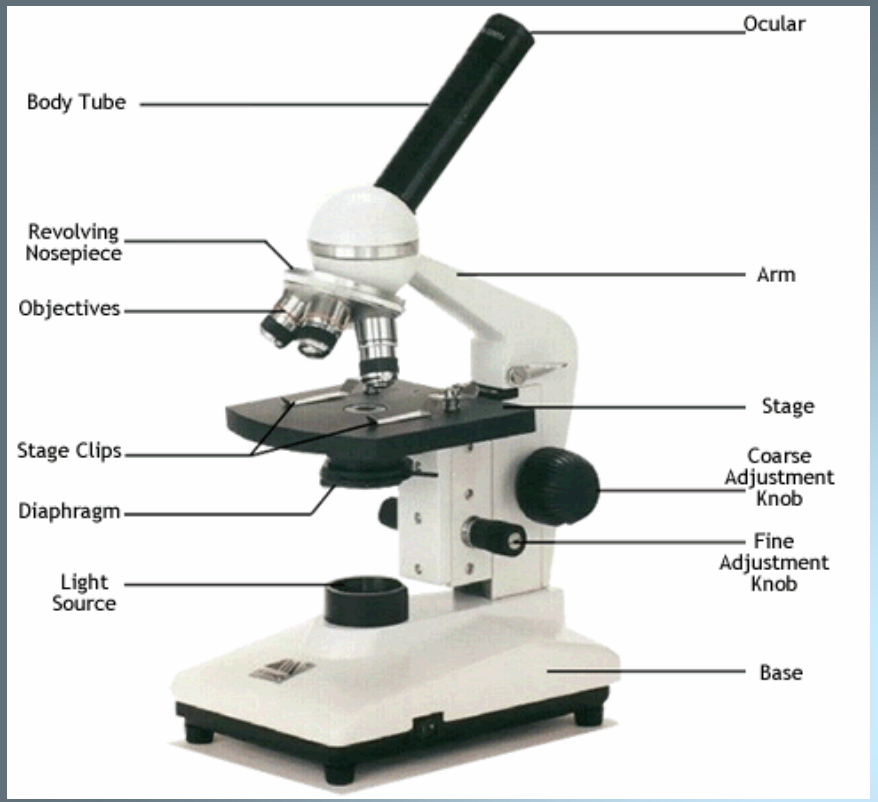

http://www.google.cz/imgres?imgurl=http://www.microscopehelp.com/

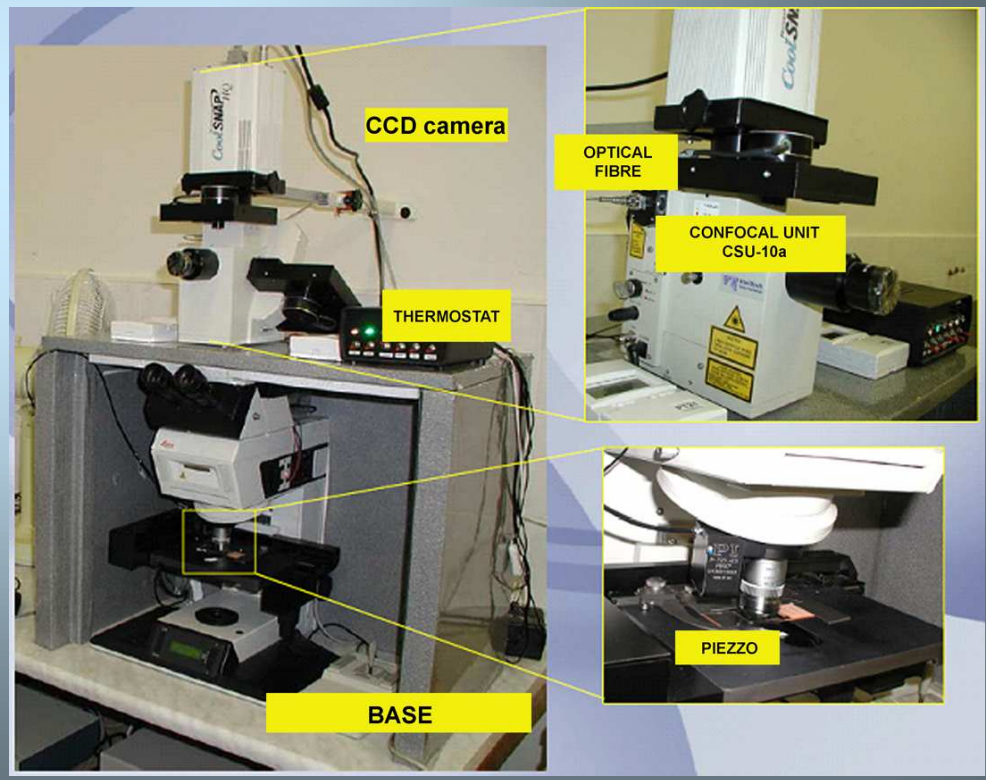

Brno laboratory at IBP

Visible Light Microscopy: Objectives: numerical aperture

- NA=ability of lens to gather light and resolve detail at a fixed distance from object.
  - Dependent on ability of lens to capture diffracted light rays.
- n=Refractive index is limiting (air=1.0, oil=1.51)
  - Do not mix mediums when using a lens
- Theoretical resolution depends on NA and the wavelength of light. NA=n·sin(μ)
  - Shorter wavelengths=higher resolution.
  - Resolution limit for green light (NA=1.4, 100X) is 0.2 μm.
    - R=0.61λ/NA

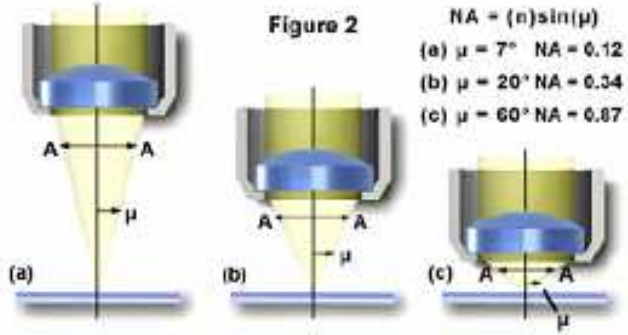

Figure 1

Tandem scanning microscopes based on Nipkow disk

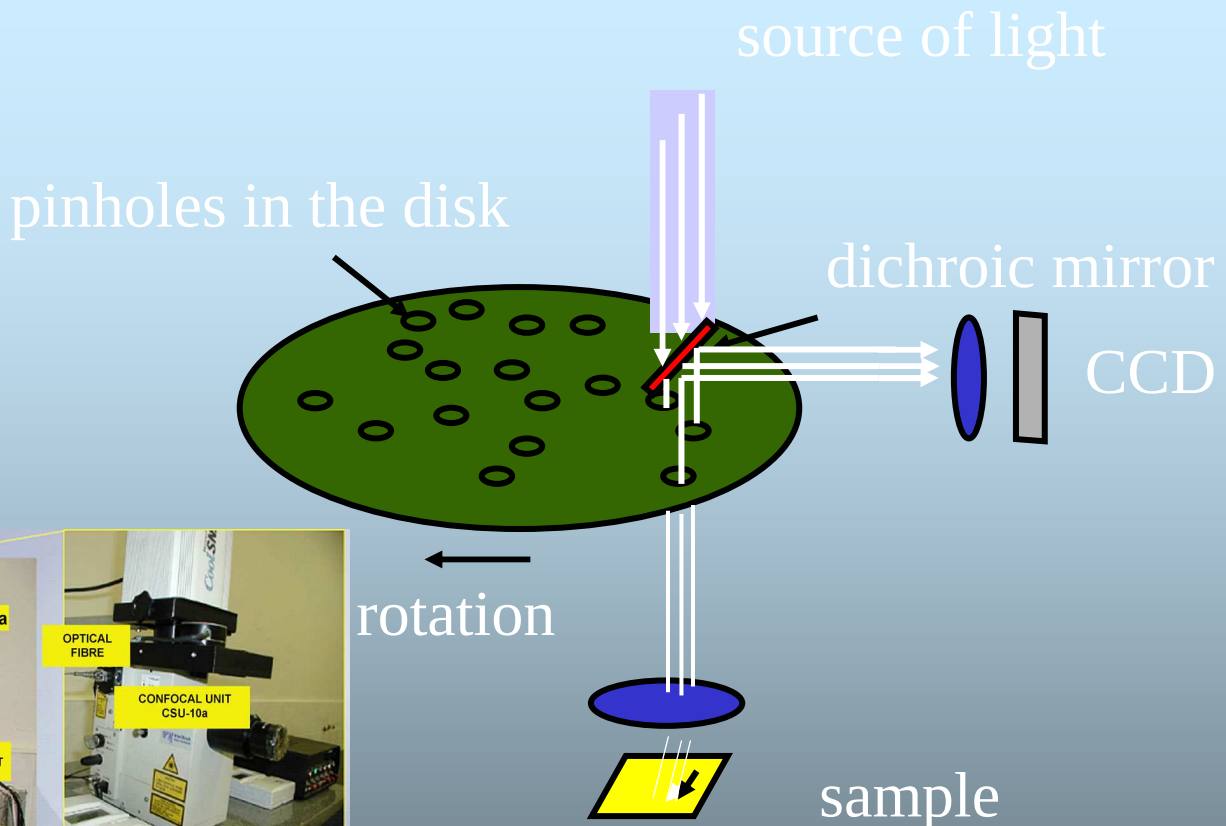

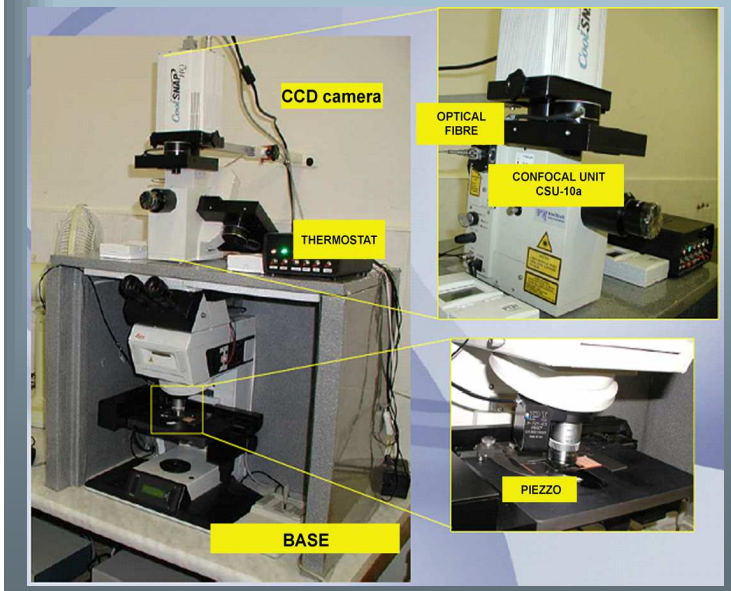

Confocal microscopy - principles

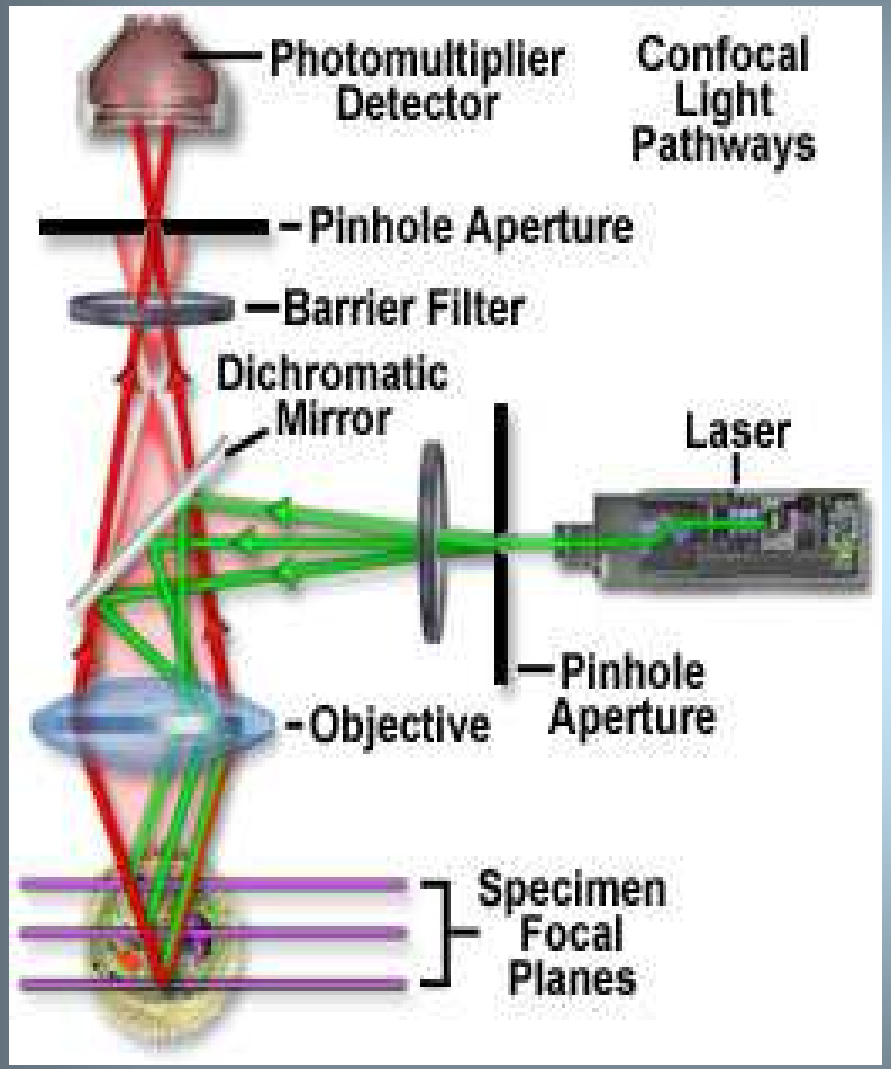

AOTF and AOBS

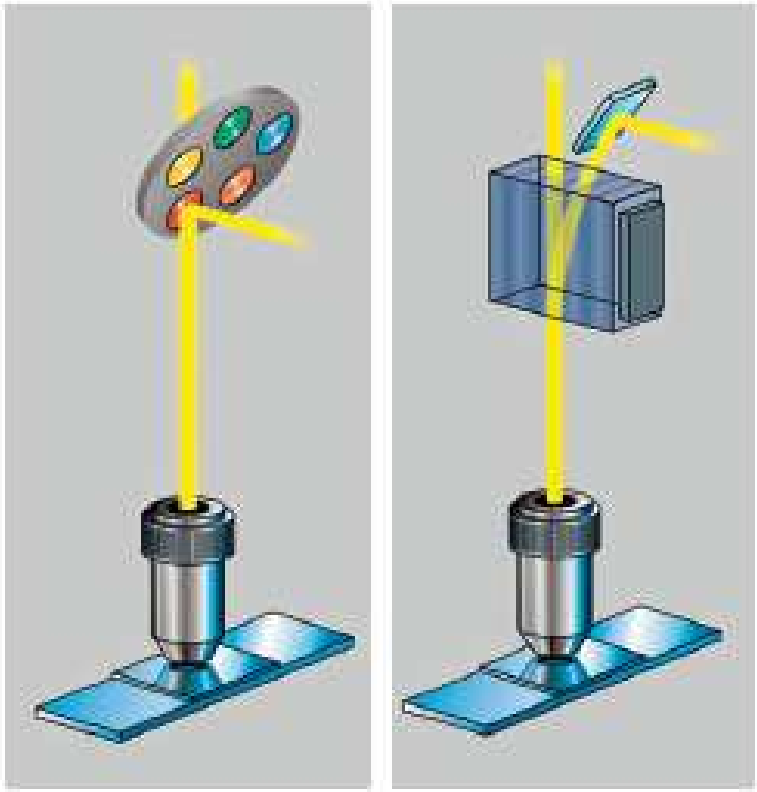

Left: conventional beam splitting by dichroic mirrors requires many optical elements with fixed properties.
Right: the AOBS® is electronically adaptable to all tasks.

3D-projection

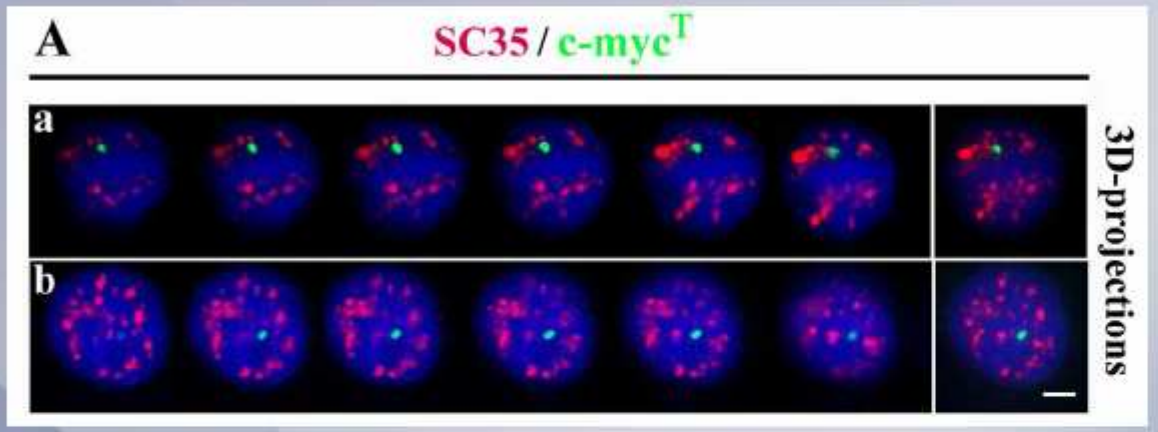

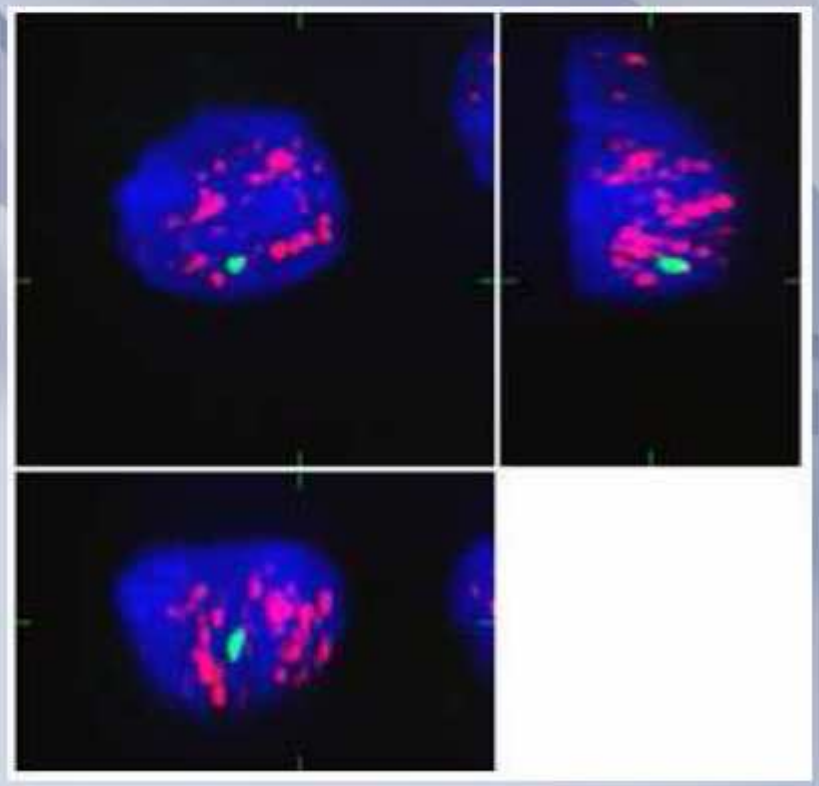

Scanning in 2D and 3D by confocal microscope

2D

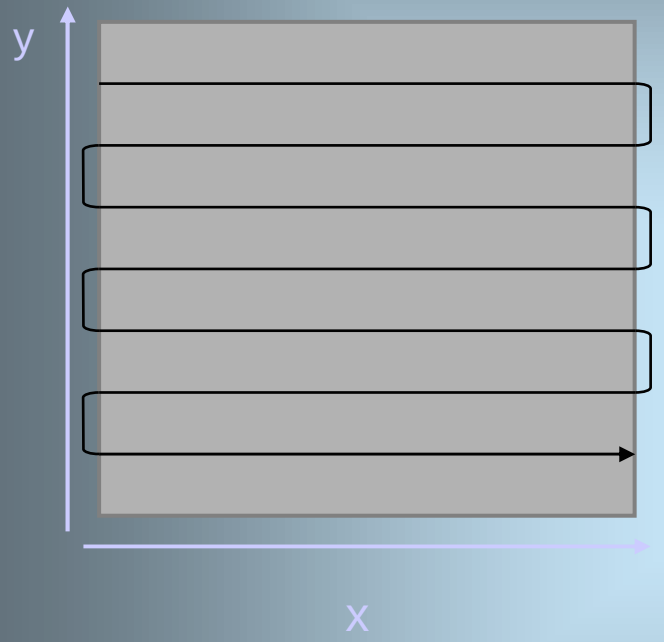

Laser beam moves firstly along *x* axis and then starts with new line in *y* axis.

3D

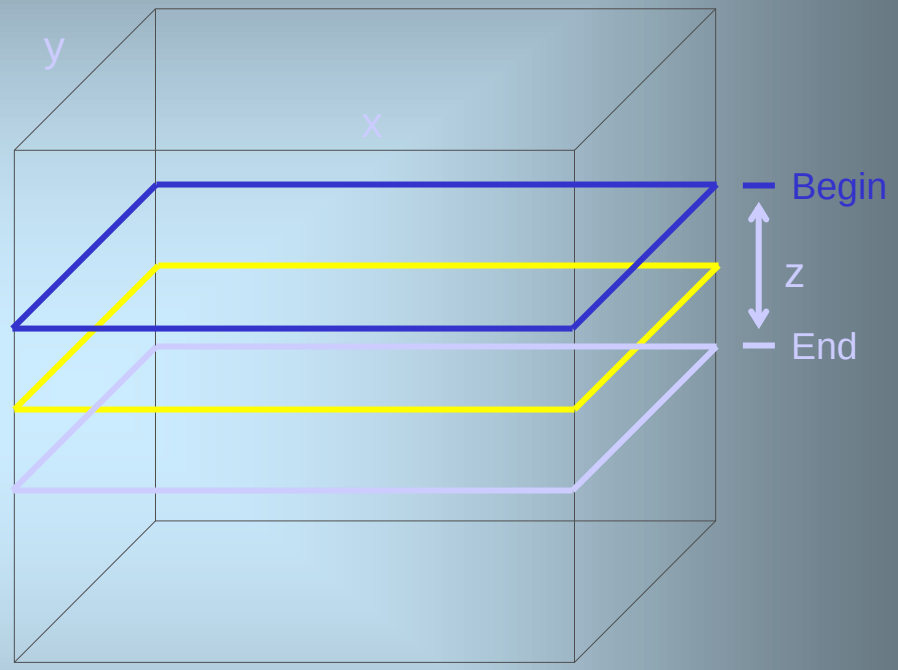

Finishing scanning of one thin optical slice in *xy* plane, the scanning plane is moved in *z* axis to other slice

Optical resolution: conventional versus confocal

Conventional

Confocal

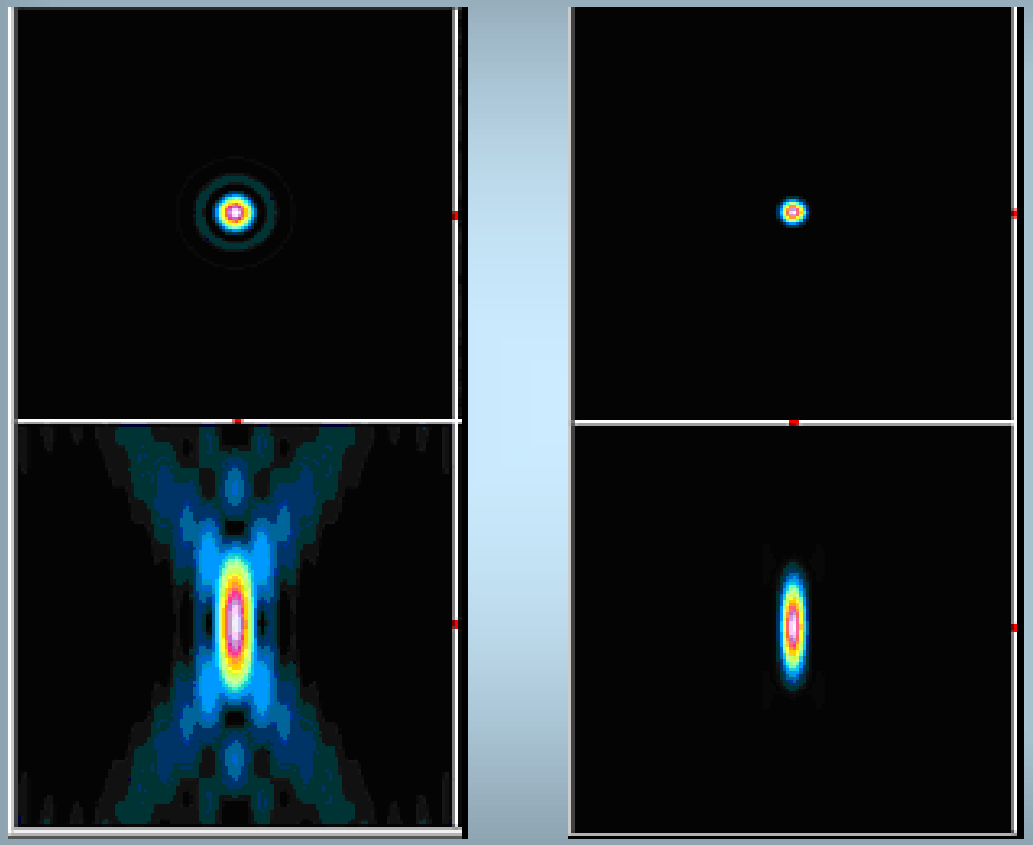

Res = 0.61*λ / NA

Res(xy) = 0.4*λ / NA

Res(xz) = 0.45*λ / n(1-cosα)

Formulas by Kino

4PI and STED resolution are much higher…

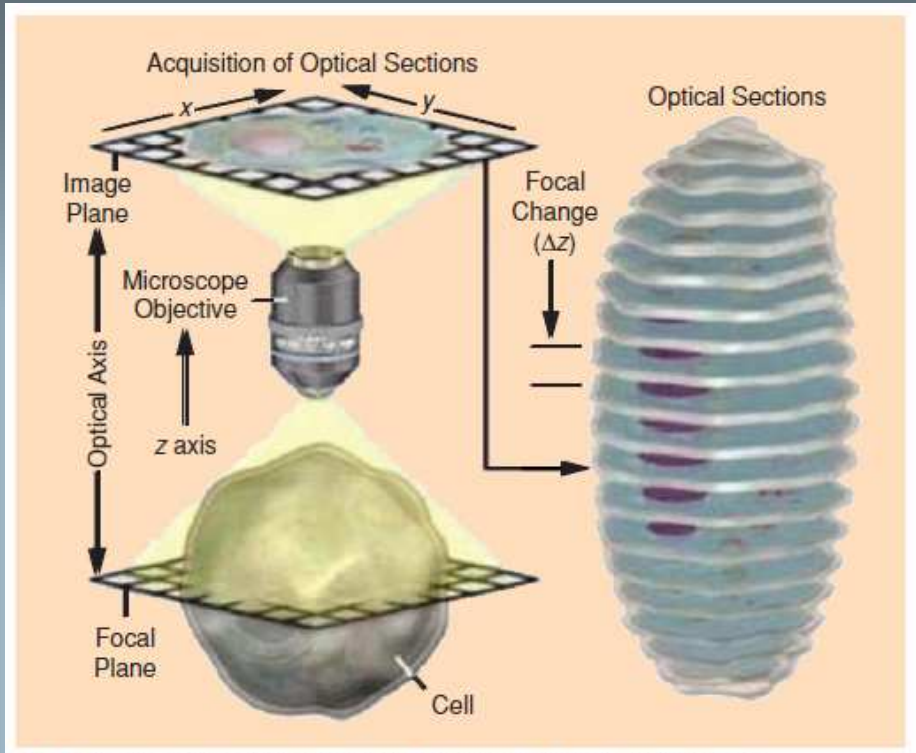

[FIG1] An example of the acquired 3-D image of a cell, captured by a fluorescence microscope.

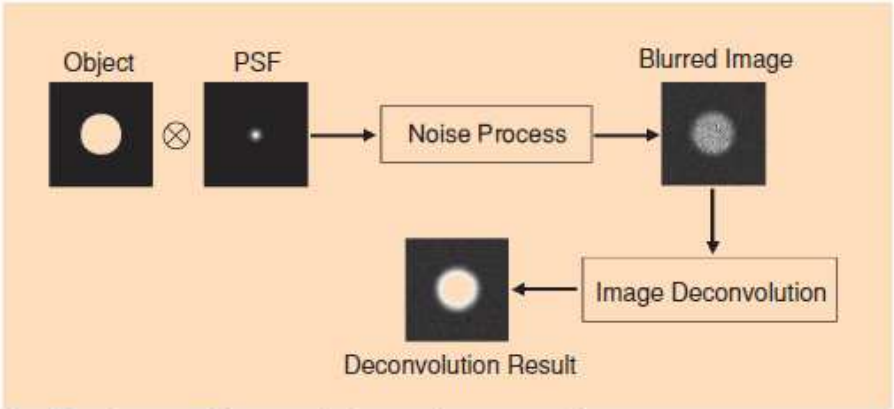

[FIG2] Schematic of a general deconvolution procedure.

Pinaki Sarder and Arye Nehorai (2006)

Deconvolution

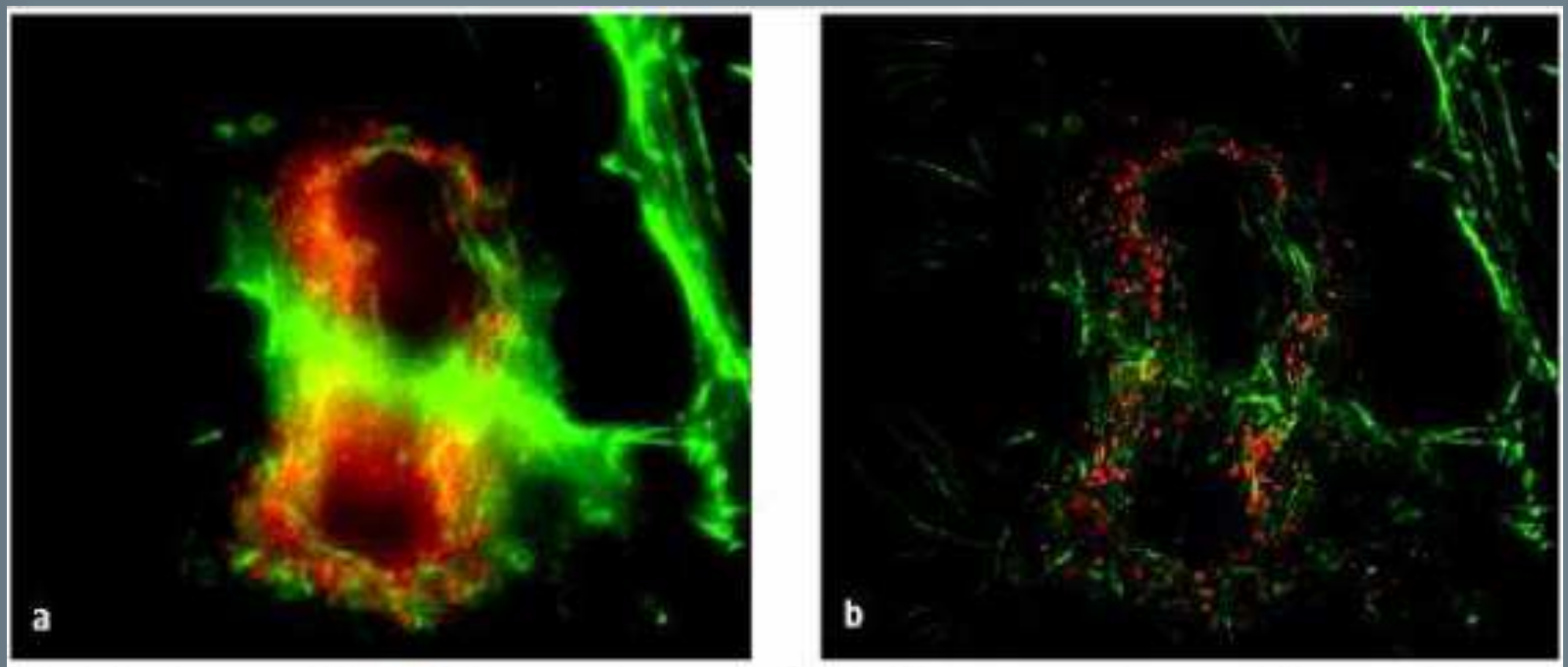

Fig. 3: Via deconvolution, artefacts can be computed out of fluorescence images. a). These artefacts are caused by the stray light from non-focused areas above and below the focus level. These phenomena, referred to as convolution, result in glare, distortion and blurriness. b). Deconvolution is a recognised mathematical procedure for eliminating such artefacts. The resulting image displayed is sharper with less noise and thus at higher resolution. This is also advantageous for more extensive analyses.

Assuming linearity, convolution of the object and the imaging system PSF is affected by noise and produces a blurred image. Deconvolution restores the original object to an improved resolution and higher signal-to-noise ratio (SNR) level.

Types of fluorochromes

Fluorochromes are essentially dyes, which accept light energy (e.g. from a laser) at a given wavelength and re-emit it at a longer wavelength. These two processes are called excitation and emission.

1. Fluorochromes conjugated with other molecule. Example represents quantum dots, used for for ultra-sensitive nonisotopic detection.

2. Fluorochormes that binds directly to some structure. For example, DAPI or PI binds to DNA

3. Fluorochromes produced by organism like *Aequorea victoria* (GFP) or octocoral *Dendronephthya sp.* (Dendra2)

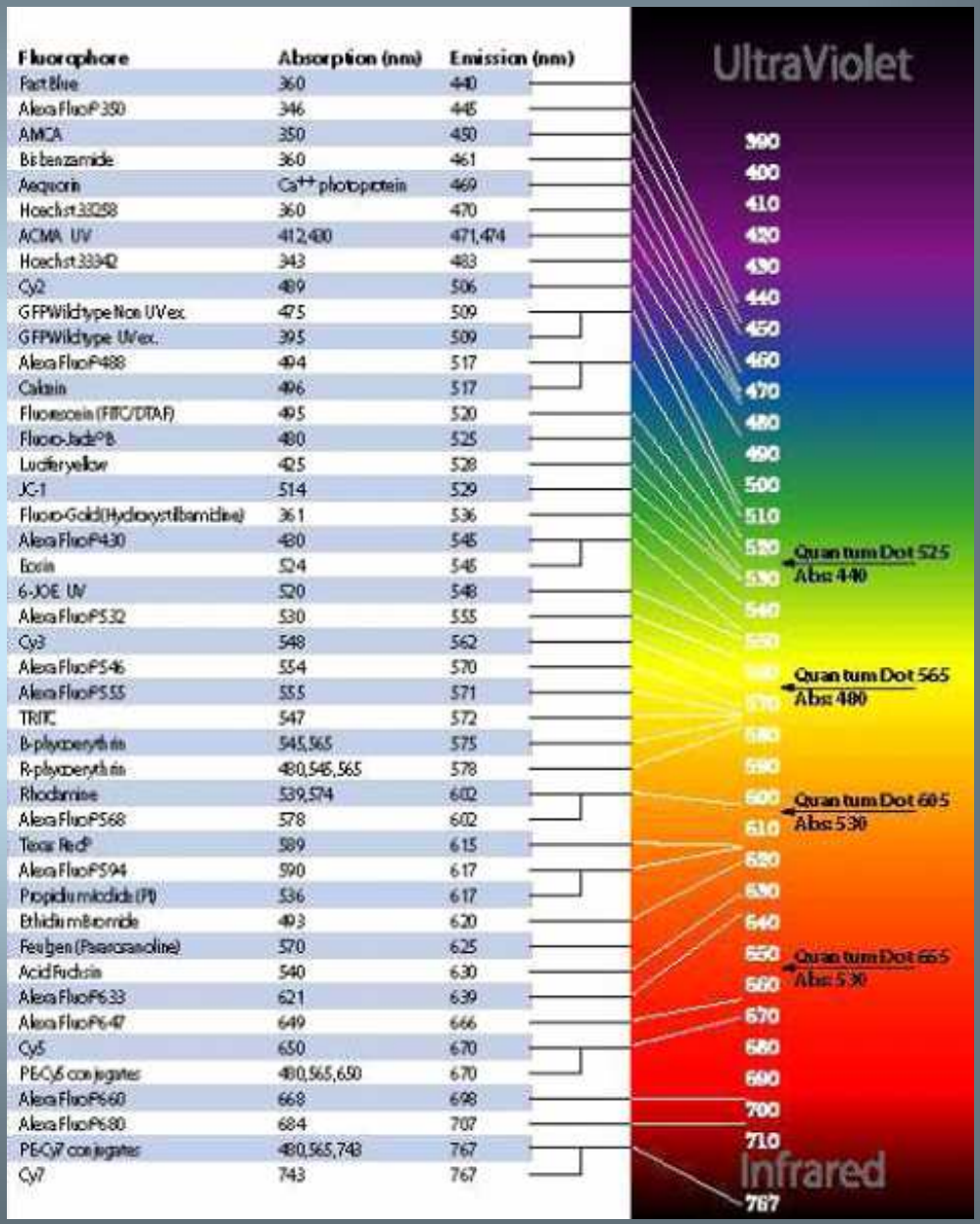

Living Cell Studies - GFP technology

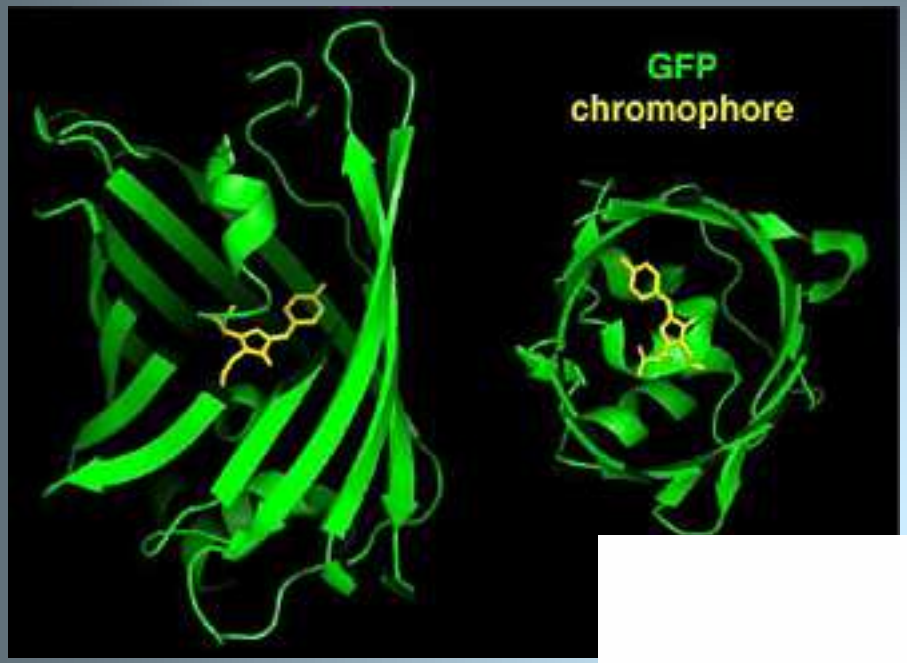

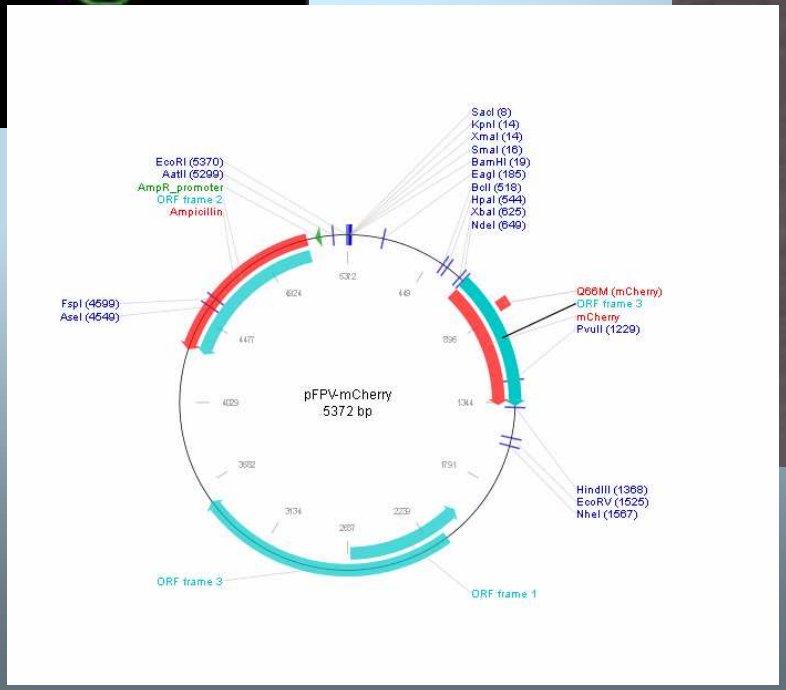

GFP-HP1 β

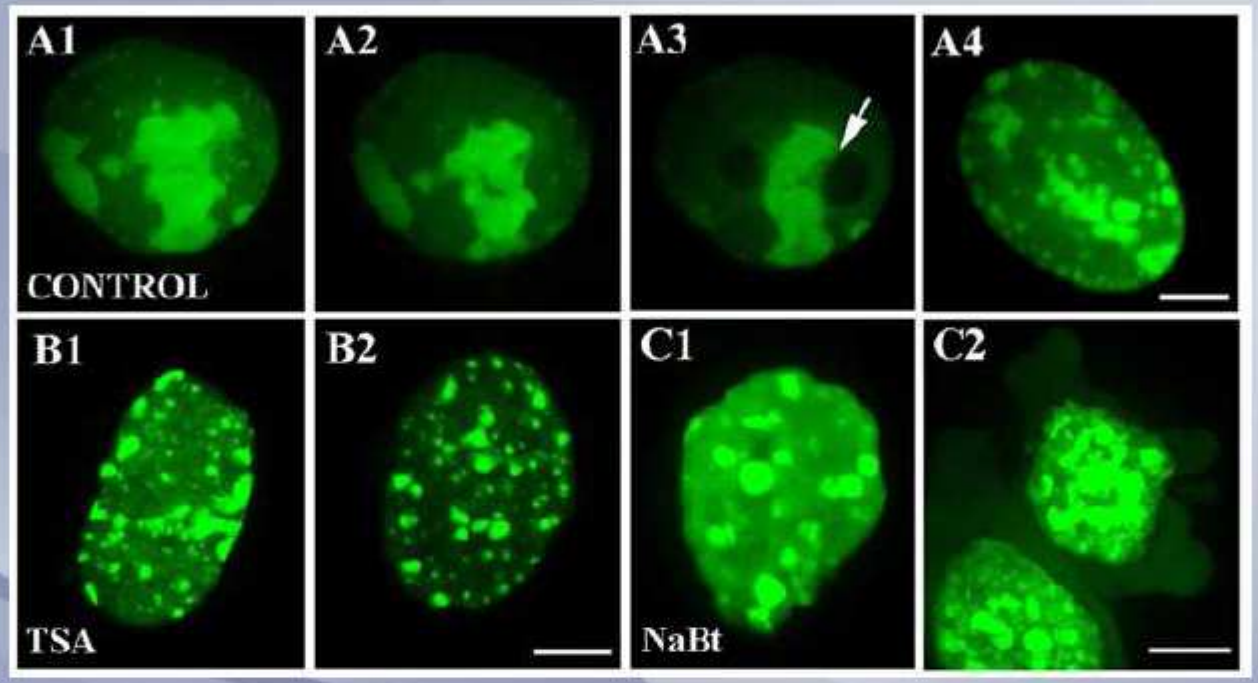
A1
A2
A3
A4
CONTROL
B1
B2
C1
C2
TSA
NaBt

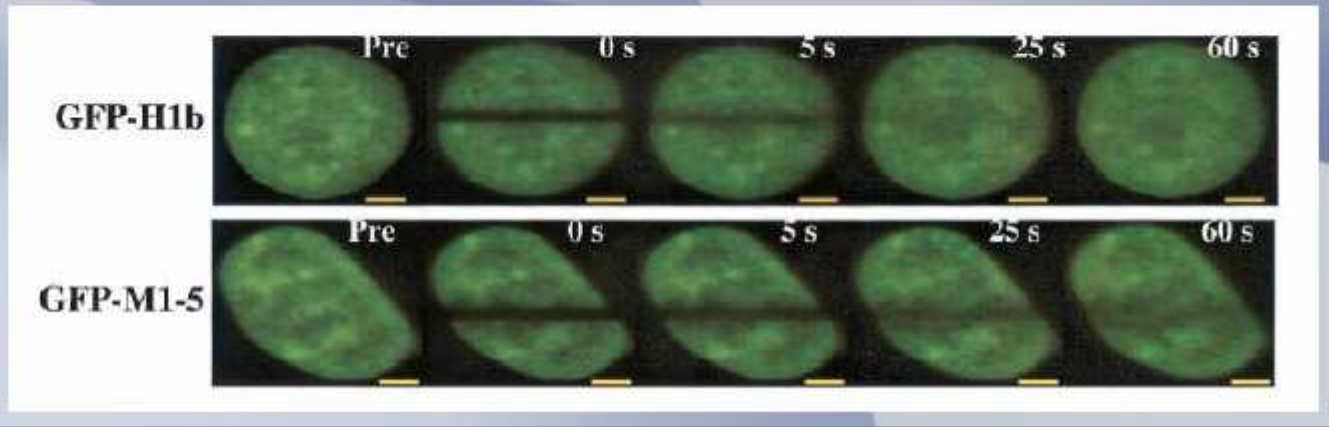
GFP-H1b
Pre
0 s
5 s
25 s
60 s
GFP-M1-5
Pre
0 s
5 s
25 s
60 s

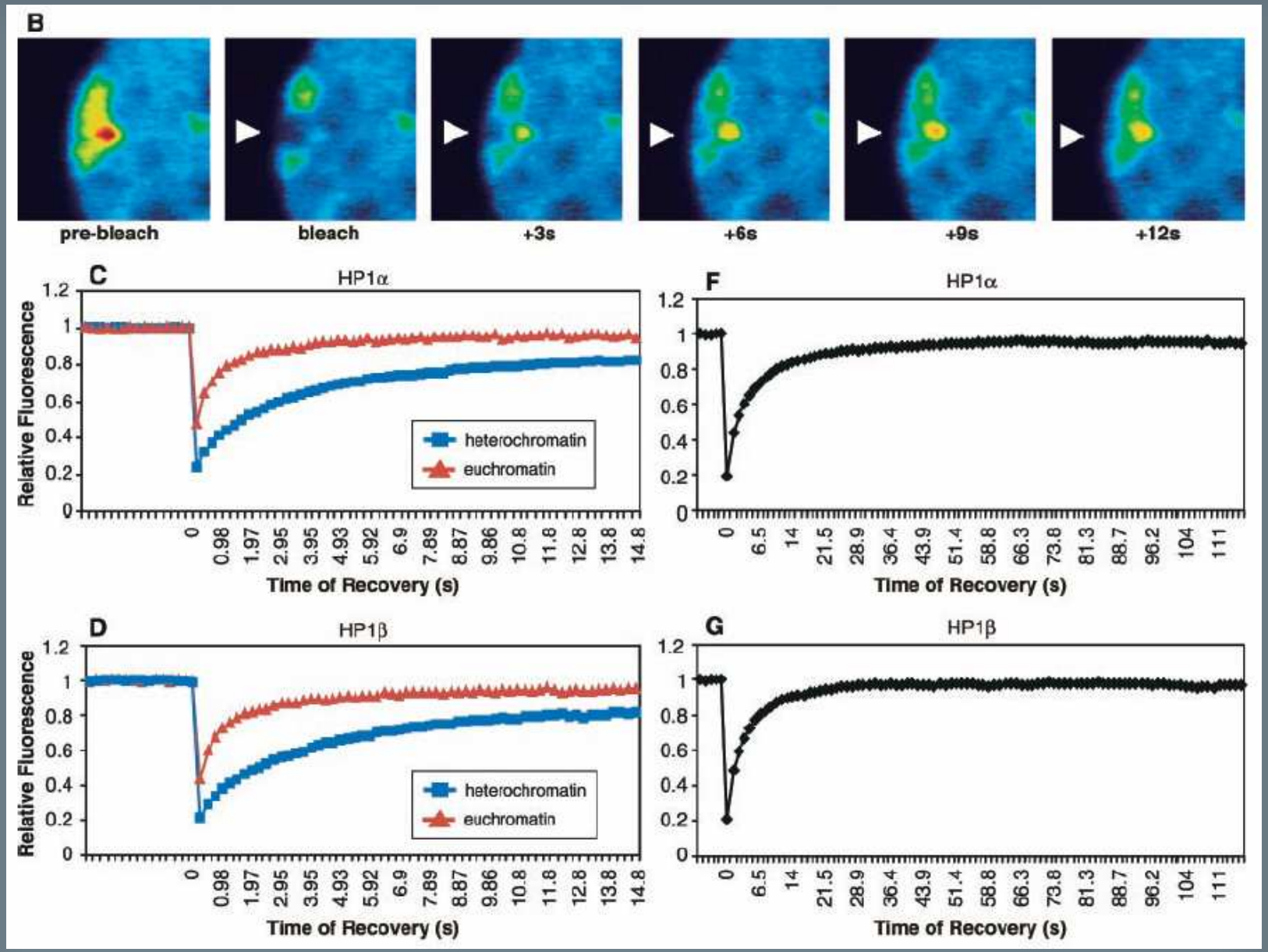

Cheutin et al. Science (2003)

Dendra2 photo-conversion

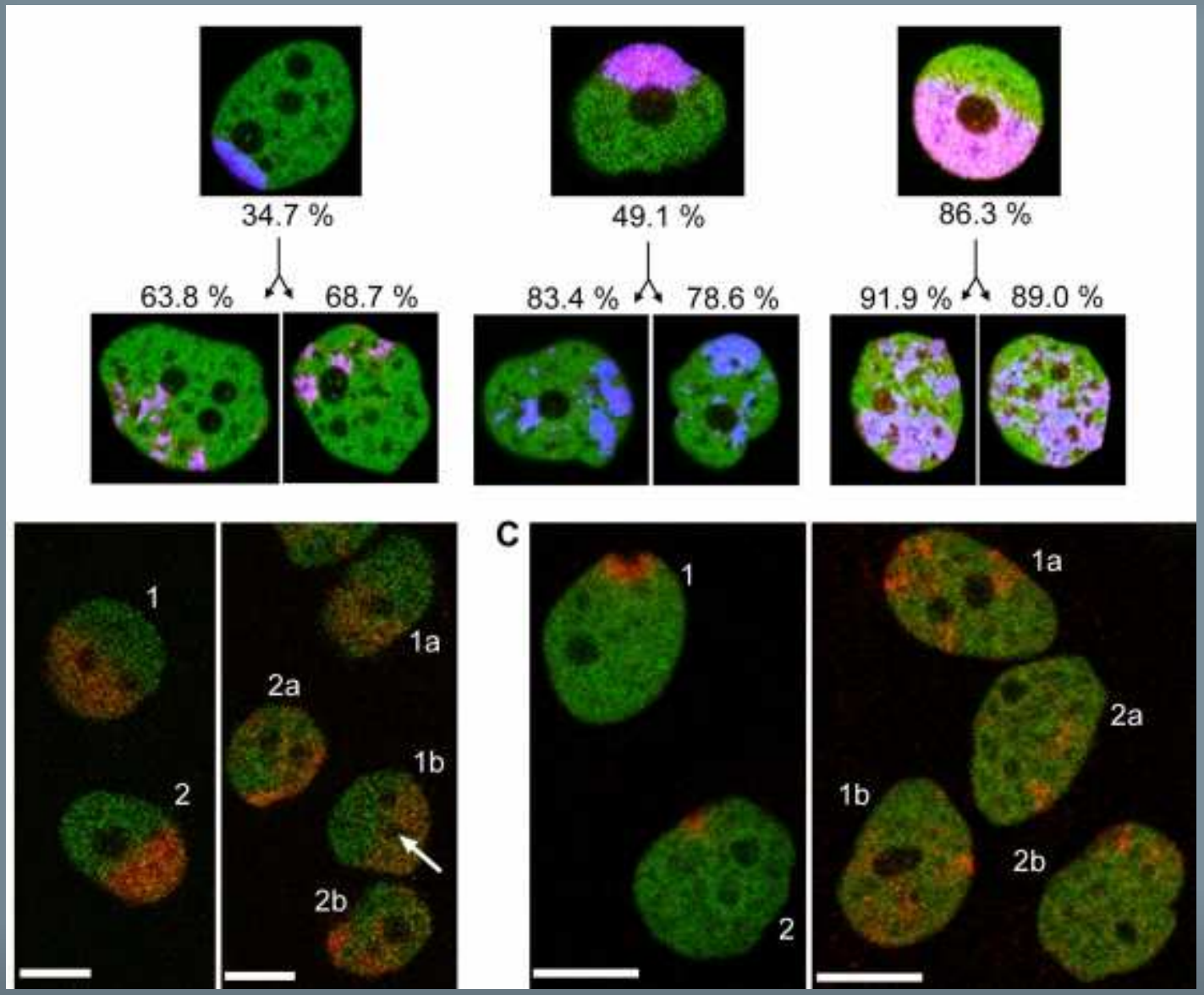

Dendra2 is an improved version of a green-to-red photoswitchable fluorescent protein Dendra, derived from octocoral *Dendronephthya* sp. (Gurskaya *et al.*, 2006).

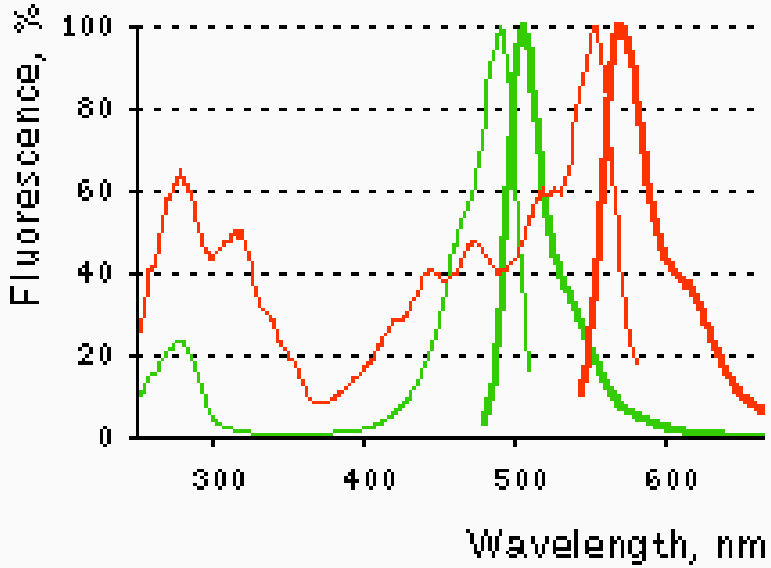

Normalized excitation (thin line) and emission (thick line) for non-activated (green) and activated (red) spectra.

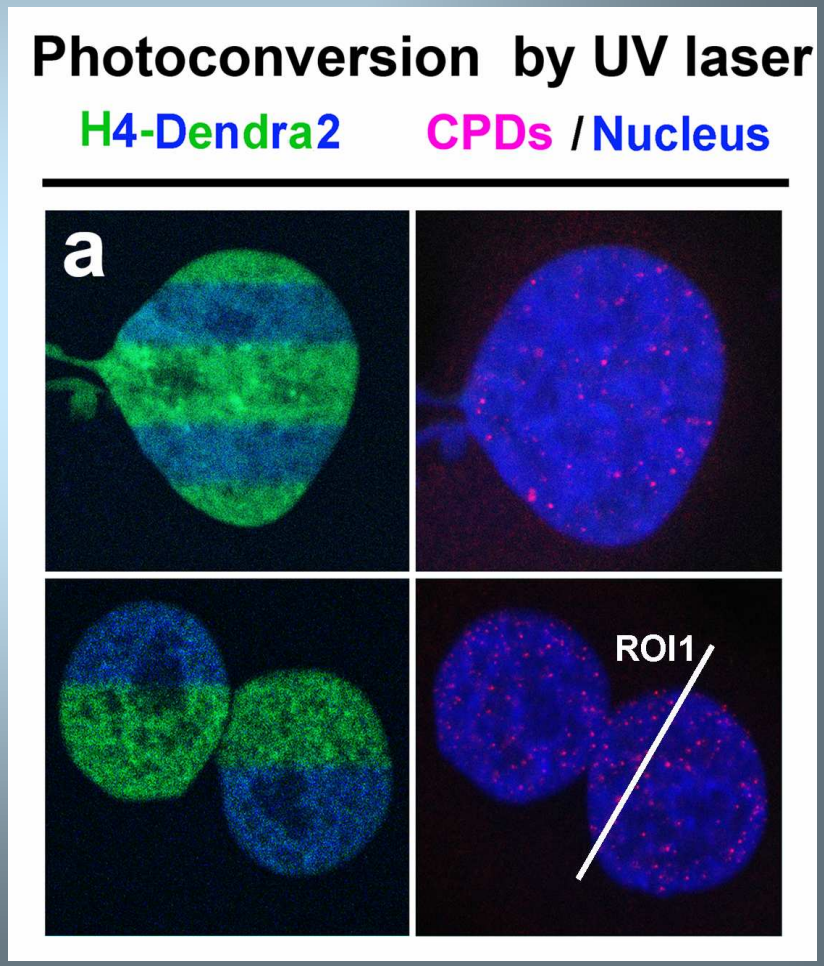

H4-Dendra2 / H4-Dendra2

Actinomycin-D
(0 min. after photoconversion)

Actinomycin-D (90 min.)

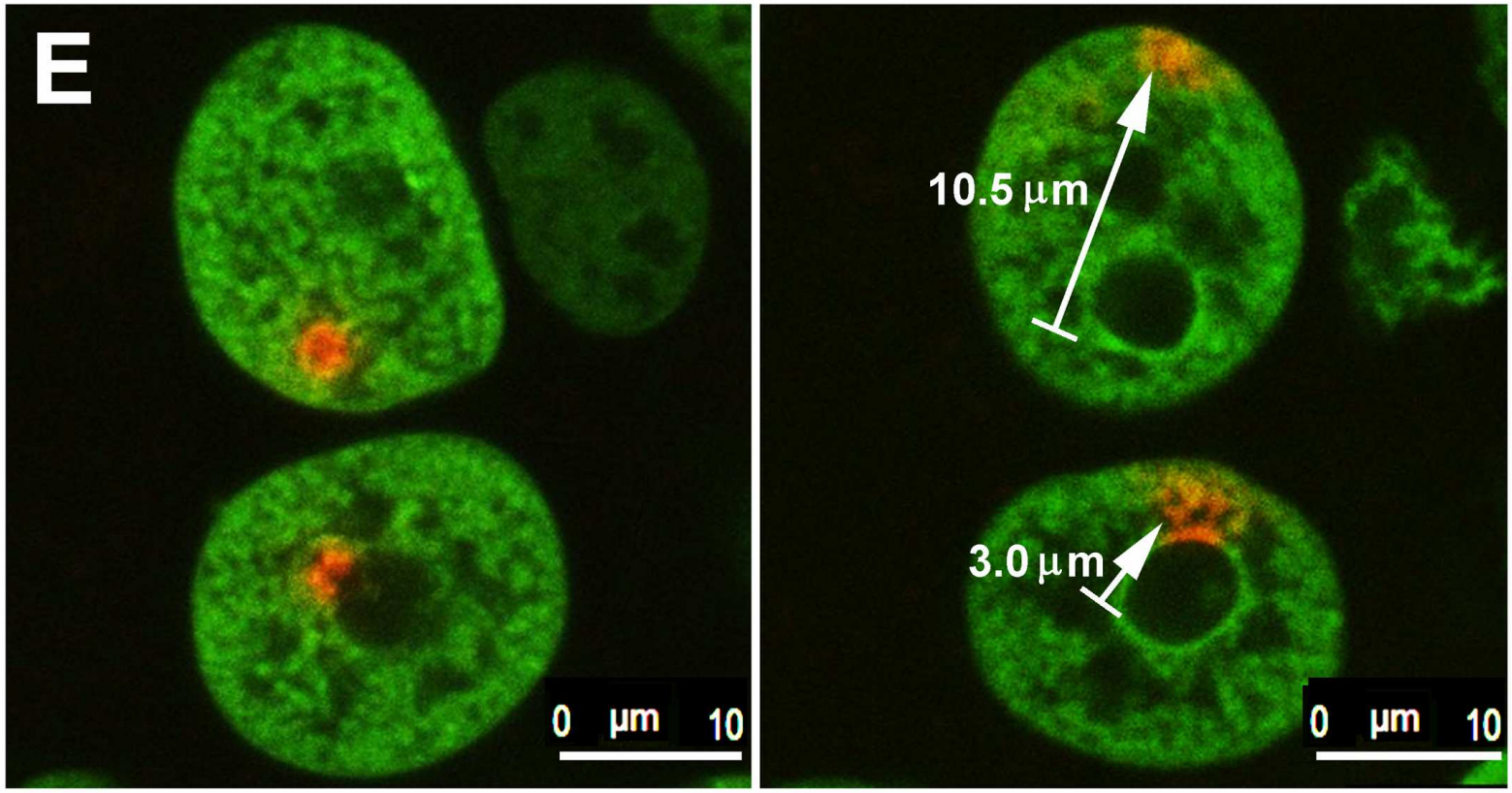


Leica TCS SP-5 X

Incubation chambers for living cell studies

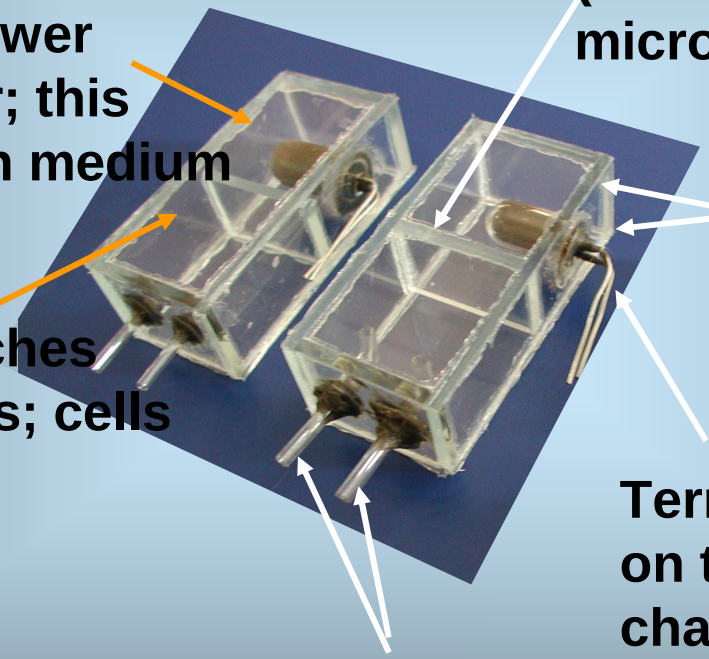

Partition with opening on the bottom of the chamber (for experiments under upright microscope)

Part I – cells can be grown on both upper and lower sides of the chamber; this part is filled fully with medium

Cover glass 24x50 mm

Part II – medium reaches under the glass tubes; cells are not grown here

Termistors in short tubes on the side of the chamber

Glass tubes bent under the upper glass (to enable CO_2 to flow above medium in the part II of the chamber)

Application of UV–laser (355 nm) in experimental studies on DNA repair

DNA repair

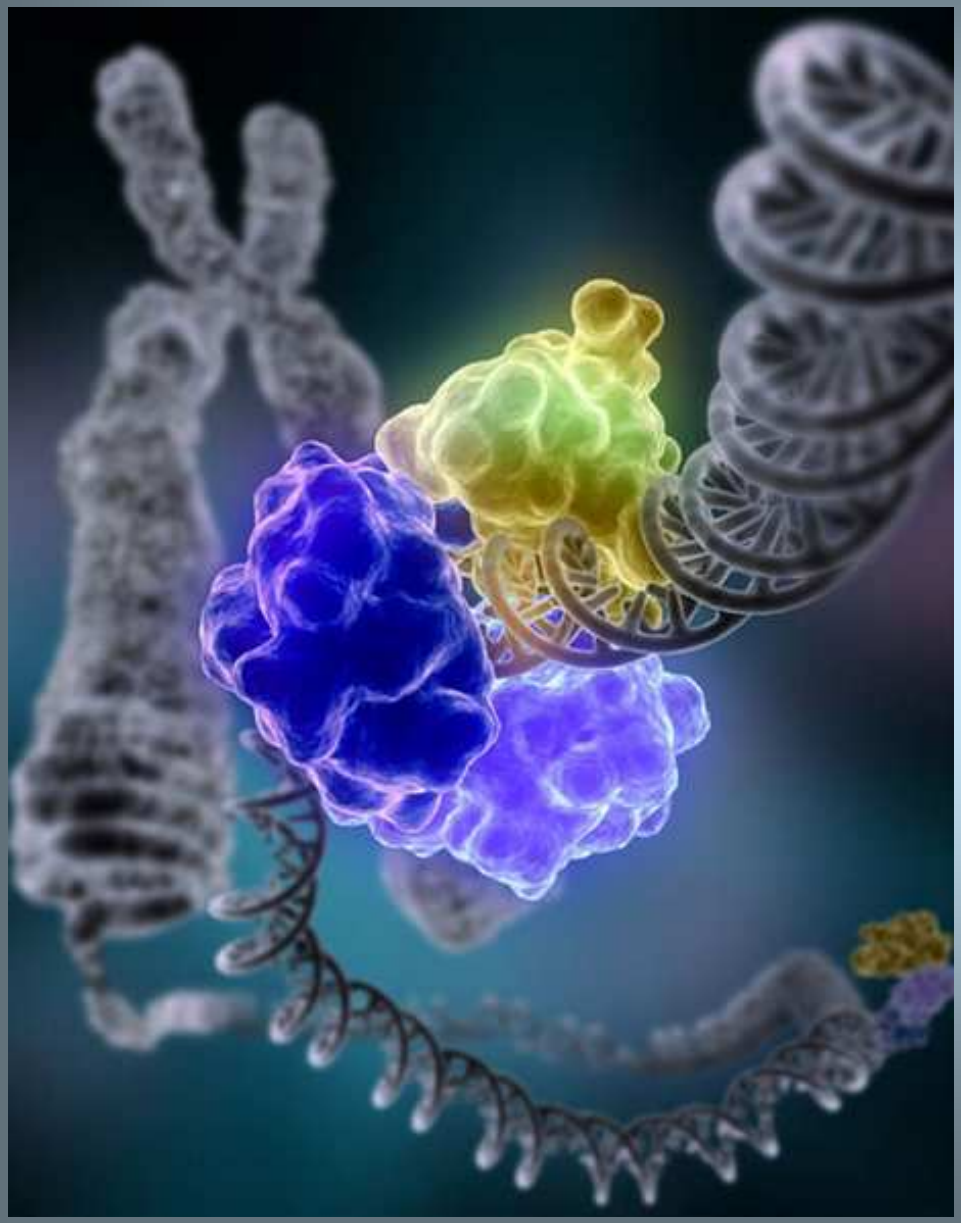

Single-strand damage

- **Base excision repair (BER), which repairs damage to a single base caused by oxidation, alkylation, hydrolysis, or deamination.**
- **Nucleotide excision repair (NER), which recognizes bulky, helix-distorting lesions such as pyrimidine dimers and 6,4 photoproducts.**
- **Mismatch repair (MMR), which corrects errors of DNA replication and recombination that result in mispaired (but undamaged) nucleotides.**

Double-strand breaks

- **non-homologous end joining (NHEJ)**
- **microhomology-mediated end joining (MMEJ)**
- **homologous recombination (HR)**

DNA repair

Box 1 | **The two main types of double-stranded DNA-break repair**

Non-homologous end joining
A DNA lesion (a double-stranded DNA break (DSB)) is sensed by the Ku80–Ku70 heterodimer, which in turn recruits the DNA-dependent protein kinase catalytic subunit DNAPKcs, resulting in assembly of the DNAPK complex and activation of its kinase activity (see the figure; left panel). Increasing evidence suggests that DNAPK functions as a regulatory component of non-homologous end joining (NHEJ), potentially facilitating and regulating the processing of DNA ends. DNAPK also increases the recruitment of XRCC4, DNA ligase IV, XLF and Artemis, which carry out the final rejoining reaction.

Homologous recombination repair
A DNA lesion is recognized by the MRN (MRE11–RAD50–NBS1) complex, which is recruited to the DSB to generate single-stranded DNA by resection (see the figure; right panel). The single-stranded ends are bound by replication protein A (RPA), RAD51 and RAD52 and can subsequently invade the homologous template, creating a D-loop and a Holliday junction, to prime DNA synthesis and to copy and ultimately restore genetic information that was disrupted by the DSB.

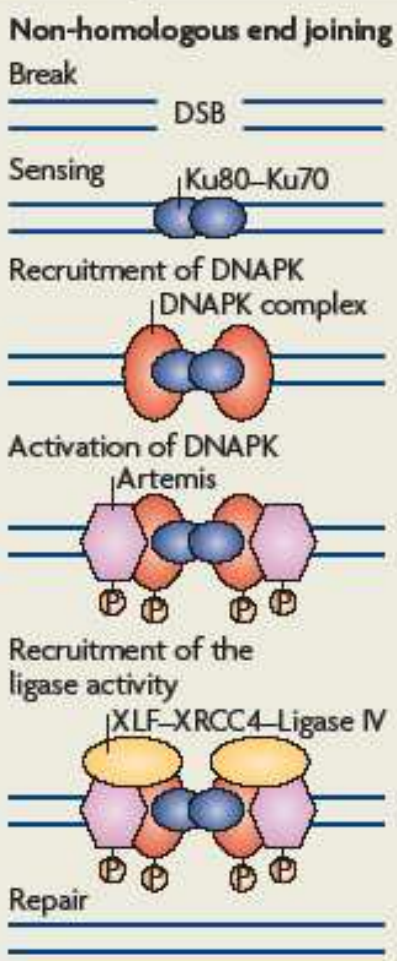

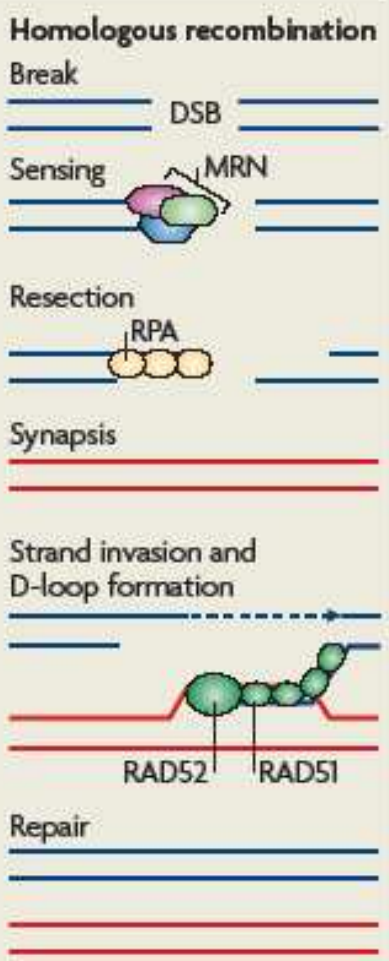

Misteli and Soutogou (2009)

DNA repair foci

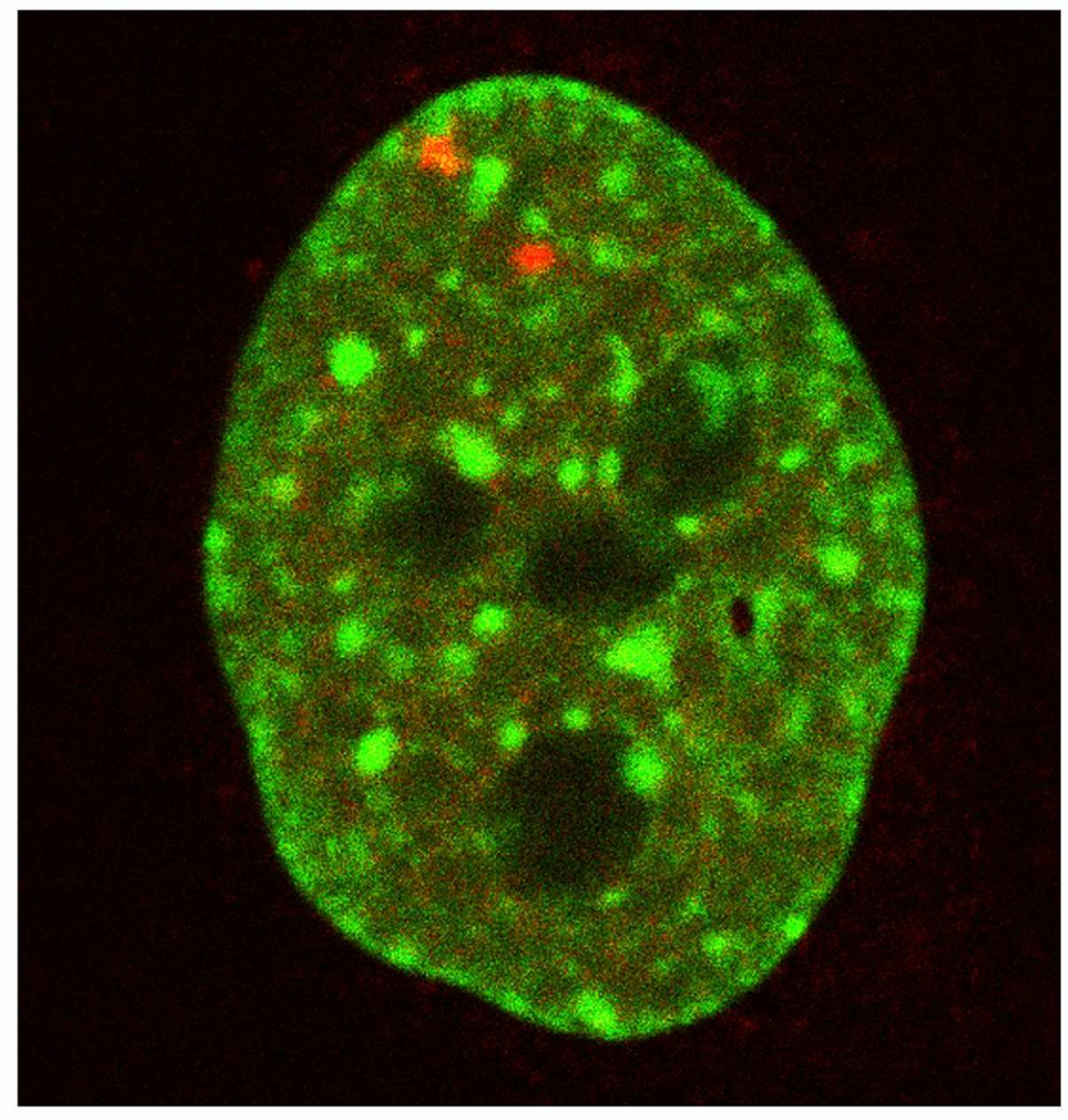

Histone signature
Brno nomenclature for histone modifications
(Turner, 2005)

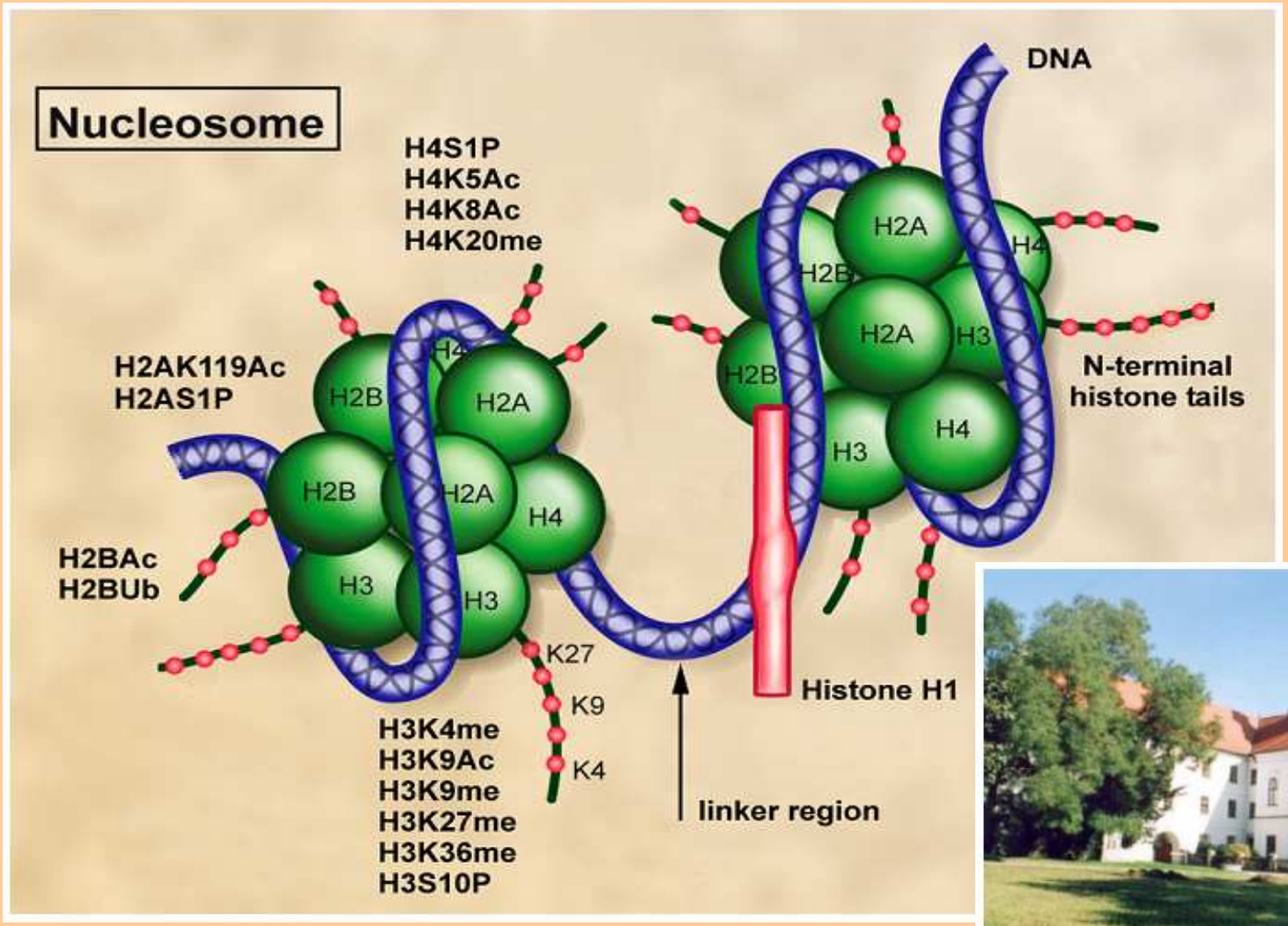

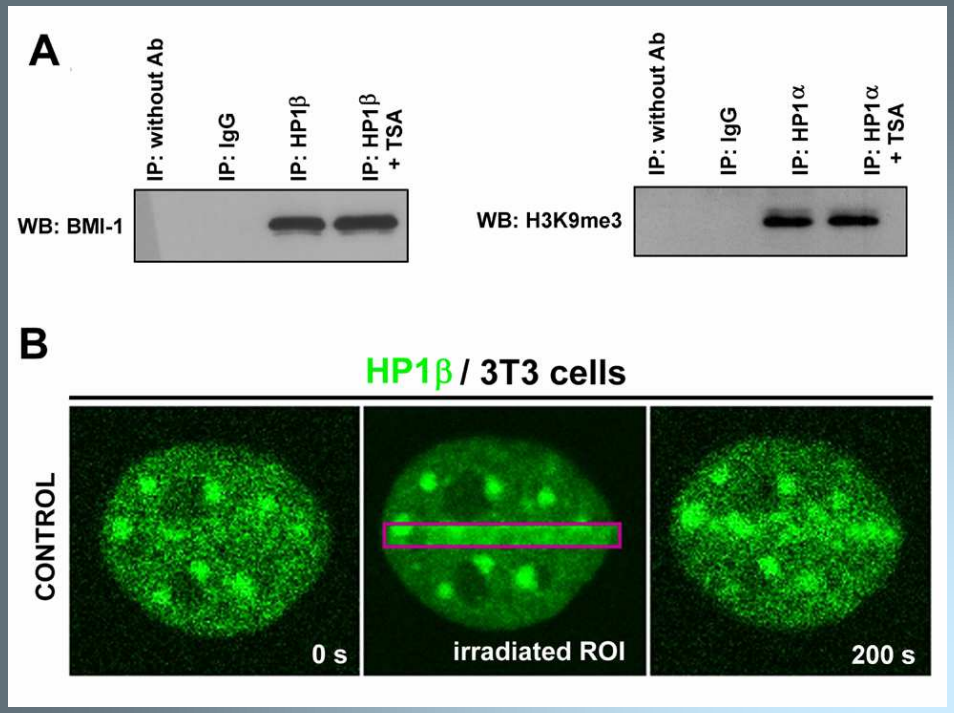

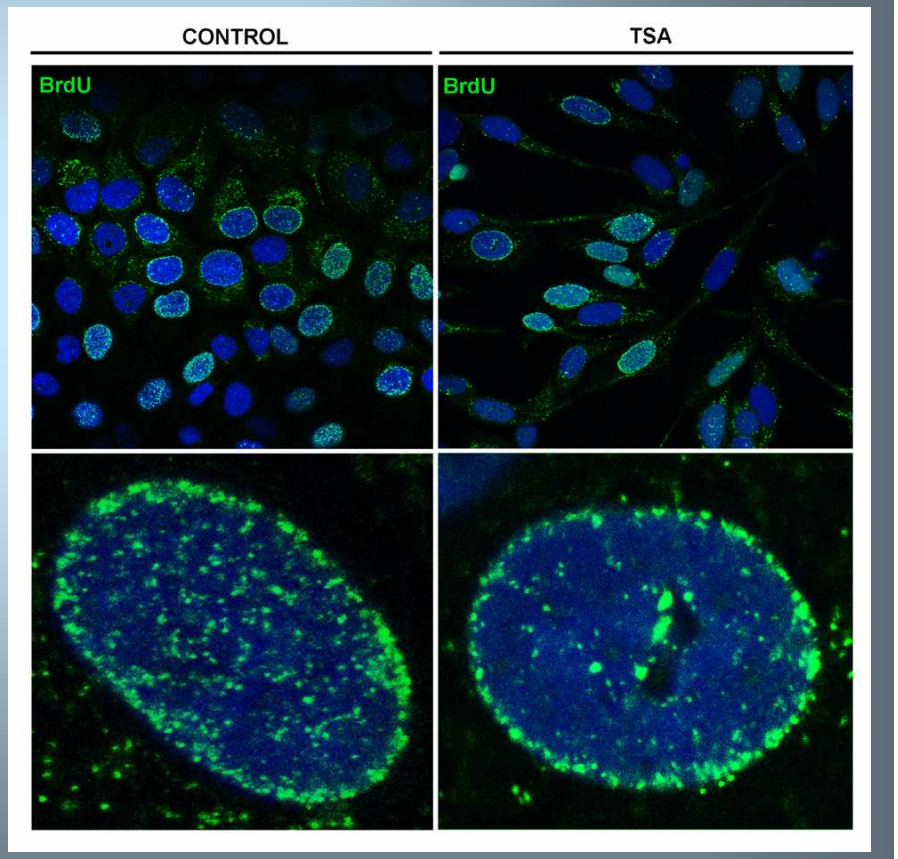

HP1β / BMI1

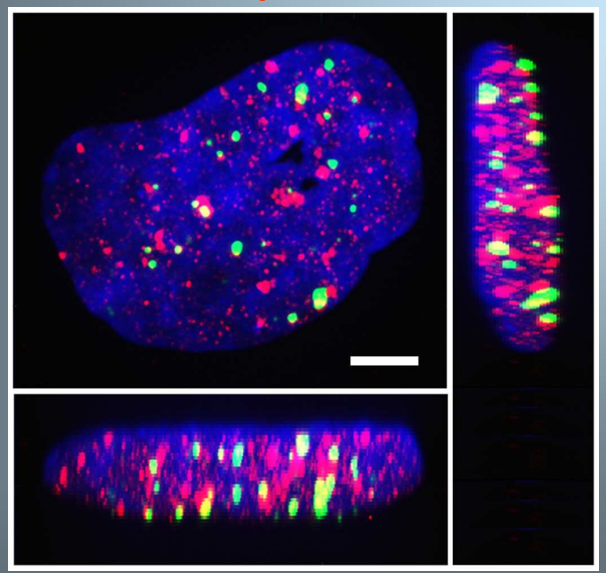

Experiments of Gabriela Šustáčková, Eva Bártová and Lenka Stixová

Využití UV laseru 355 nm ke studiu DNA reparace

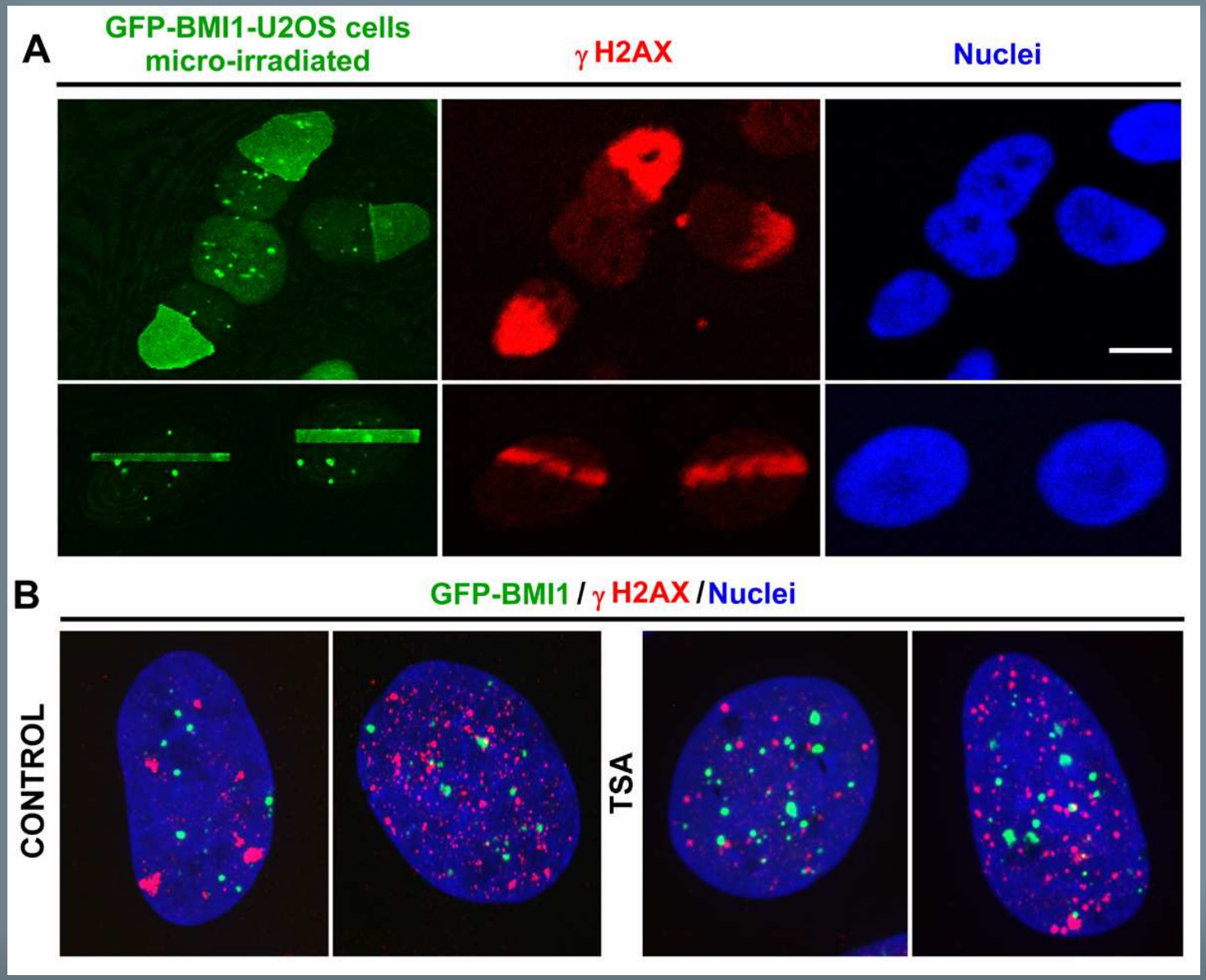

Experiments of Gabriela Galiová

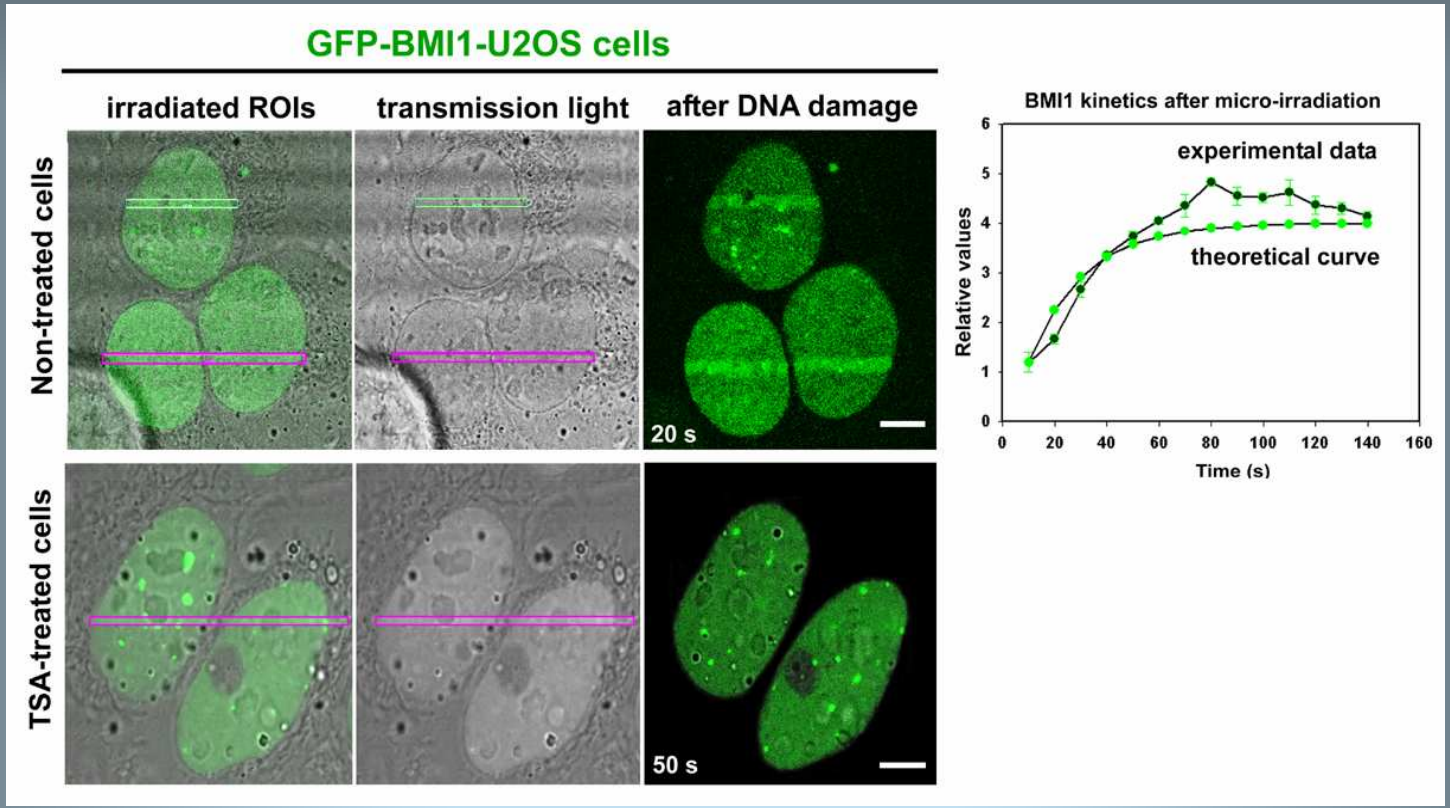

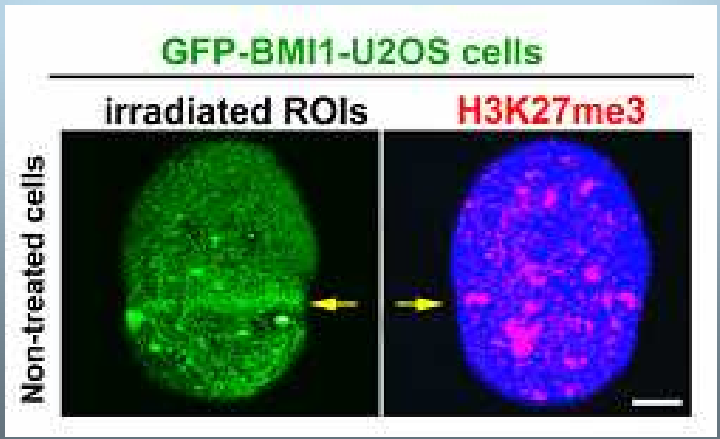

Experiments of Gabriela Galiová

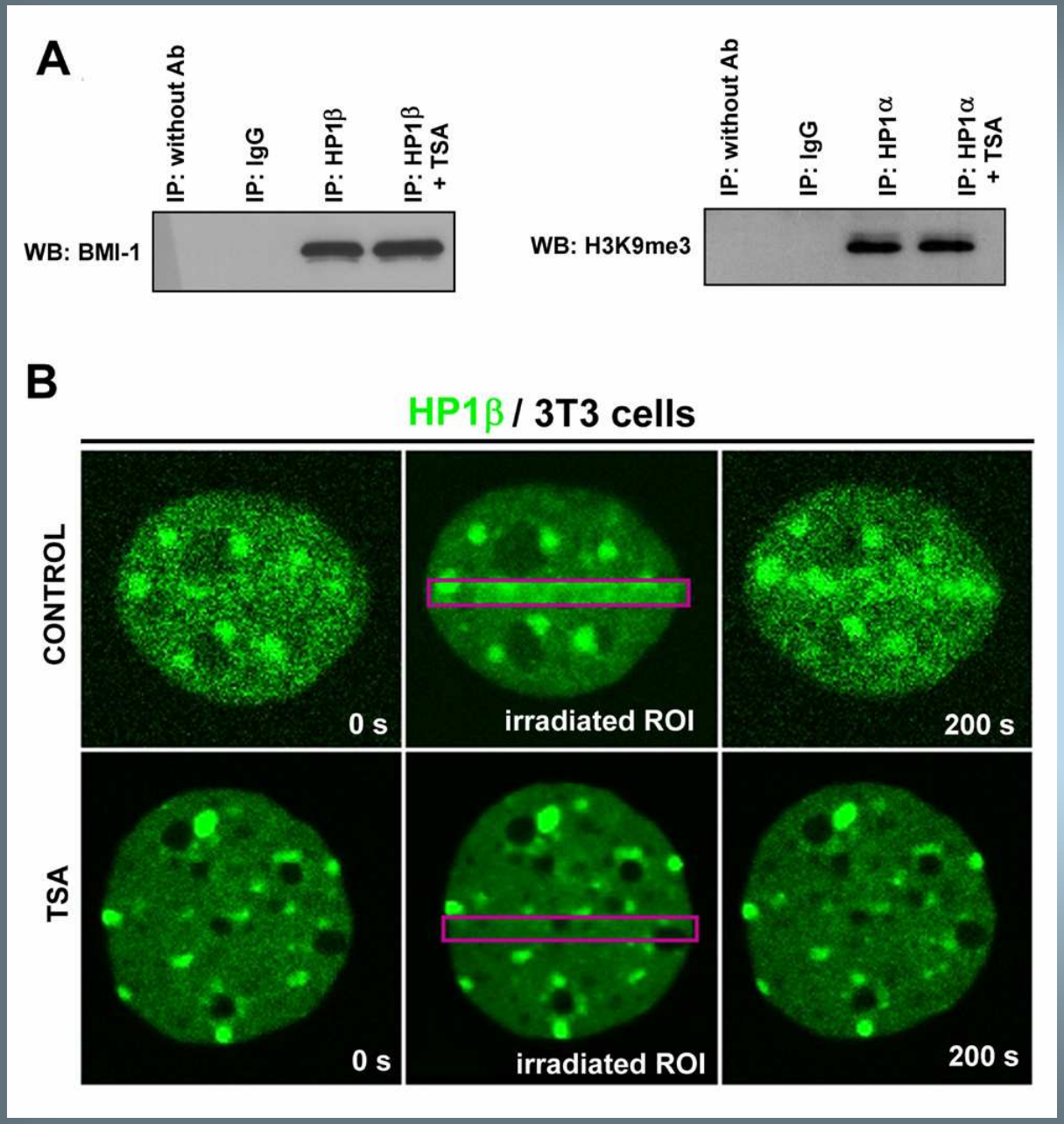

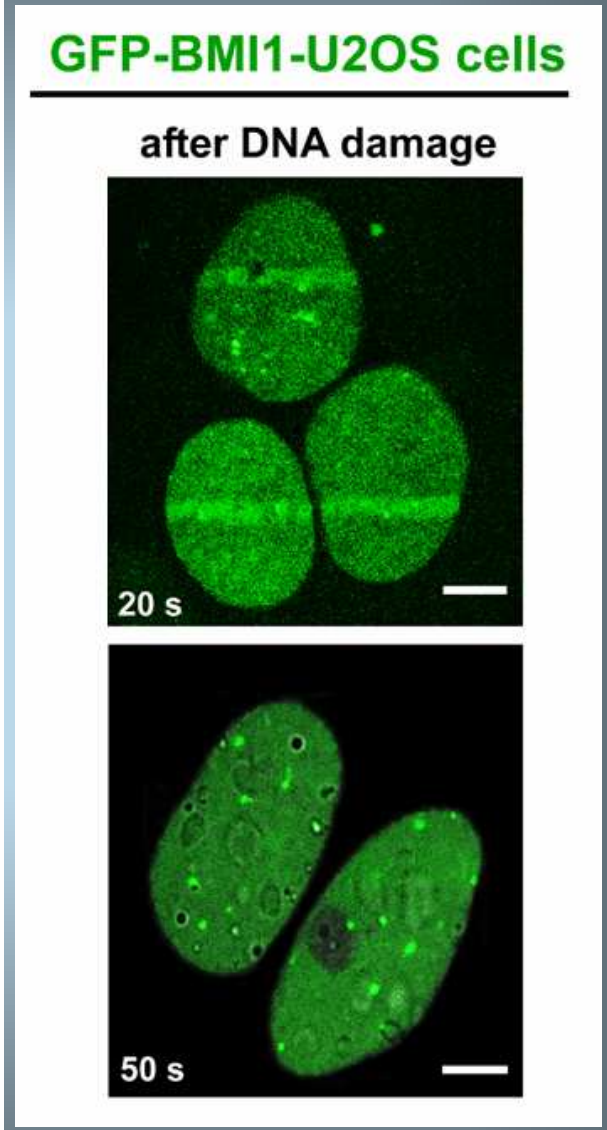

Experiments of Gabriela Galiová and Lenka Stixová

ATP depletion

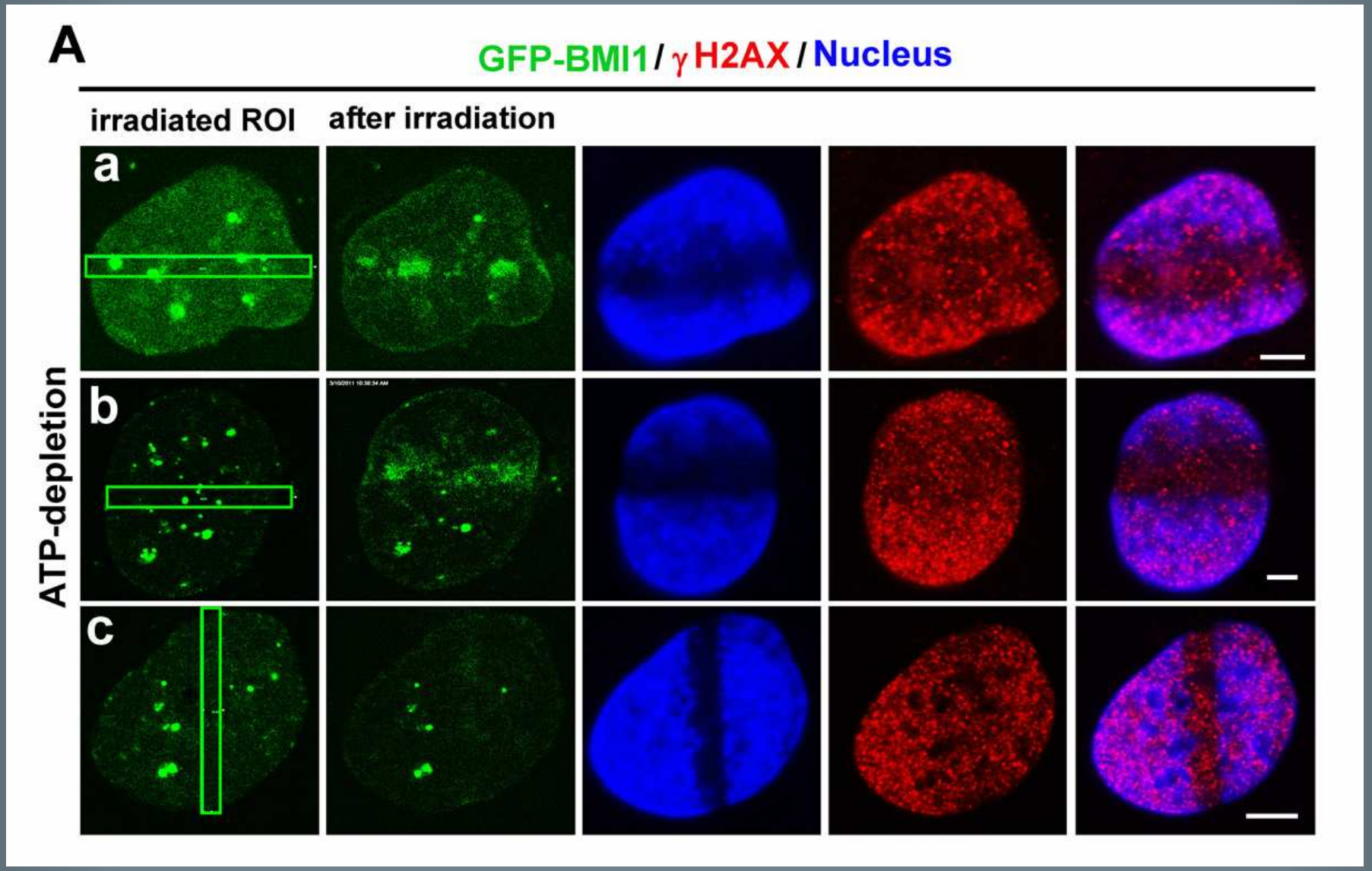

Šustáčková et al., JCP, 2011

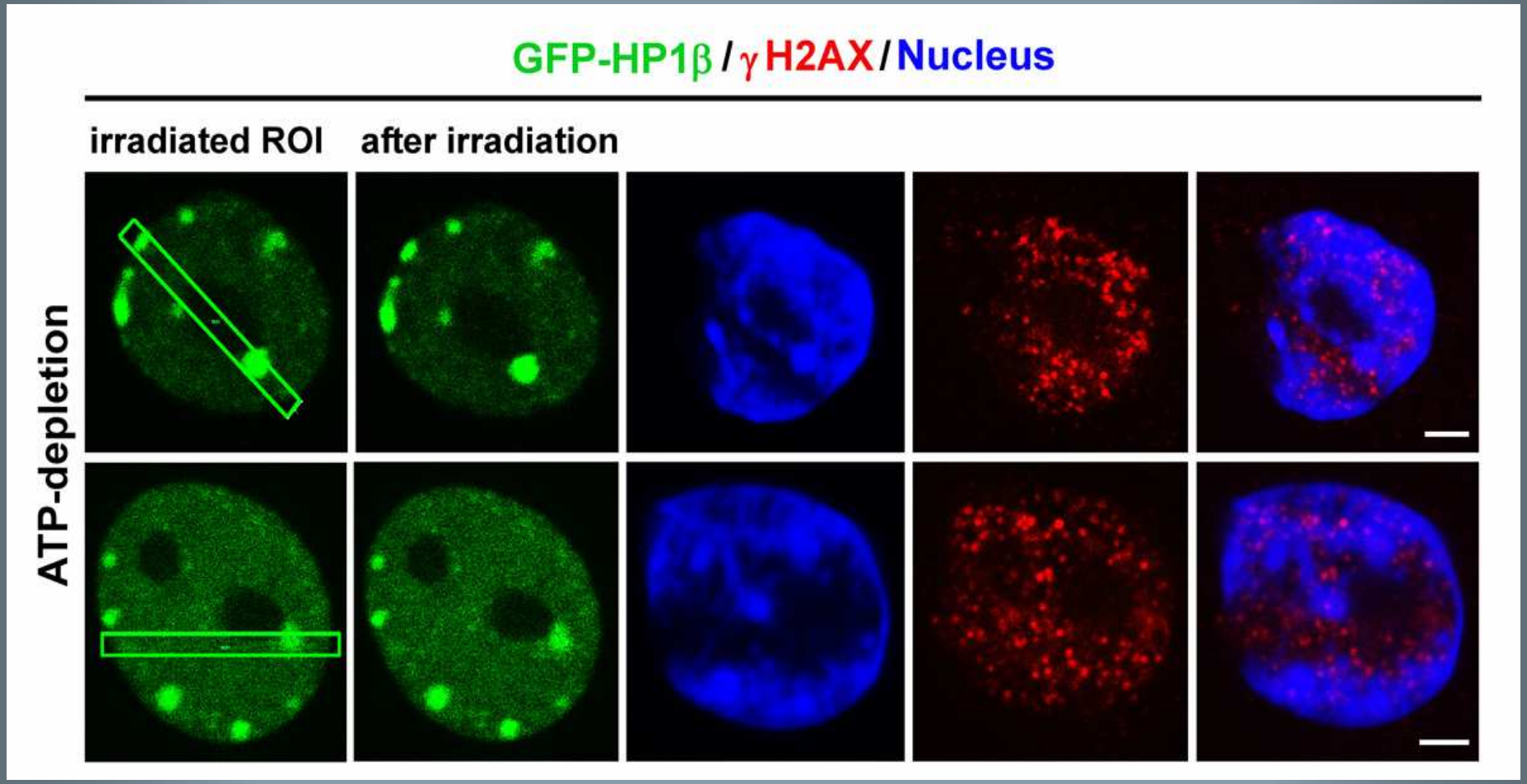

Experiments of Gabriela Šustáčková

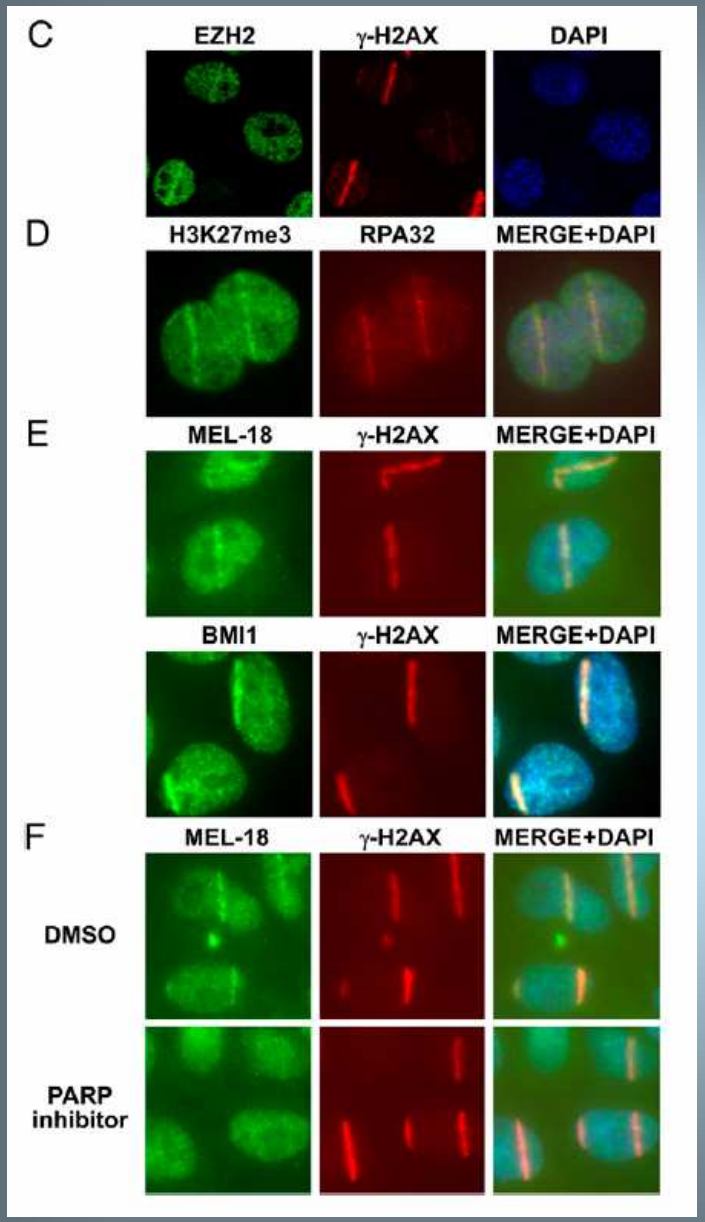

Chou et al., PNAS (2010)

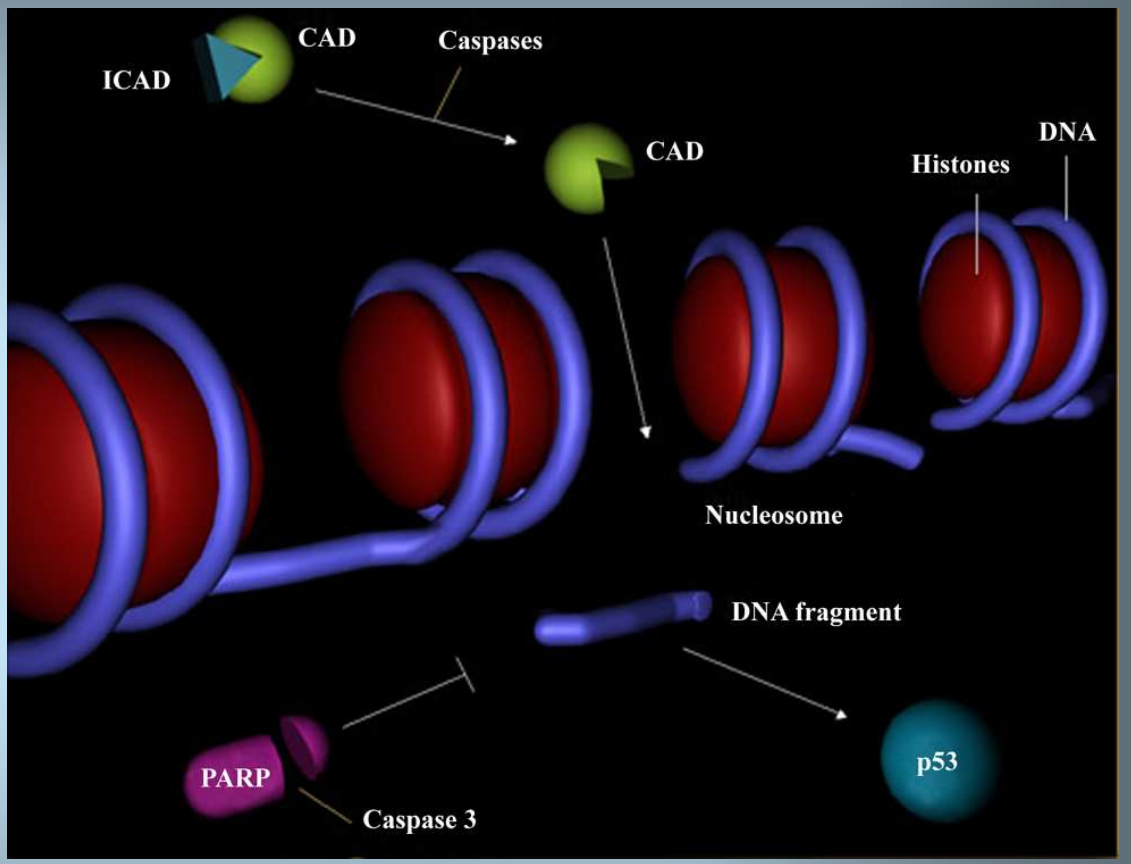

DNA repair

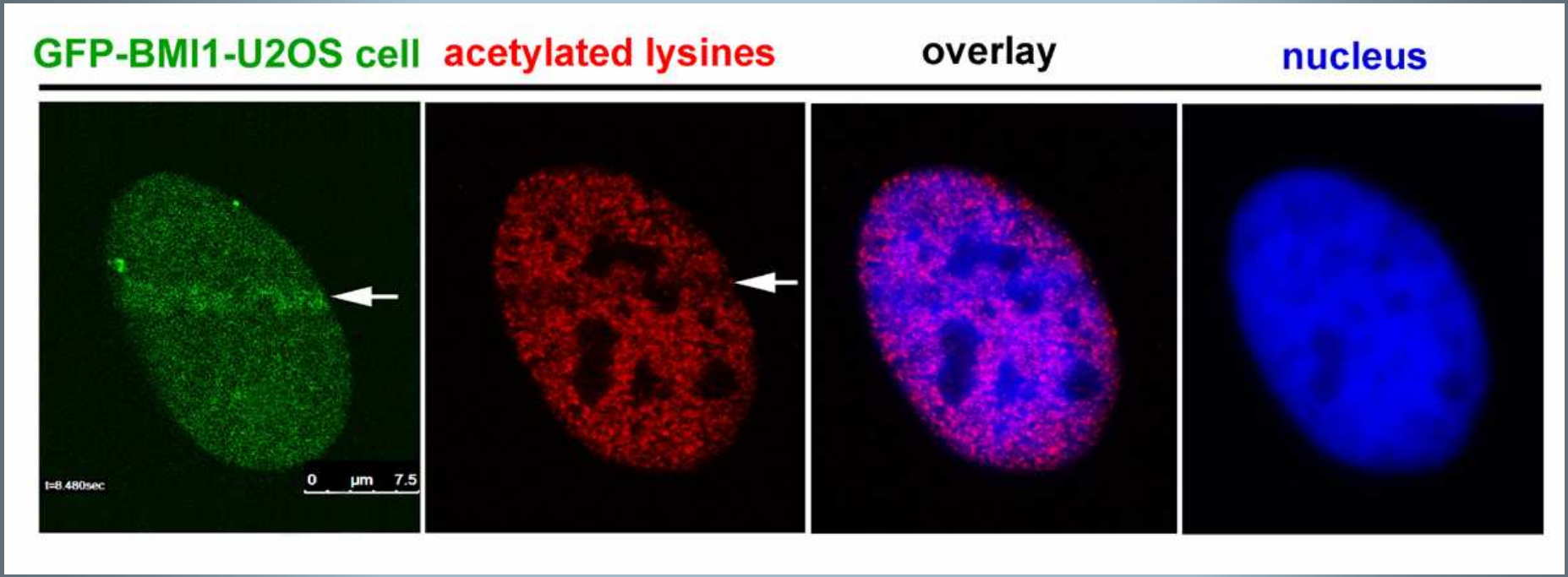

Experiments of Gabriela Šustáčková and Soňa Legartová

FRAP in UV-damaged chromatin with accumulated BMI1 and HP1β

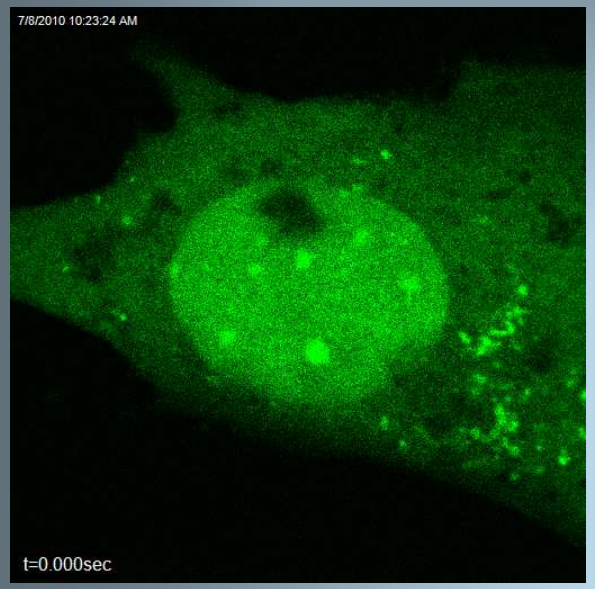

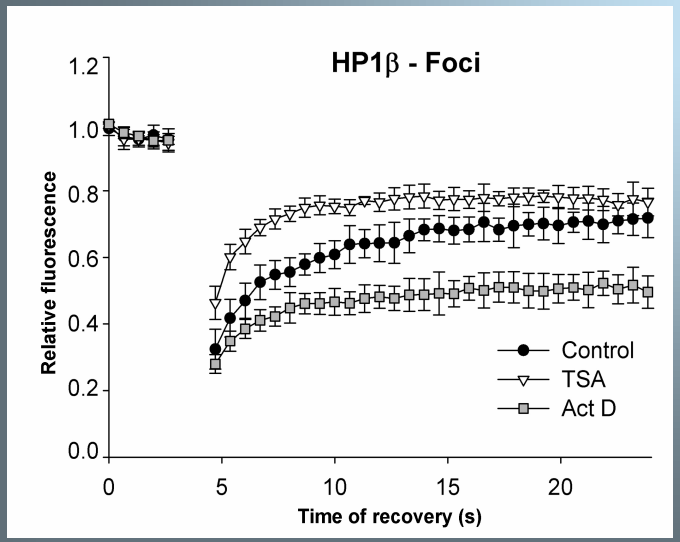

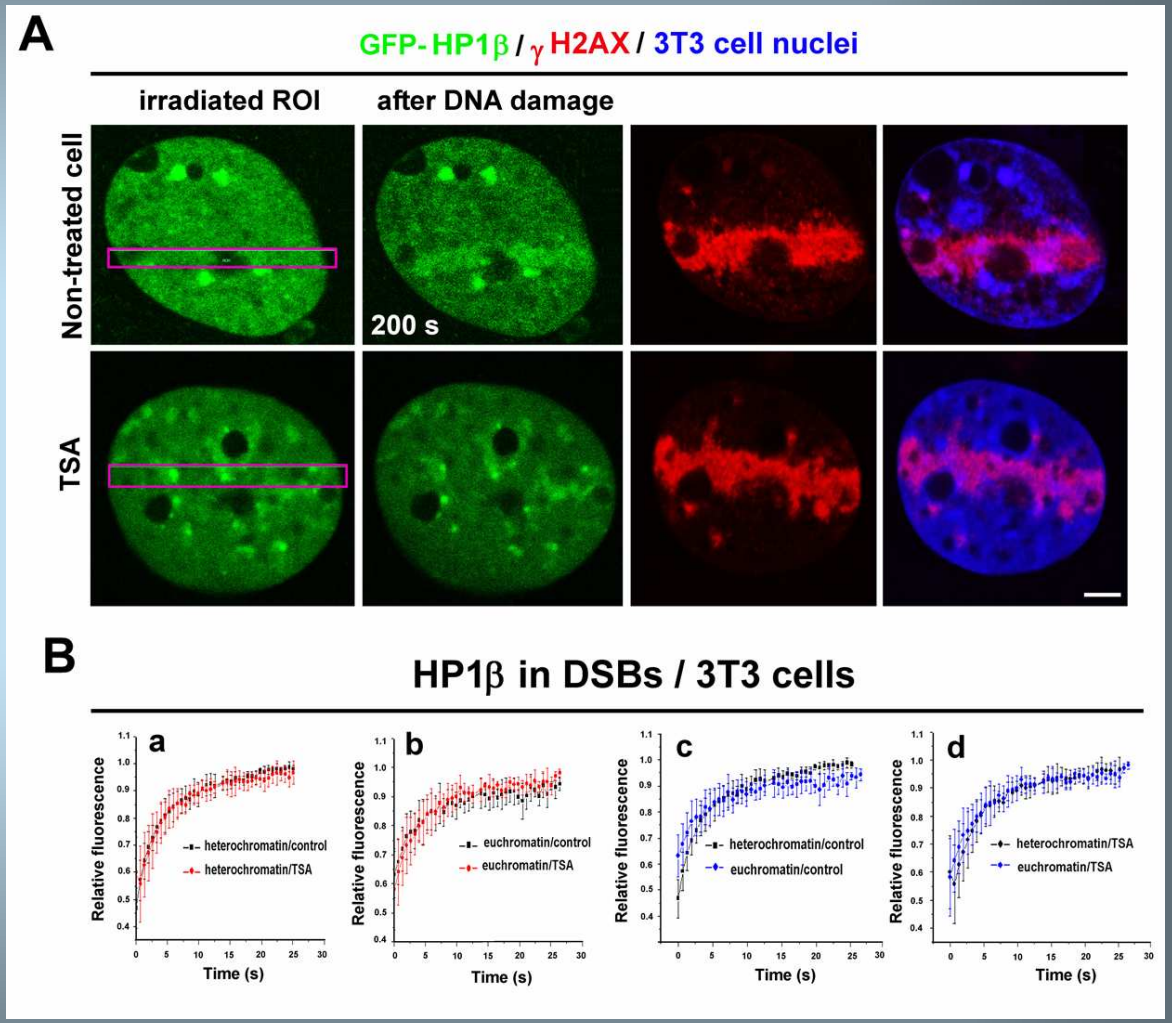

Experiments of Gabriela Šustáčková and Darya Orlova

FRAP – BMI1

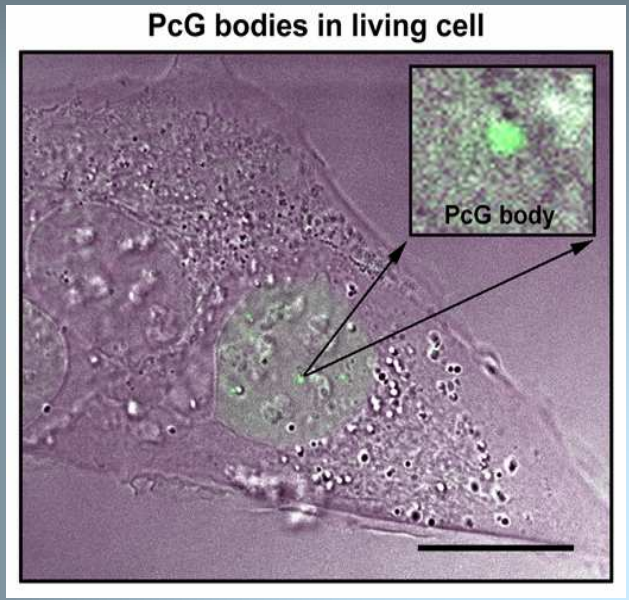

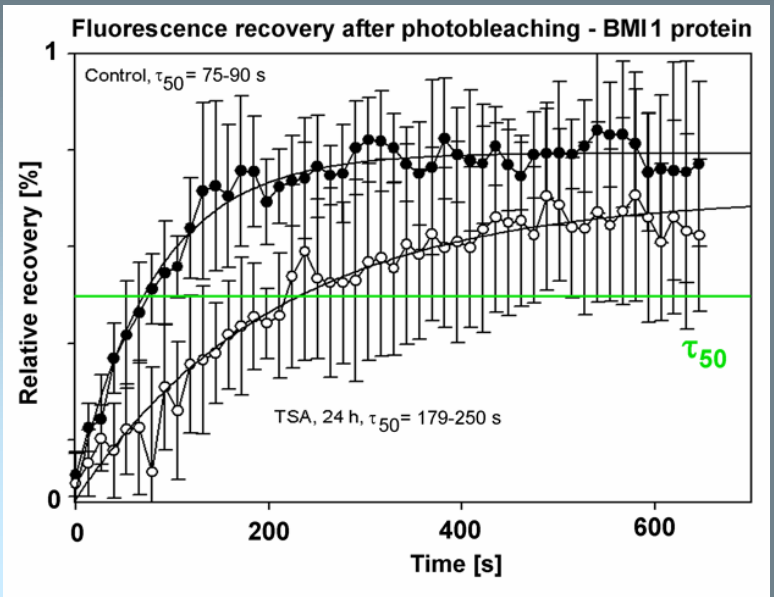

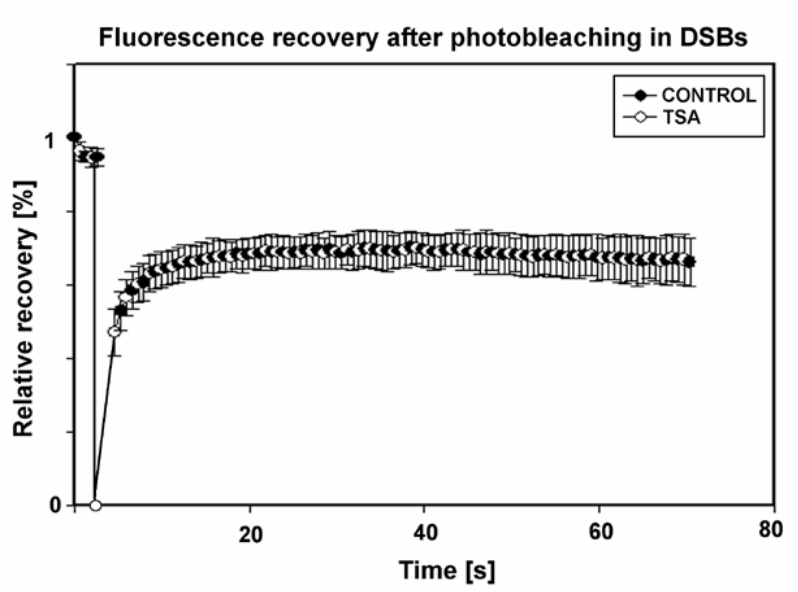

Experiments of Stanislav Kozubek

Additional molecular-biology methods with application for confocal microscopy

FRET (Fluorescence Resonance Energy Transfer) is a technique for measuring interactions between two proteins in vivo. In this technique, two different fluorescent molecules (fluorophores) are genetically fused the two proteins of interest.

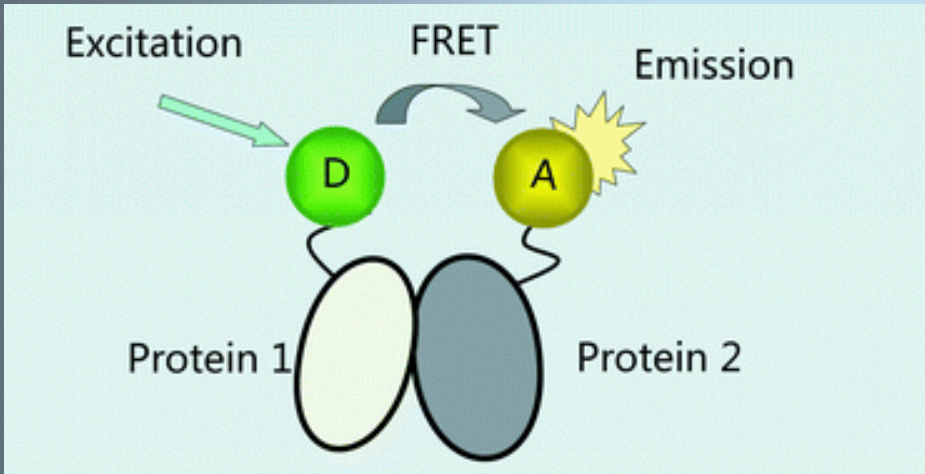

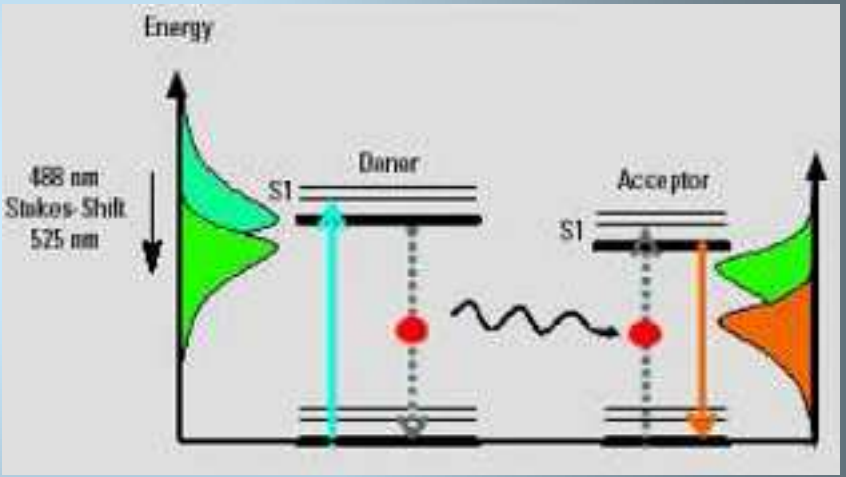

http://www.rsc.org/publishing/journals/

$$E_A(i) = \frac{B - A \times b - C \times (c - a \times b)}{C}$$

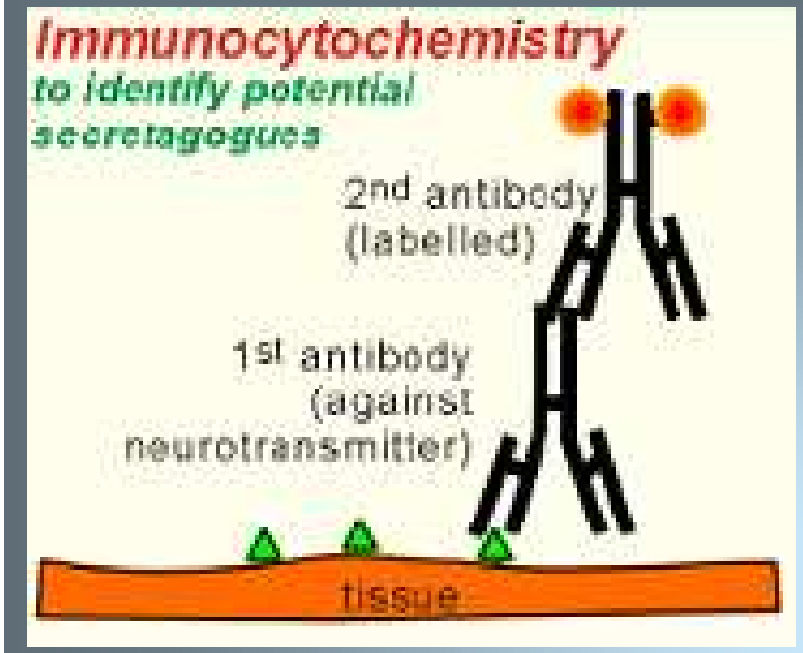

http://www.celanphy.science.ru.nl/Bruce%20web/construction.htm

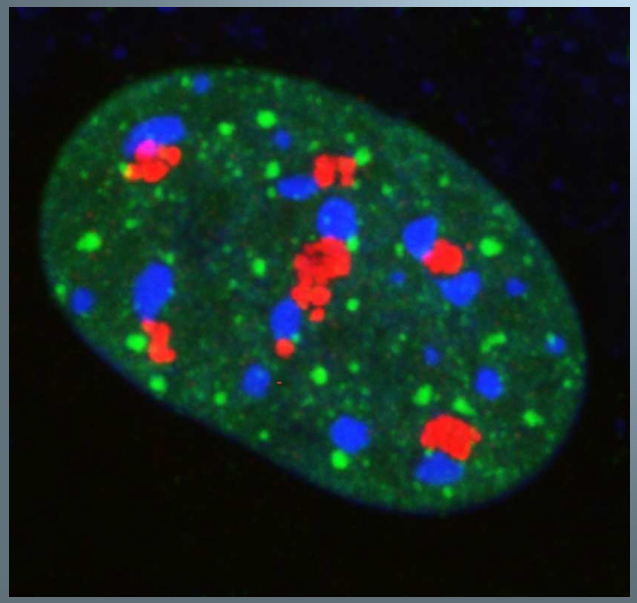

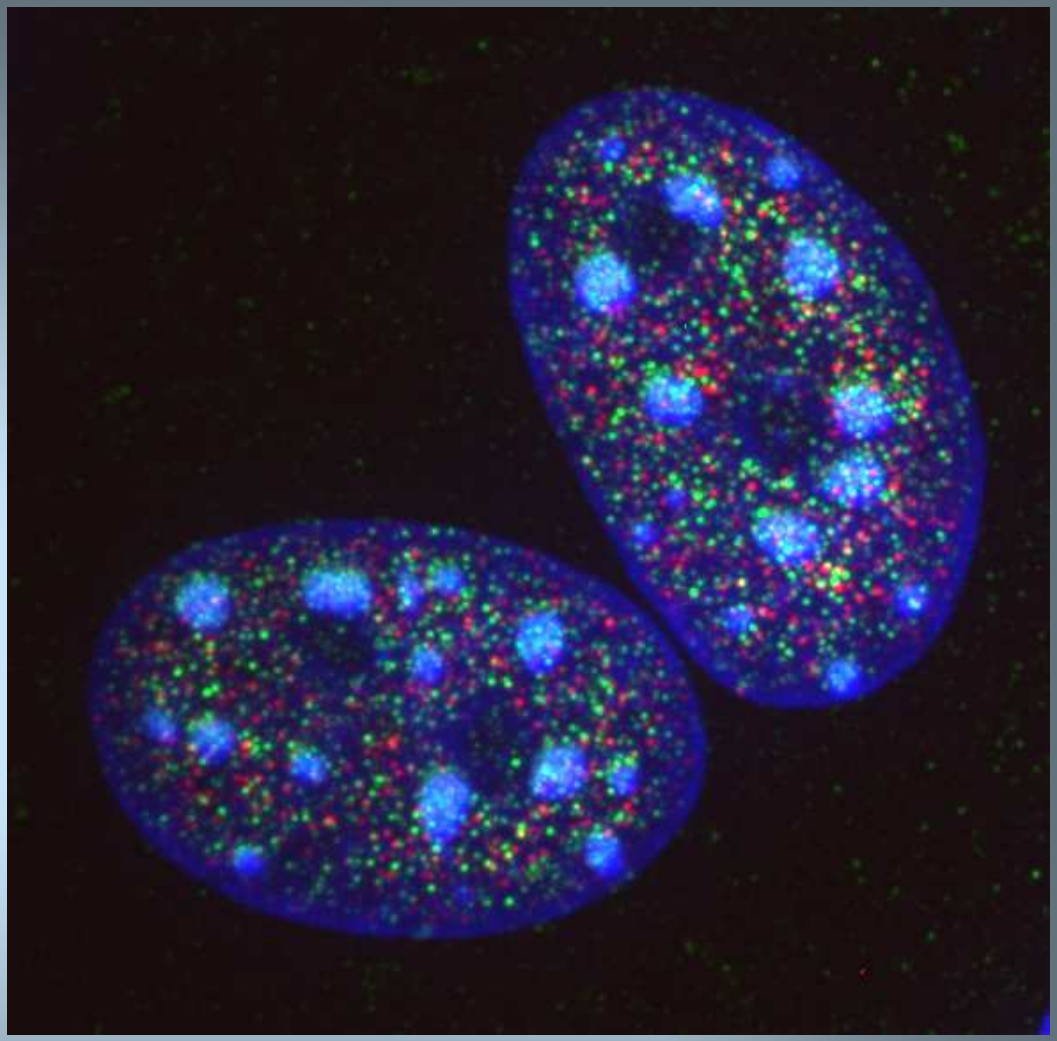

EB group, IBP, Brno

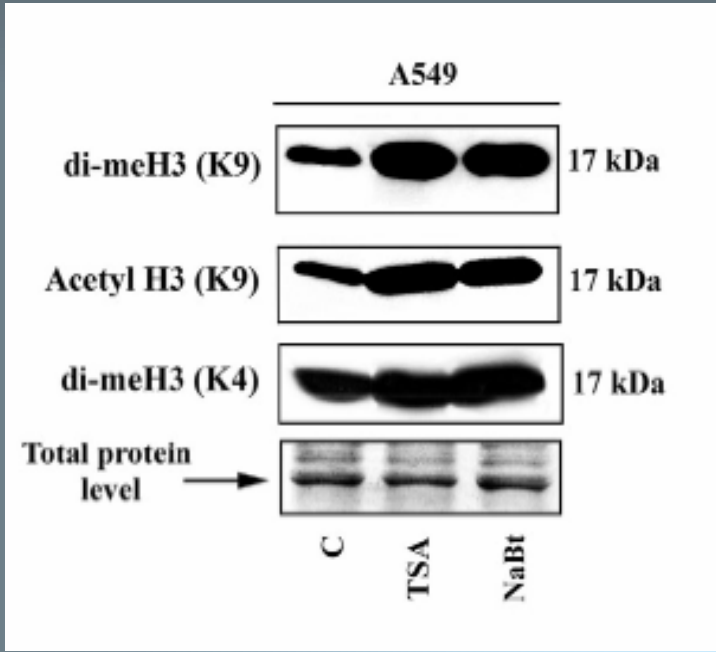

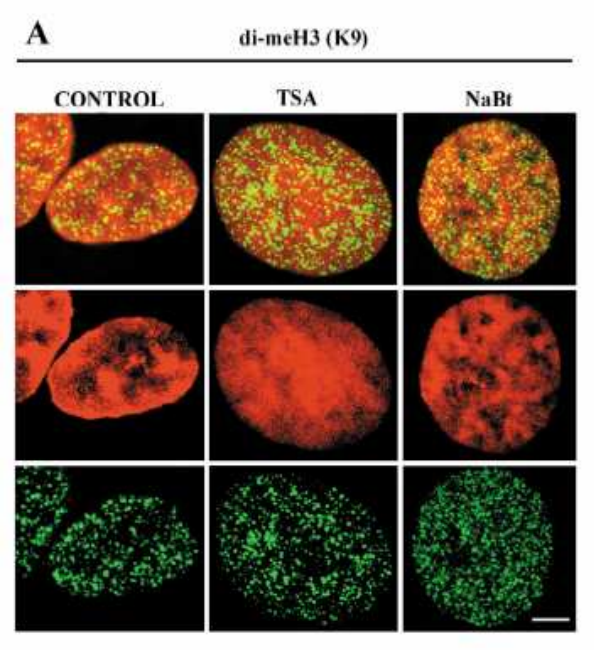

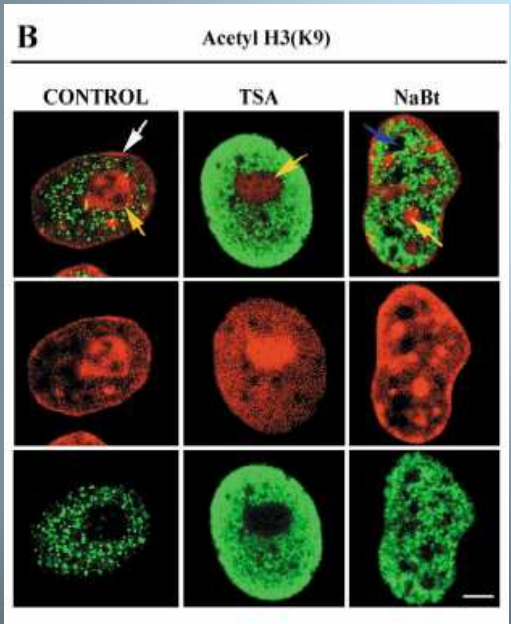

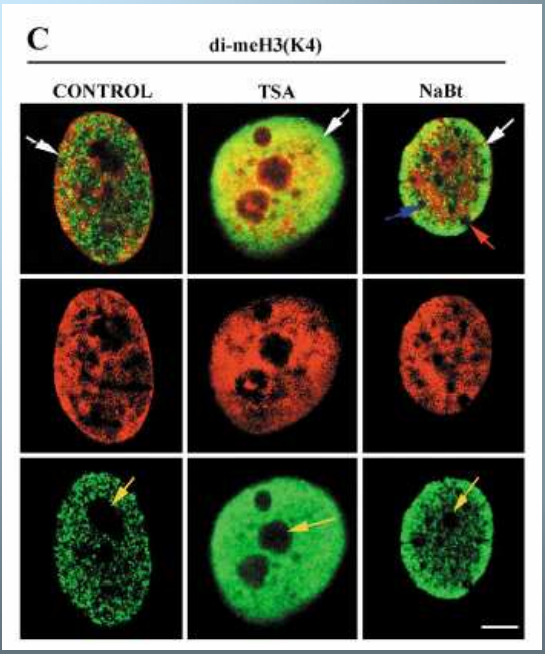

Bártová et al., JCS (2005)

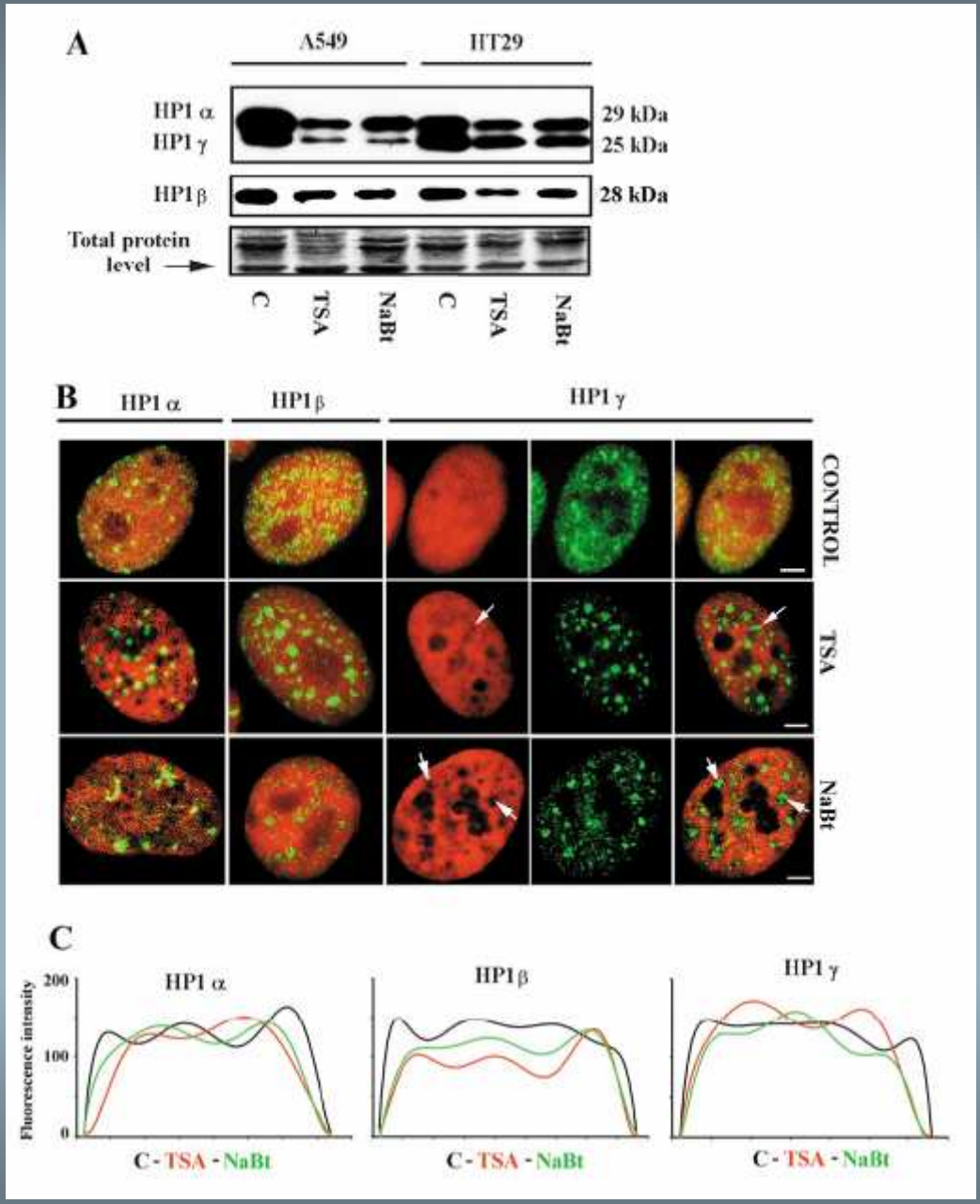

Bártová et al., JCS (2005)

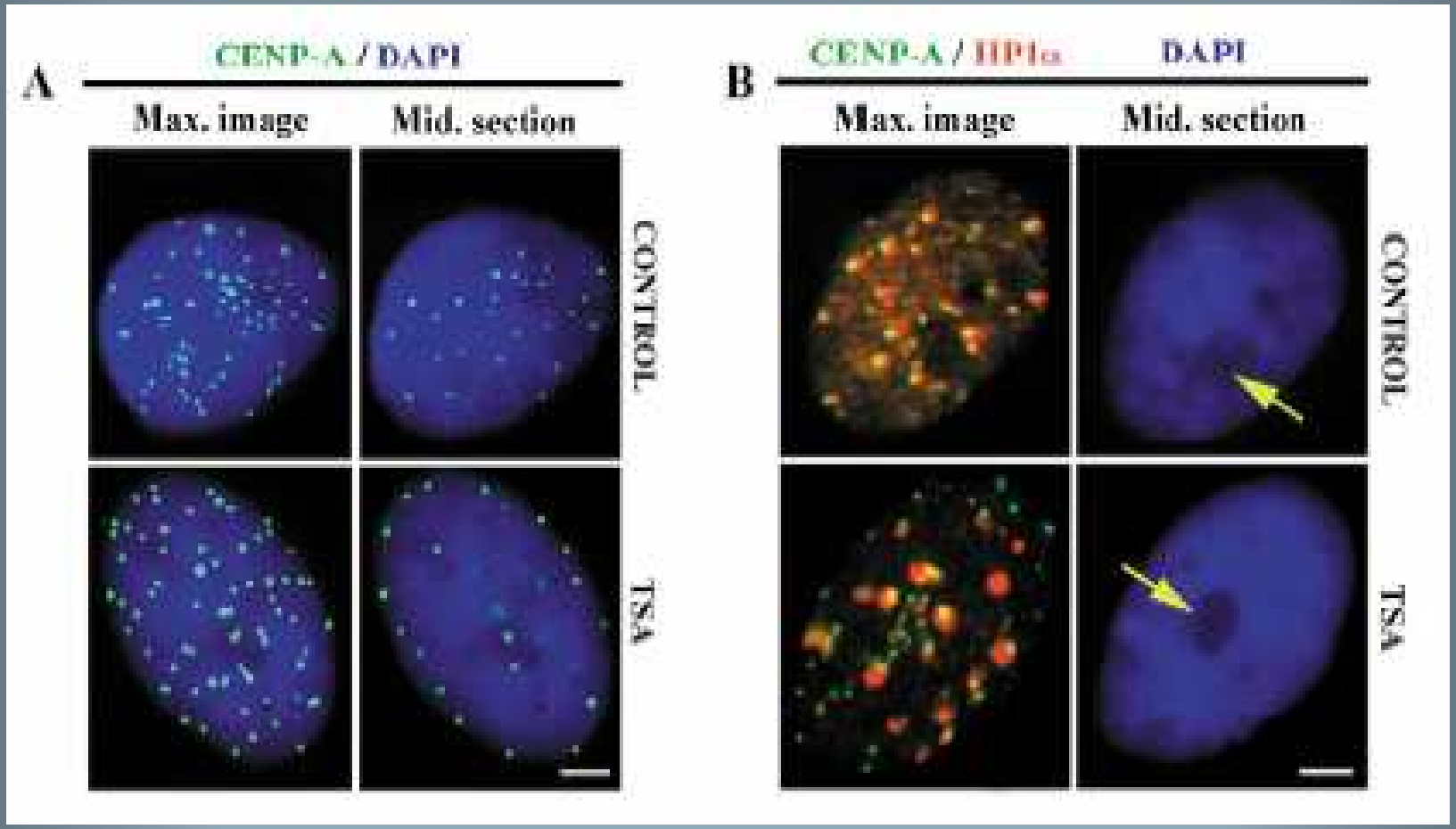

Bártová et al., JCS (2005)

Single particle tracking

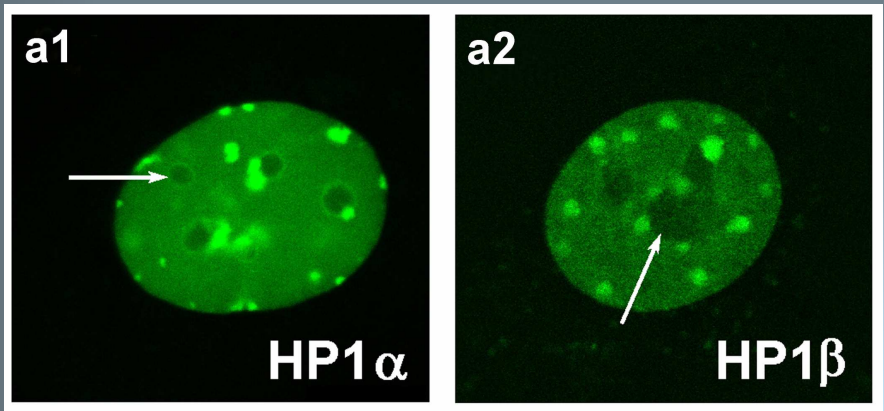

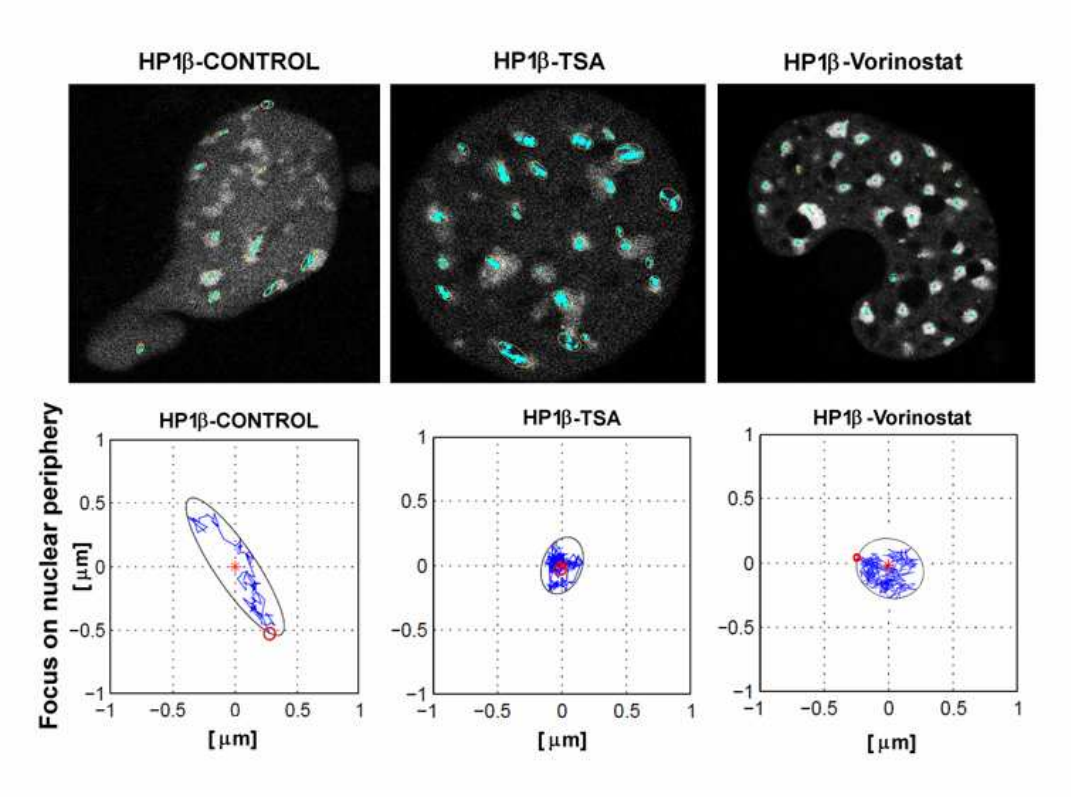

Experiments of Lenka Stixová and Pavel Matula

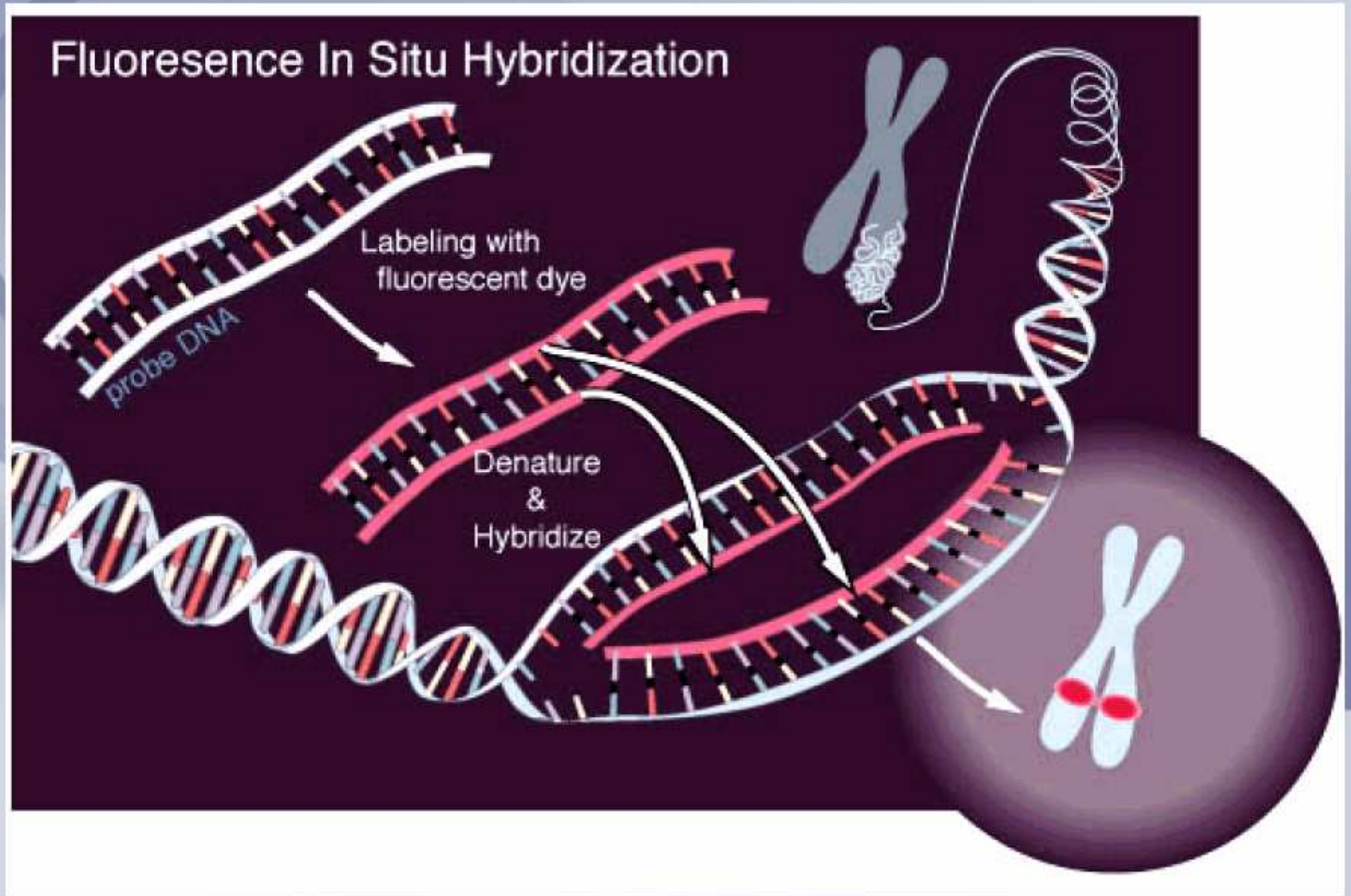

http://www.accessexcellence.org/RC/VL/GG/fish.html

3D-FISH a konfokální mikroskopie

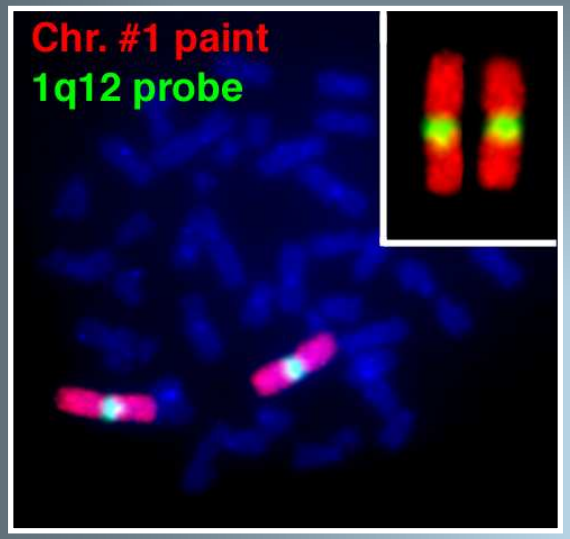

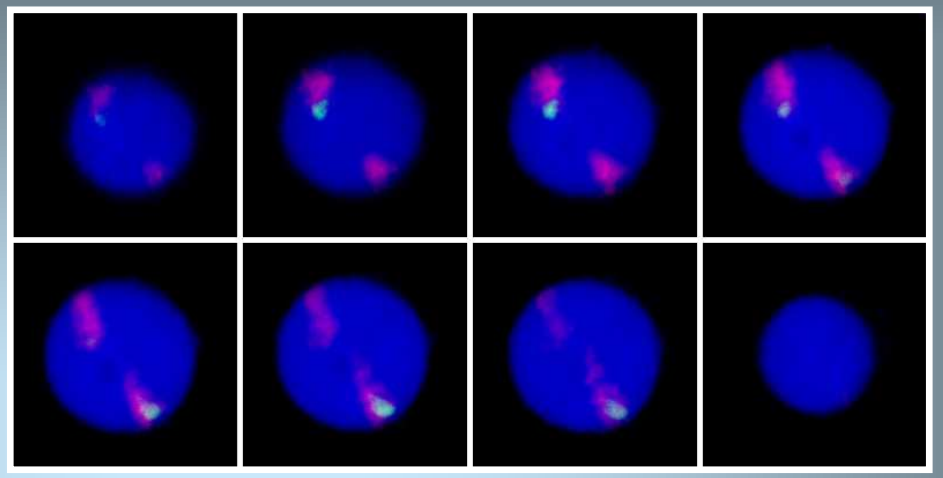

Galerie optických řezů

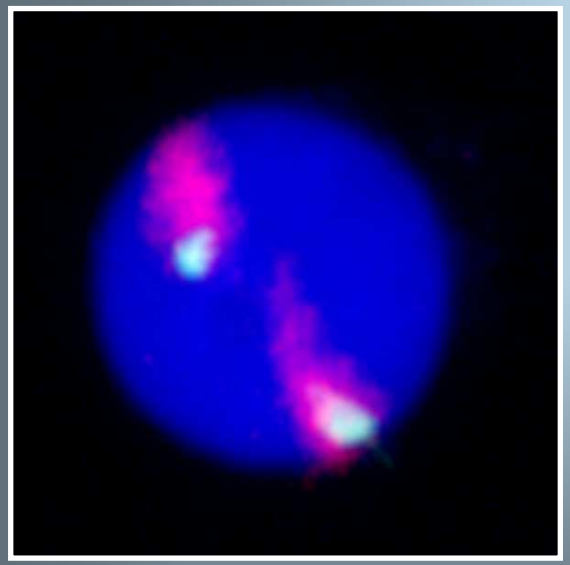

Maximální obraz
Všech řezů

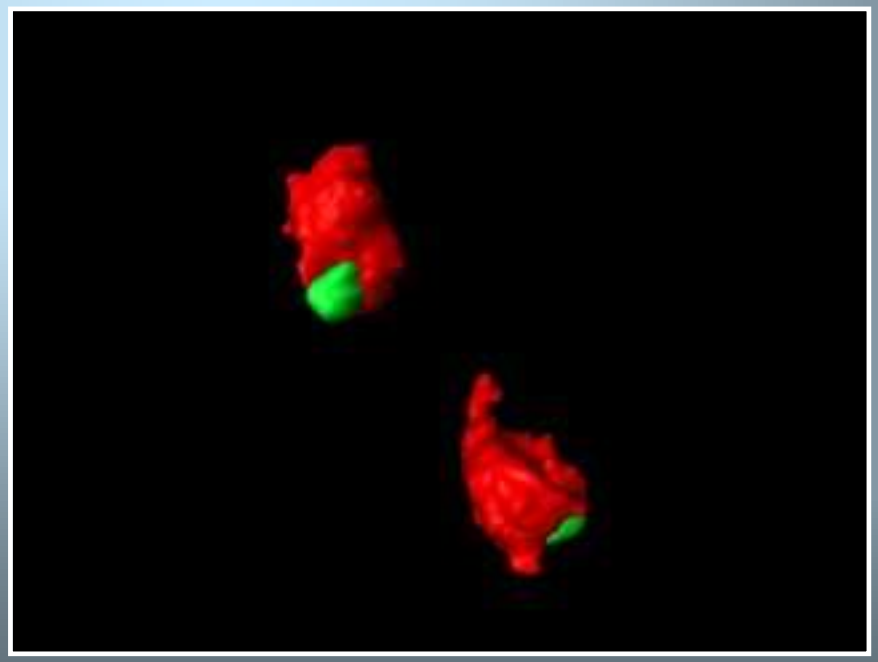

3D reconstrukce CT

Weierich et al., (2003) in press

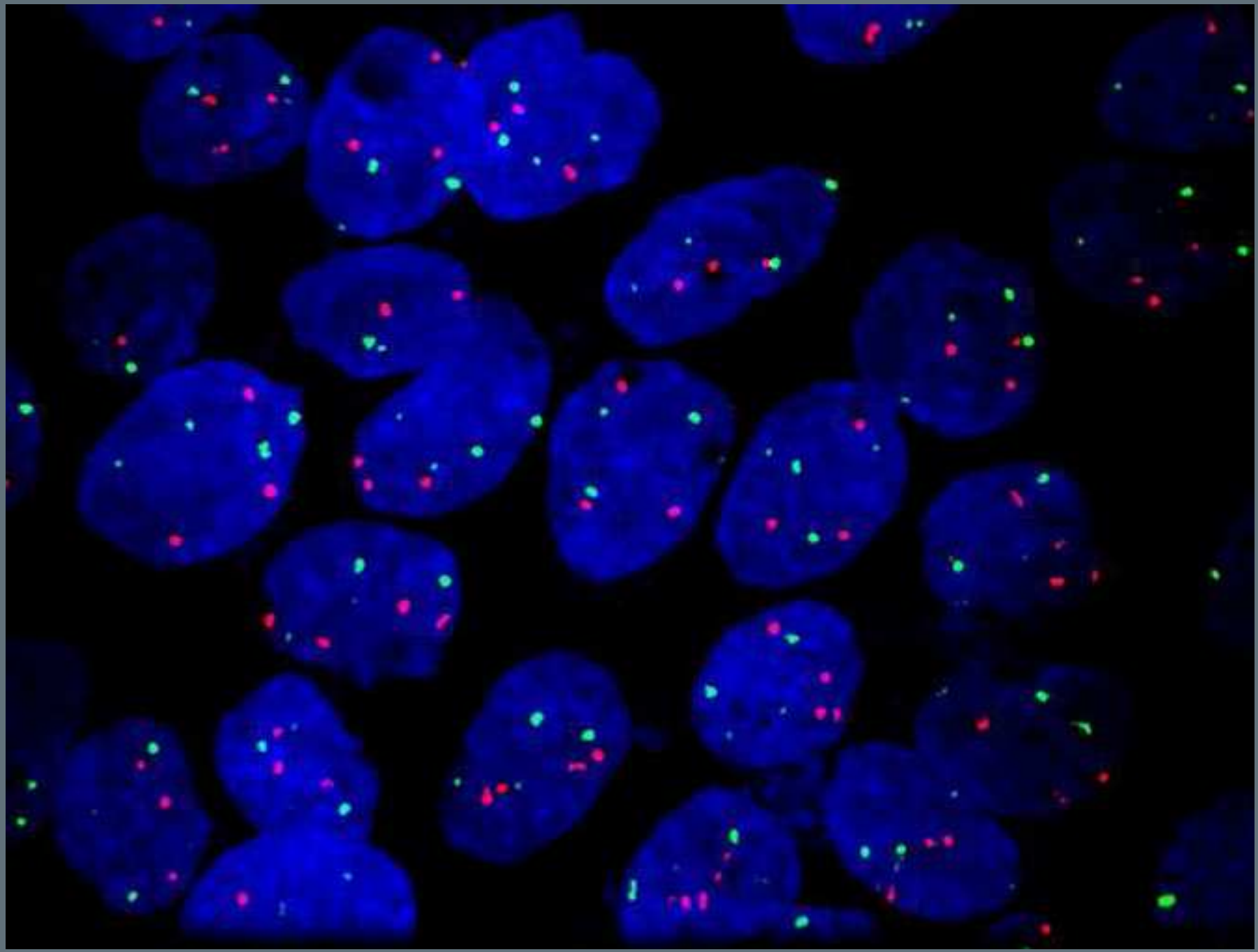

Image analysis and studies on nuclear radial distribution of selected genomic regions

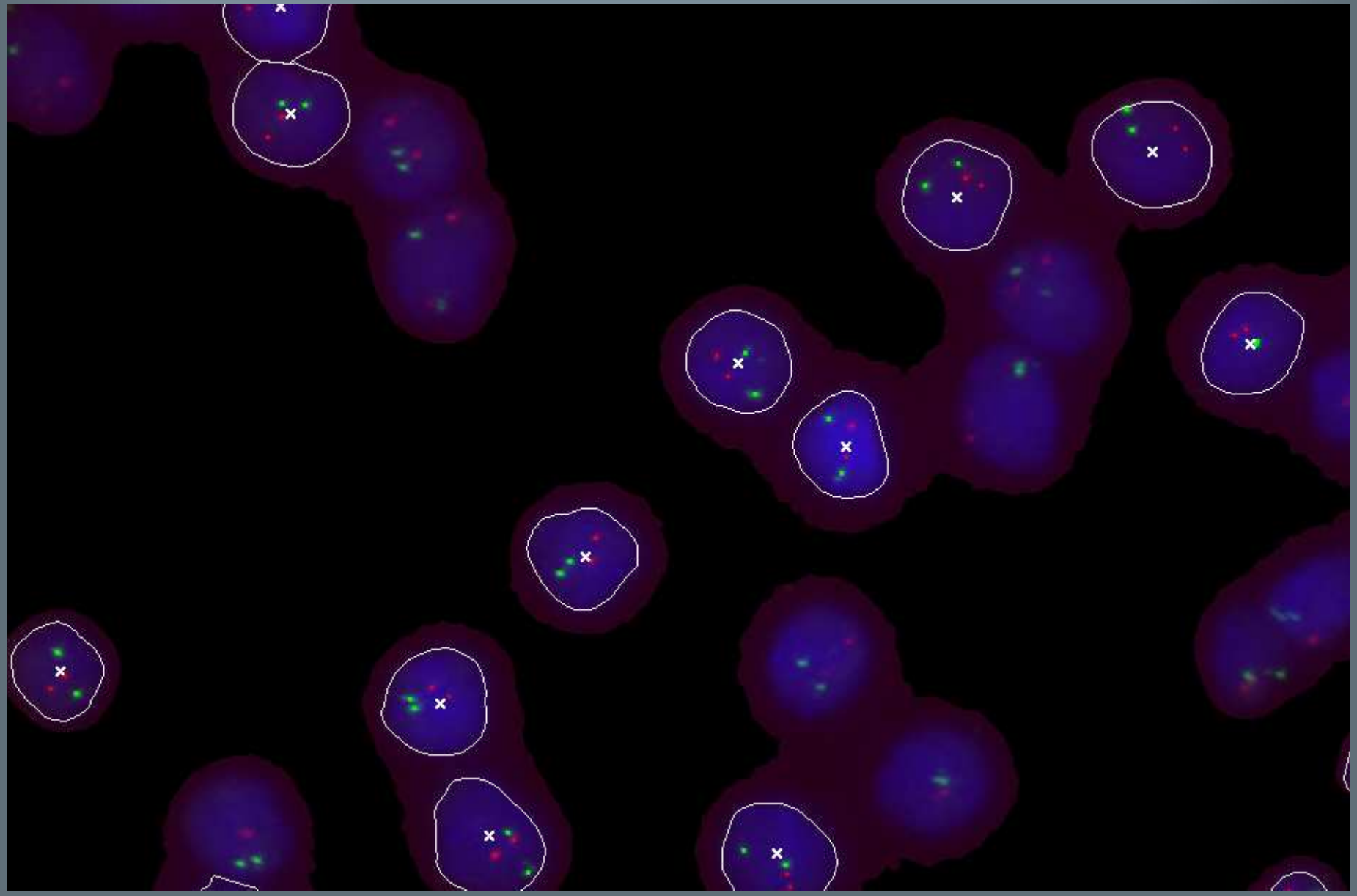

Comparative genome hybridization

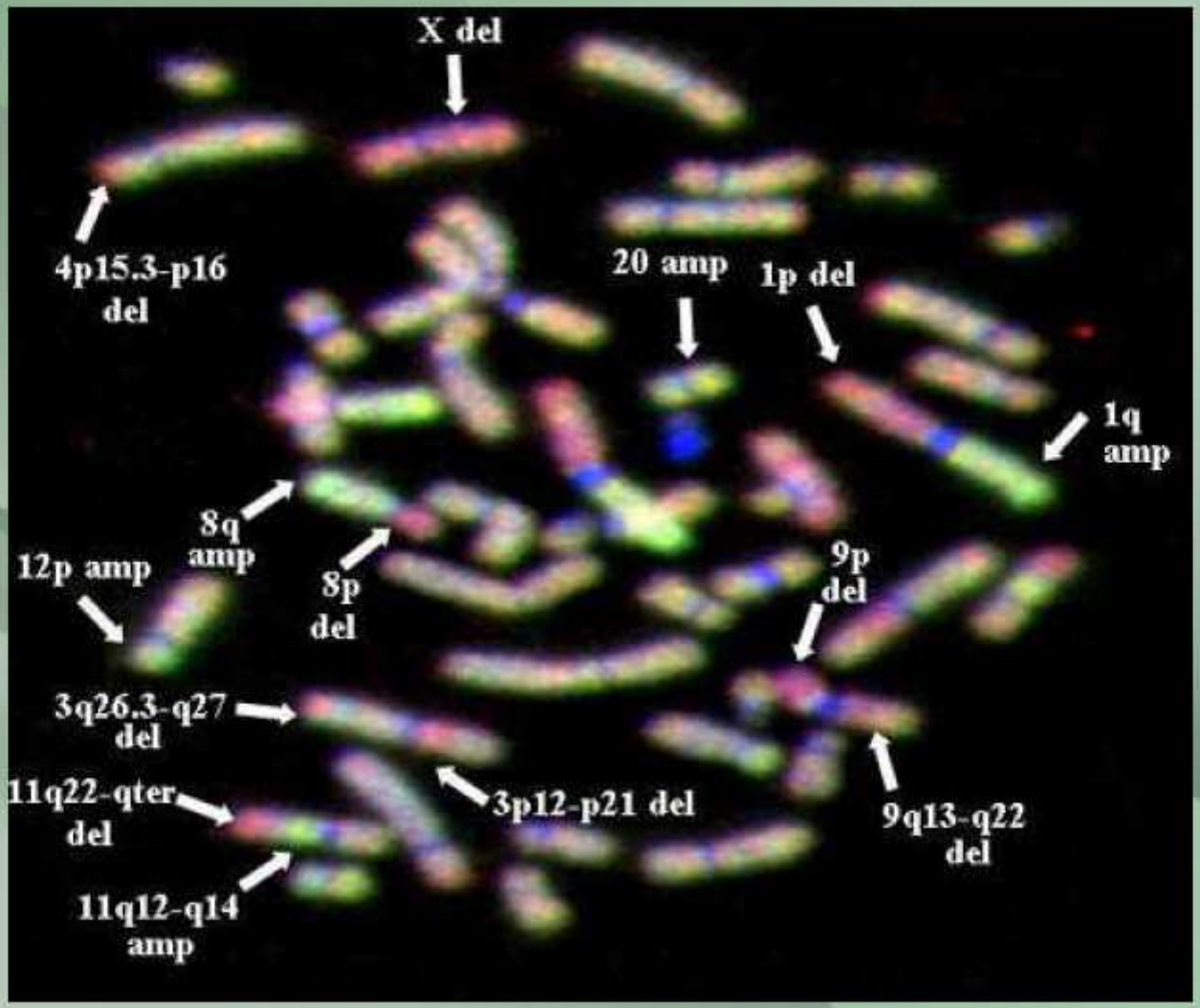

CGH on metaphase spreads

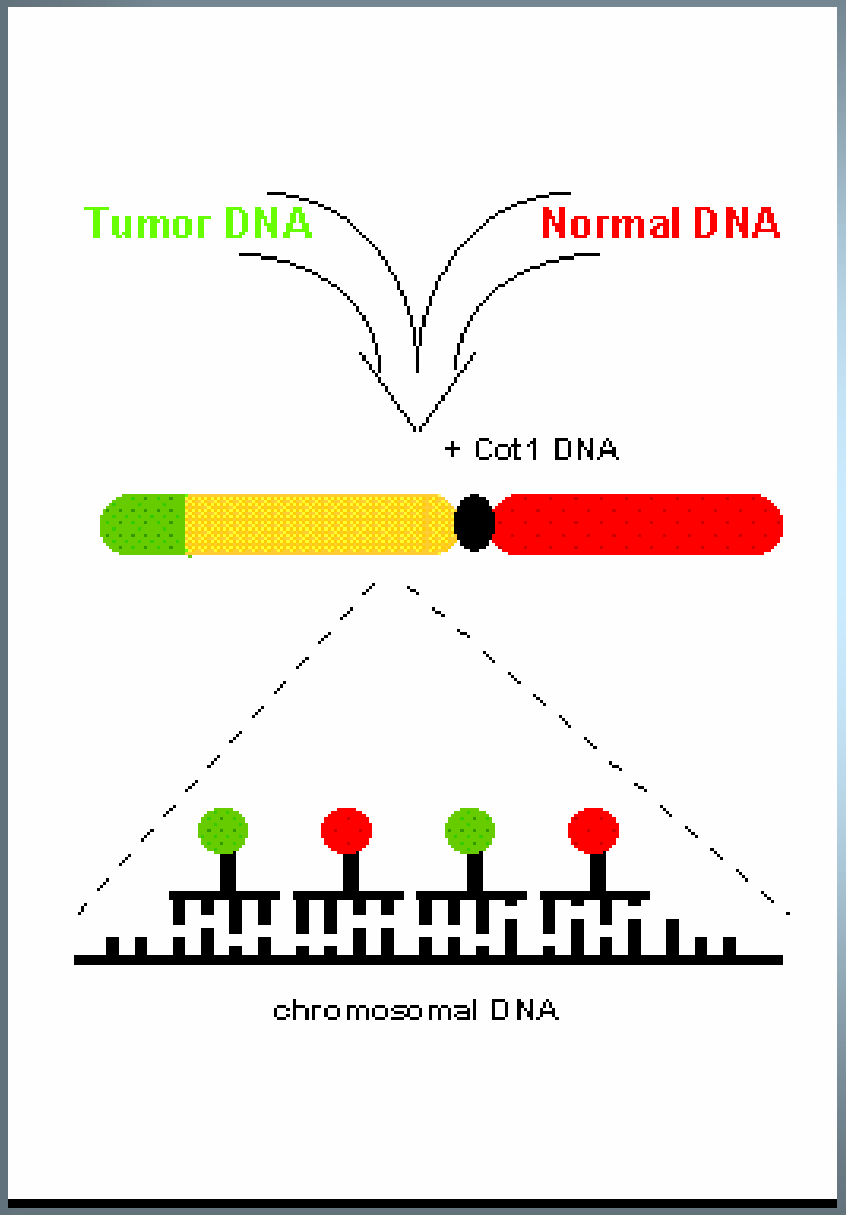

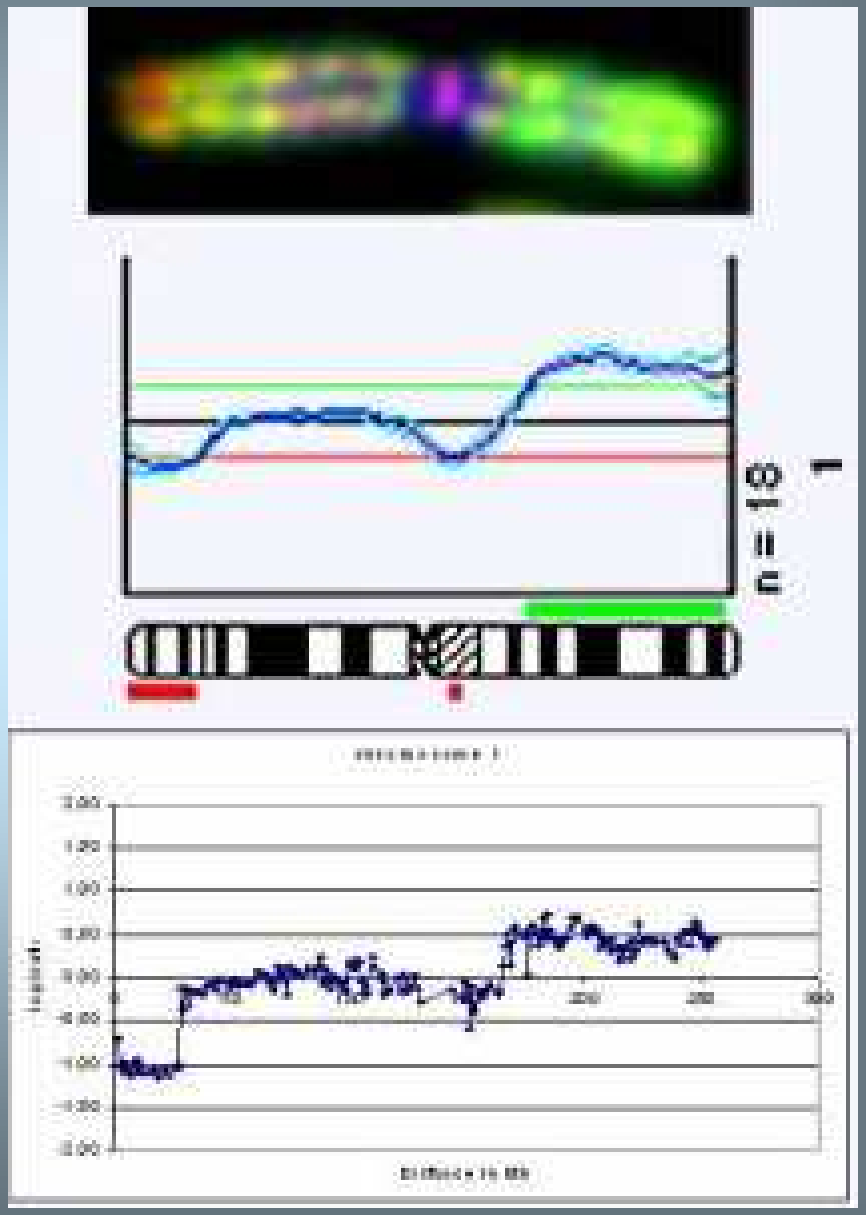

Comparative genome hybridization

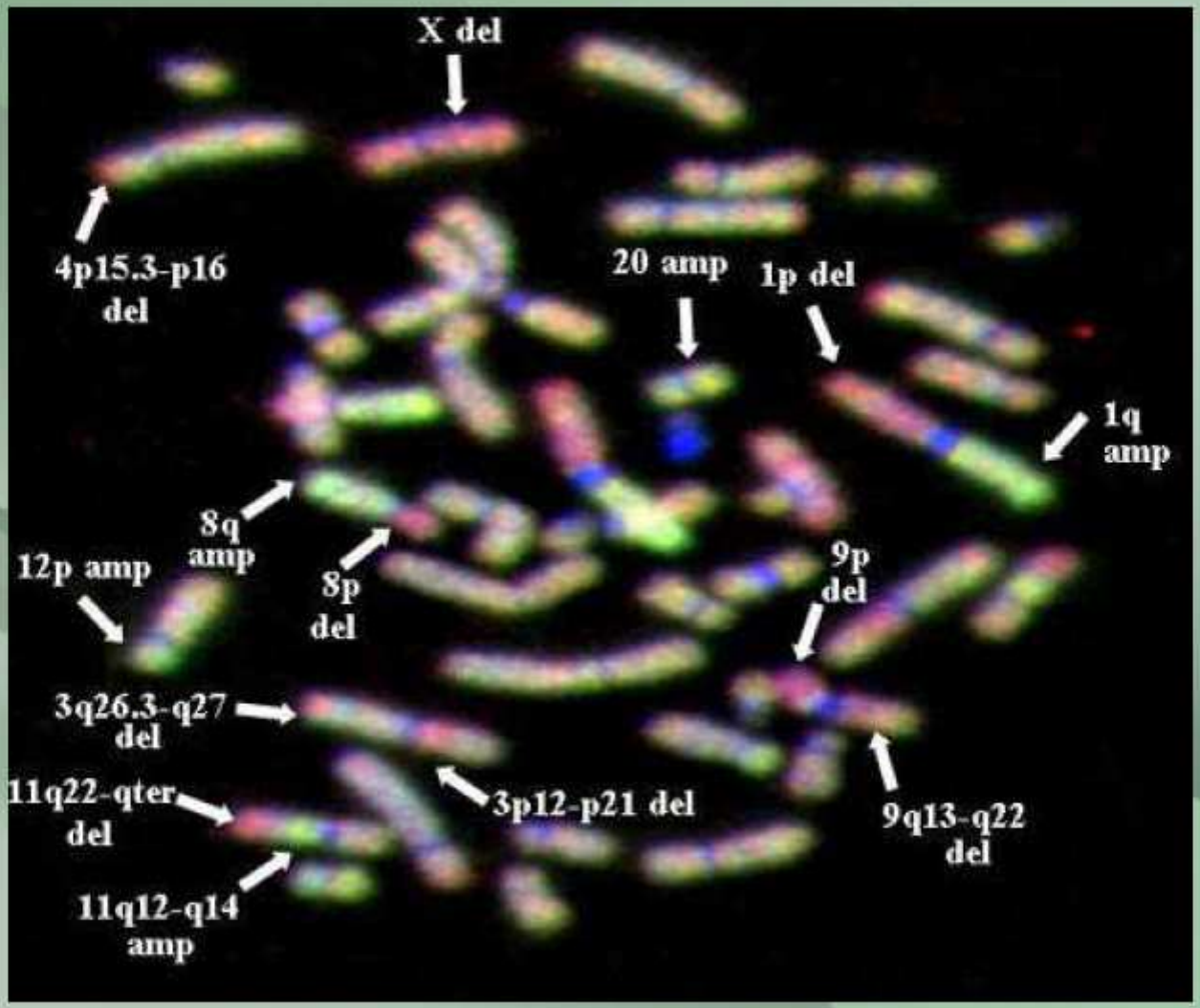

Advanced microscopic techniques

Electron Microscopes are: **scientific instruments that use a beam of highly energetic electrons to examine objects on a very fine scale. This examination can yield the following information:**

Topography

The surface features of an object or "how it looks", its texture; direct relation between these features and materials properties (hardness, reflectivity...etc.)

Morphology

The shape and size of the particles making up the object; direct relation between these structures and materials properties (ductility, strength, reactivity...etc.)

Composition

The elements and compounds that the object is composed of and the relative amounts of them; direct relationship between composition and materials properties (melting point, reactivity, hardness...etc.)

Crystallographic Information

How the atoms are arranged in the object; direct relation between these arrangements and materials properties (conductivity, electrical properties, strength, etc.)

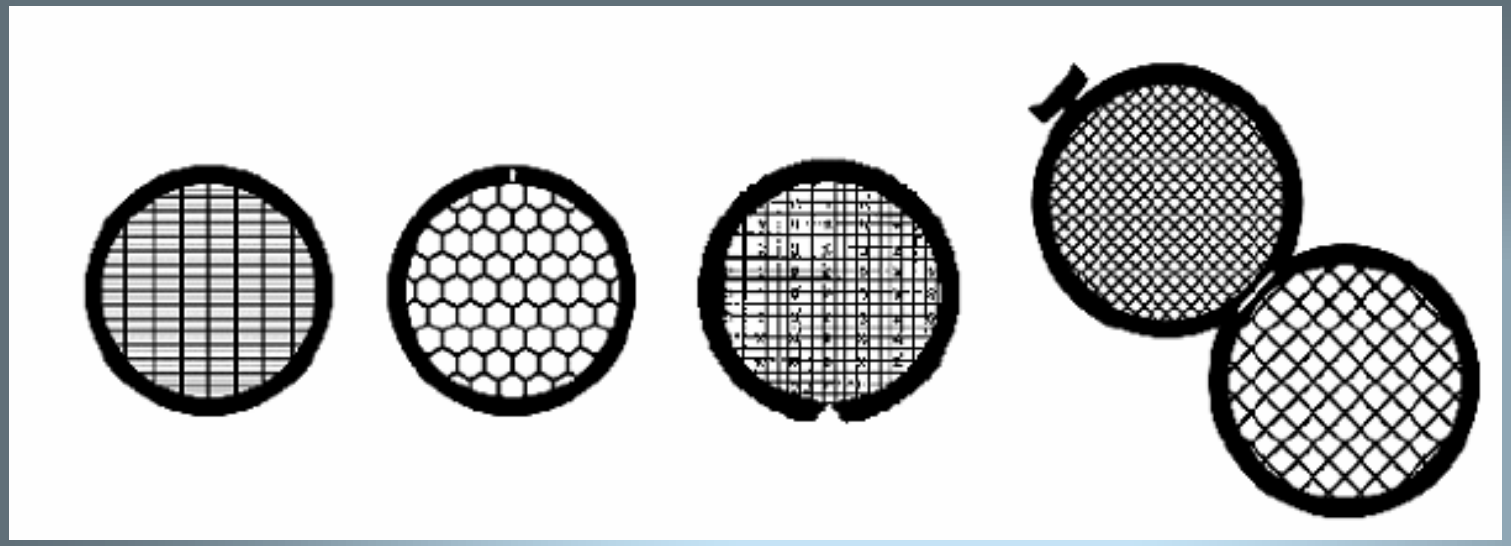

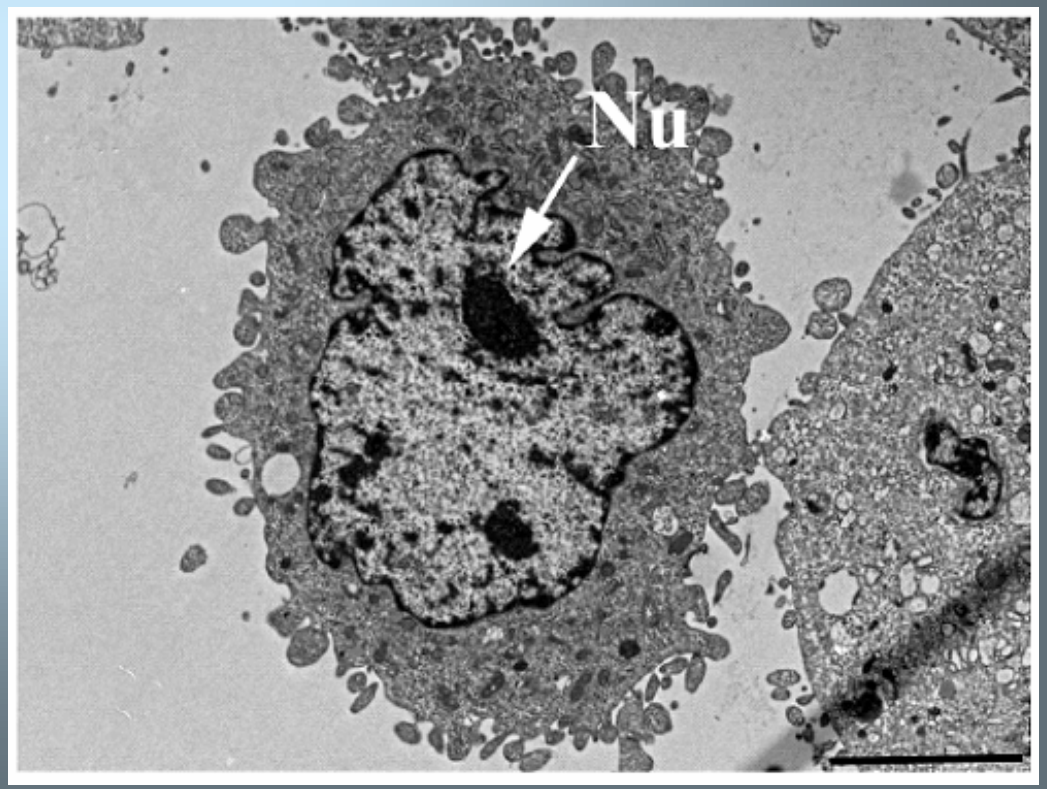
Nu

Transmission Electron Microscopes (TEM)

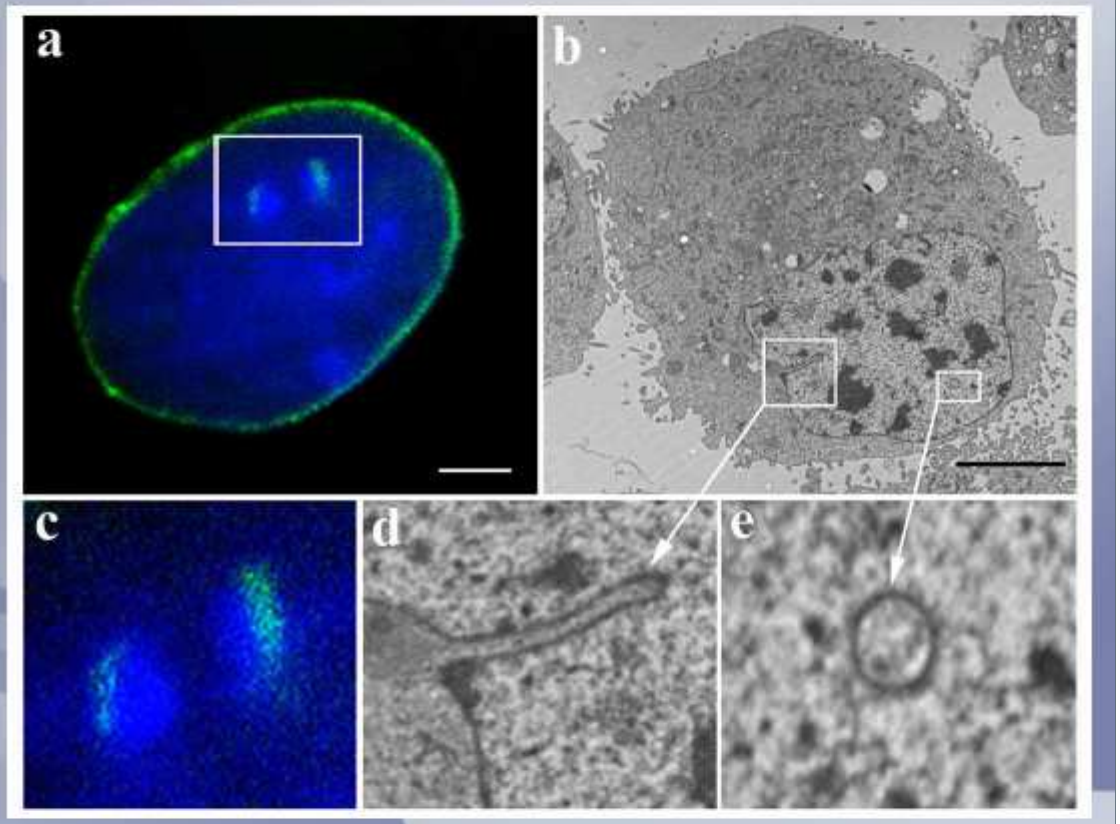

Galiová et al. EJCB (2008)

Scanning Electron Microscopes

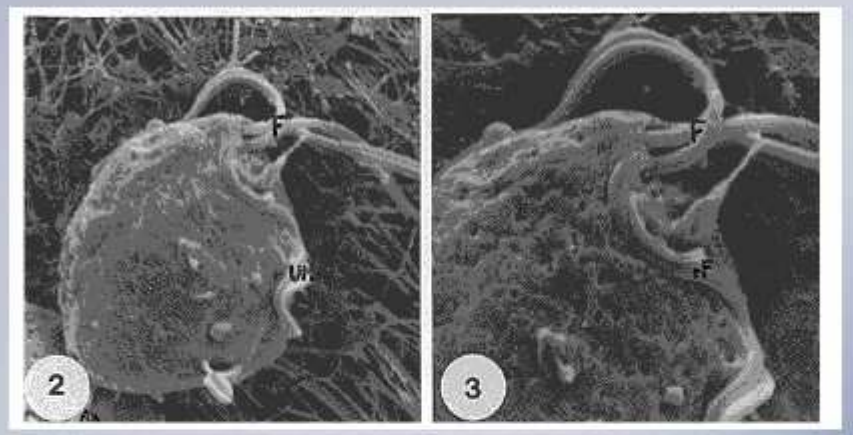

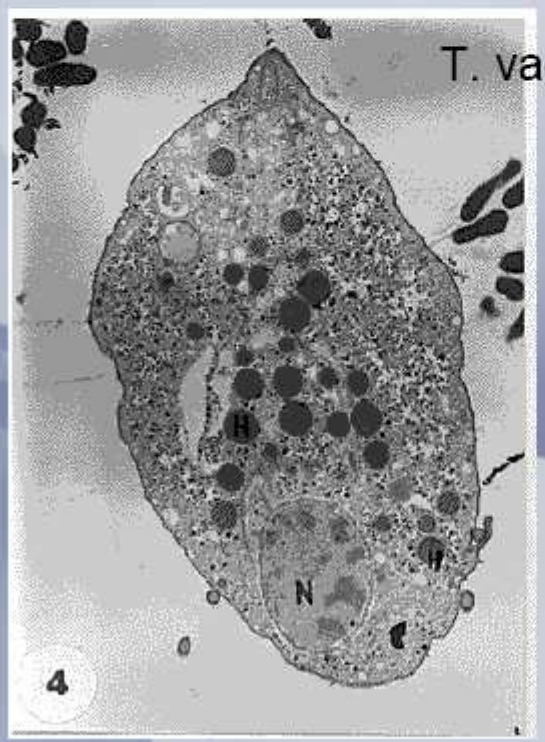

4-pi microscopy (CC lab in Heidelberg)

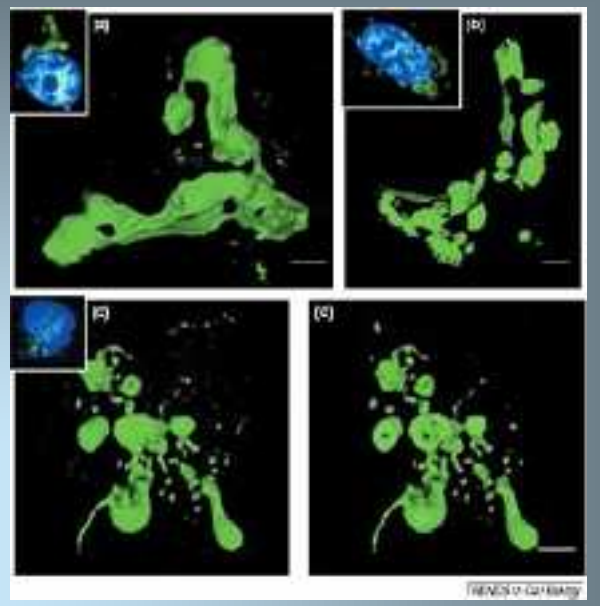

4pi: improved axial resolution. The typical value of 500-700 nm can be improved to 100-150 nm which corresponds to an almost spherical focal spot with 5-7 times less volume than that of standard confocal microscopy.

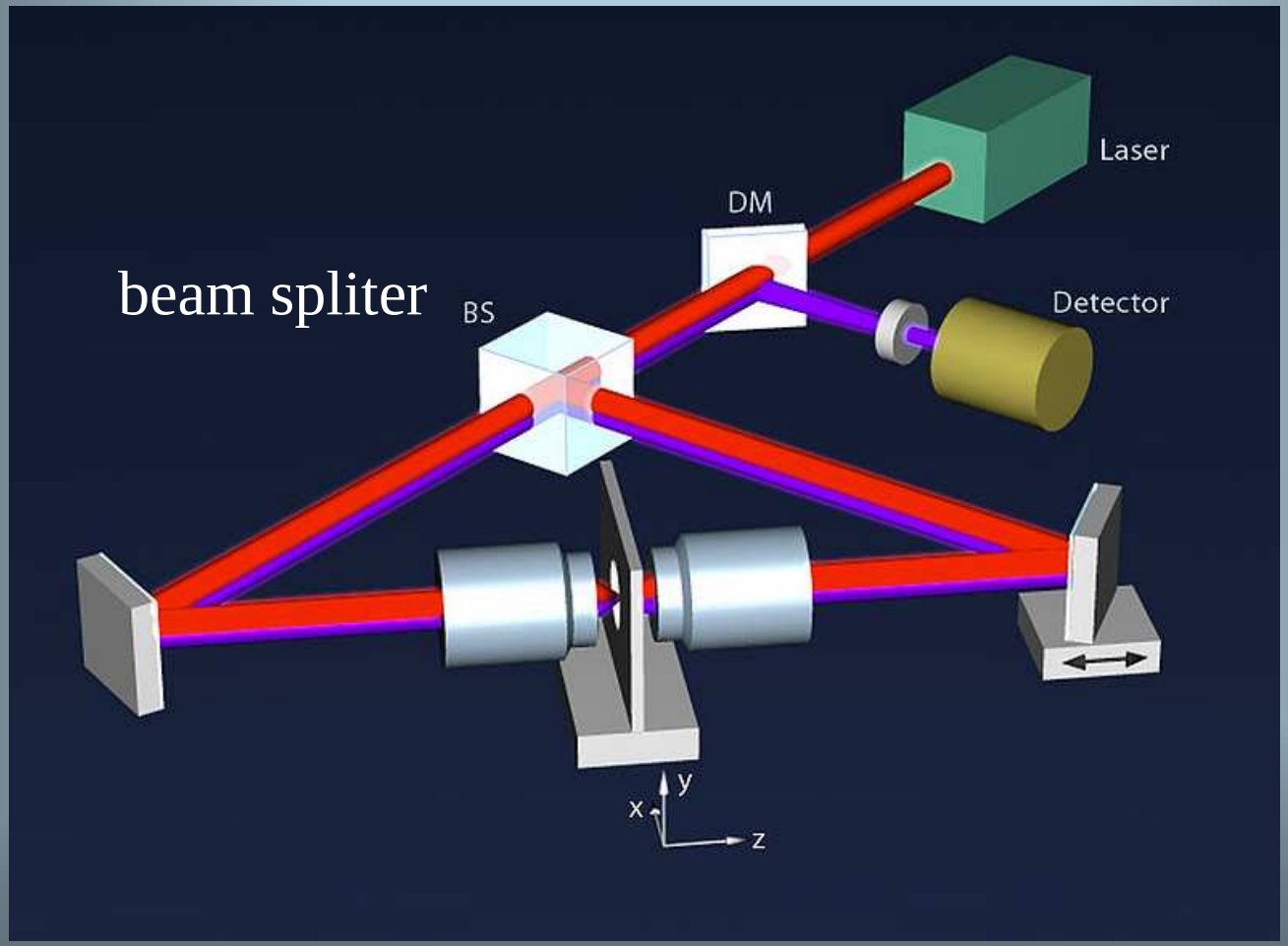

The operation mode of a 4Pi microscope is shown in the figure. The laser light is divided by a beam splitter (BS) and directed by mirrors towards the two opposing objective lenses. At the common focal point superposition of both focused light beams occurs. Excited molecules at this position emit fluorescence light which is collected by both objective lenses, combined by the same beam splitter and deflected by a dichroic mirror (DM) onto a detector. There superposition of both emitted light pathways can take place again.

X-RAY MICROSCOPY

Soft X-ray microscopes can be used to study hydrated cells up to 10 µm thick and produce images of 30 nm resolutions. X-ray microscopy, that has the more pronounced properties of laser scanning confocal microscopy (LSCM), has been a long-standing goal for experimental science (Seres et al., 2005). Since the cells are imaged in the X-ray transmissive "water window", where organic material absorbs approximately an order of magnitude more strongly than water, chemical contrast enhancement agents are not required to view the distribution of cellular structures (Meyer-Ilse et al., 2001). In such experiments, cells must be rapidly frozen to be studied on a cryostage, showing information which is closely similar to 4D-living cell observation by LSCM.

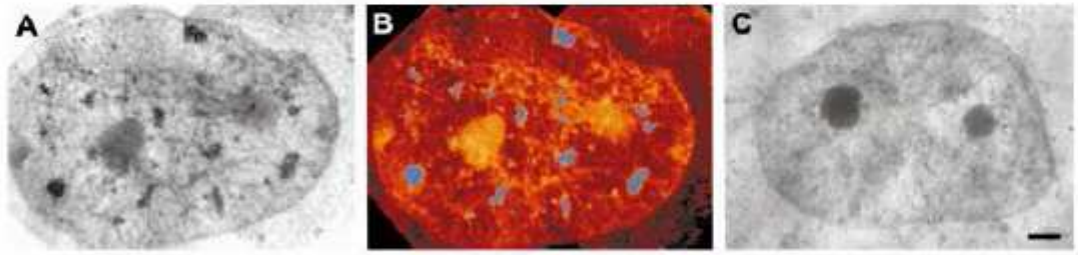

Fig. 4. Nuclei of human mammary epithelial cells (T4) labelled for RNA splicing factor (SRm300). (A) X-ray micrograph of a single nucleus after silver enhancement. This image is a montage compiled from two individual X-ray microscope images. (B) Same nucleus after colour coding to emphasize the label. (C) Control; single nucleus that was exposed to secondary antibodies and silver enhancement but not primary antibodies. This image is a montage compiled from two individual X-ray microscope images. Magnification = 2400×, 0.034 NA with 20 nm pixel size at 517 eV (λ = 2.4 nm).

(Meyer-Ilse et al., 2000)

WHAT IS A SYNCHROTRON

A synchrotron is a device that accelerates electrons to almost the speed of light. As the electrons are deflected through magnetic fields they create extremely bright light. The light is channelled down beamlines to experimental workstations where it is used for research.

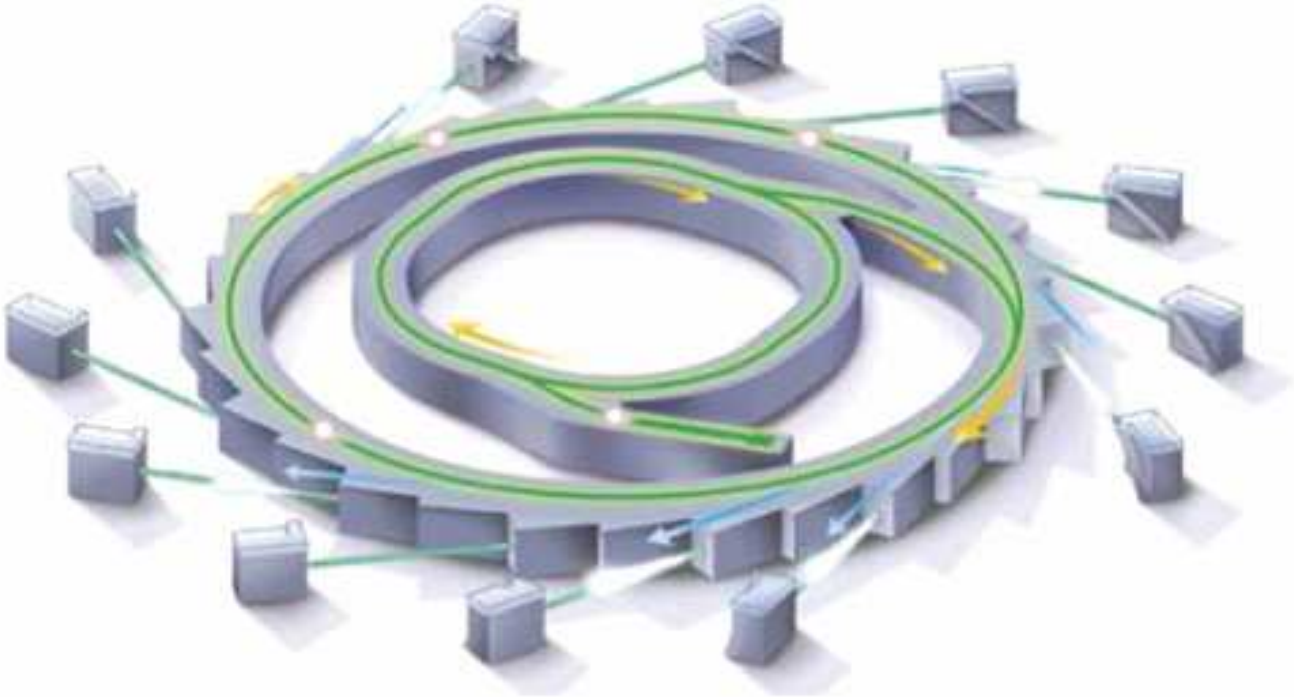

Subdiffraction Multicolor Imaging of the Nuclear Periphery with 3D Structured Illumination Microscopy

Lothar Schermelleh,[1]* Peter M. Carlton,[2]* Sebastian Haase,[2,4] Lin Shao,[2] Lukman Winoto,[2] Peter Kner,[2] Brian Burke,[3] M. Cristina Cardoso,[4] David A. Agard,[2] Mats G. L. Gustafsson,[5] Heinrich Leonhardt,[1]*† John W. Sedat[2]*†

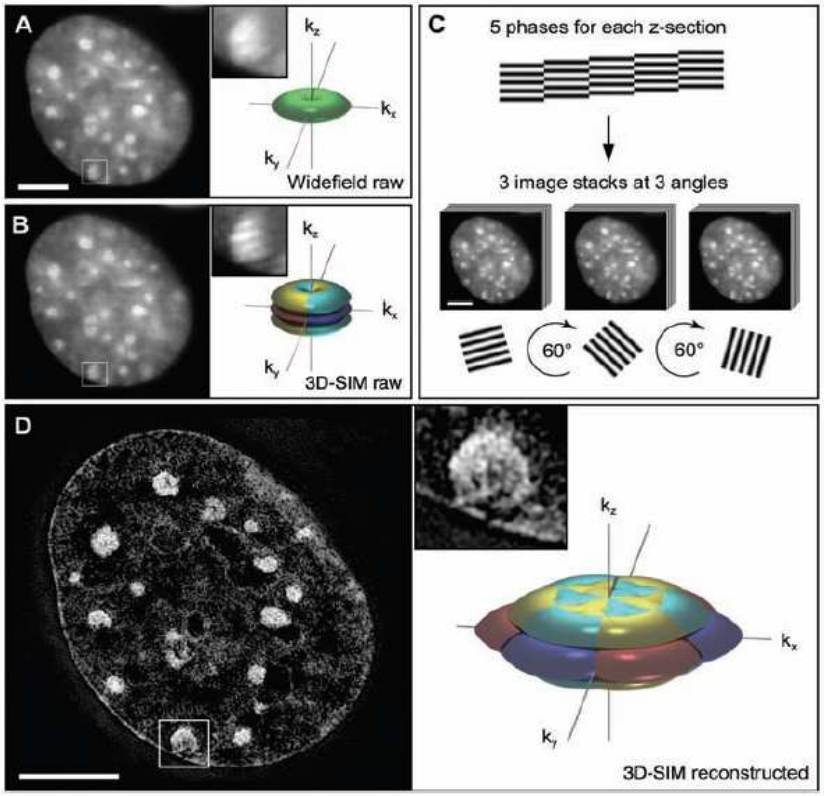

Fig. 1. Subdiffraction resolution imaging with 3D-SIM. (**A** and **B**) Cross section through a DAPI-stained C2C12 cell nucleus acquired with conventional wide-field illumination (A) and with structured illumination (B), showing the striped interference pattern (inset). The renderings to the right illustrate the respective support of detection in frequency space. The axes k_x, k_y, and k_z indicate spatial frequencies along the x, y, and z directions. The surfaces of the renderings represent the corresponding resolution limit. The depression of the frequency support ("missing cone") in z direction in (A) indicates the restriction in axial resolution of conventional wide-field microscopy. With 3D-SIM, the axial support is extended but remains within the resolution limit. (**C**) Five phases of the sine wave pattern are recorded at each z position, allowing the shifted components to be separated and returned to their proper location in frequency space. Three image stacks are recorded with the diffraction grating sequentially rotated into three positions 60° apart, resulting in nearly rotationally symmetric support over a larger region of frequency space. (**D**) The same cross section of the reconstructed 3D-SIM image shows enhanced image details compared with the original image (insets). The increase in resolution is shown in frequency space on the right, with the coverage extending two times farther from the origin. Scale bars indicate 5 μm.

Stimulated Emission Depletion microscopy, or STED microscopy, is a fluorescence microscopy technique that uses the non-linear de-excitation of fluorescent dyes to overcome the resolution limit imposed by diffraction with standard confocal laser scanning microscopes and conventional far-field optical microscopes.

STED

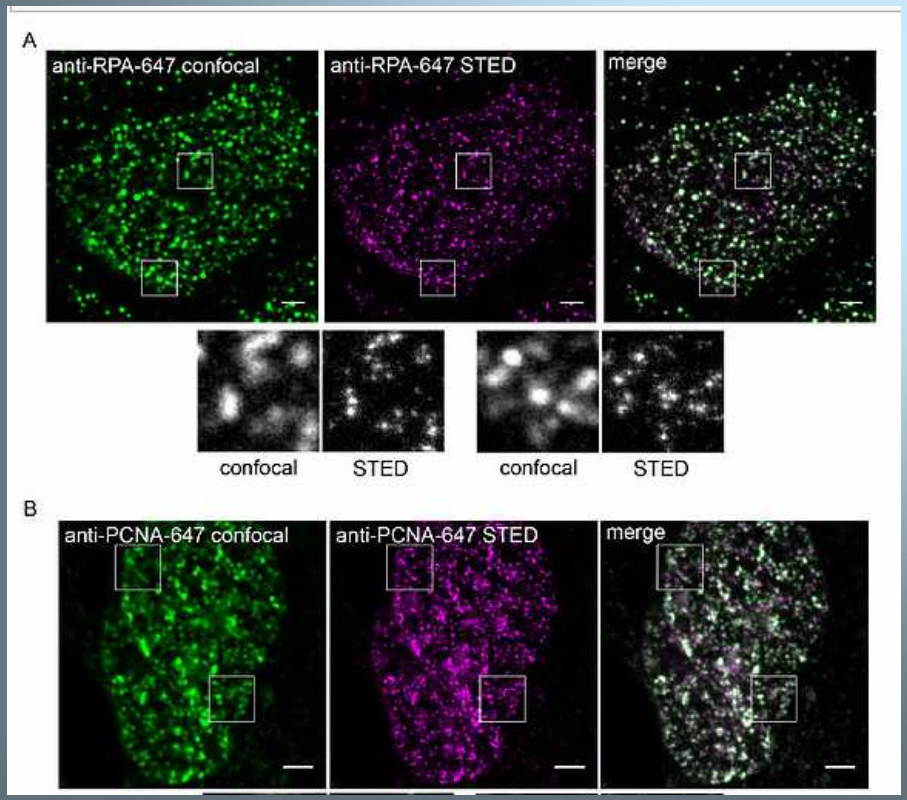

SP-5 LSCM

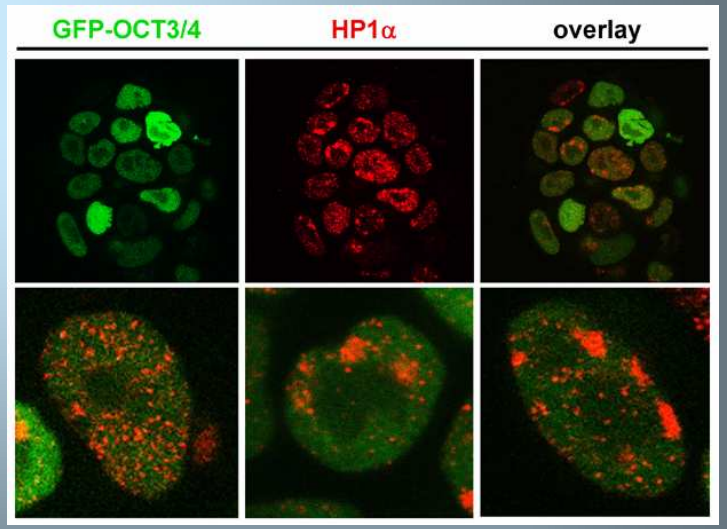

Leica STED – STimulated Emission Depletion
SUPERRESOLUTION (subdiffraction) in xy plane

Hell, S. W. and J. Wichmann (1994). *Opt. Lett.*
"Breaking the diffraction resolution limit by stimulated emission"

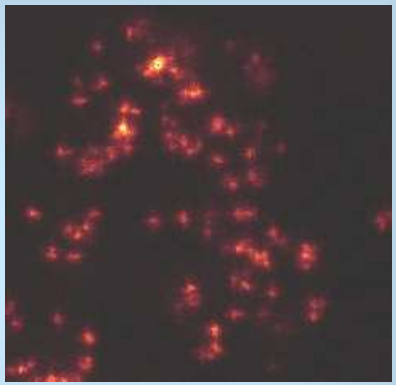

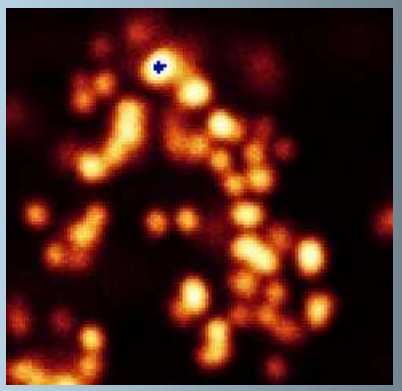

neurobiology
membrane biology
membrane rafts
intracellular transport

Willig KI et al. *Nature* 2006
Sieber JJ et al. *Biophy J* 2006
Kittel RJ et al. *Science* 2006
Fitzner D et al. *EMBO J* 2006

Kellner RR et al. *Neurosience* 2007
Lin W et al. *PNAS* 2007
Seebach J *Cardiovas. Res.* 2007
Sieber JJ *Science* 2007

Unique

Super-resolution microscope systems from Carl Zeiss ELYRA combines PAL-M (Photo-activated localization microscopy) and SR-SIM technology

Fluorescence microscopy technique comparison

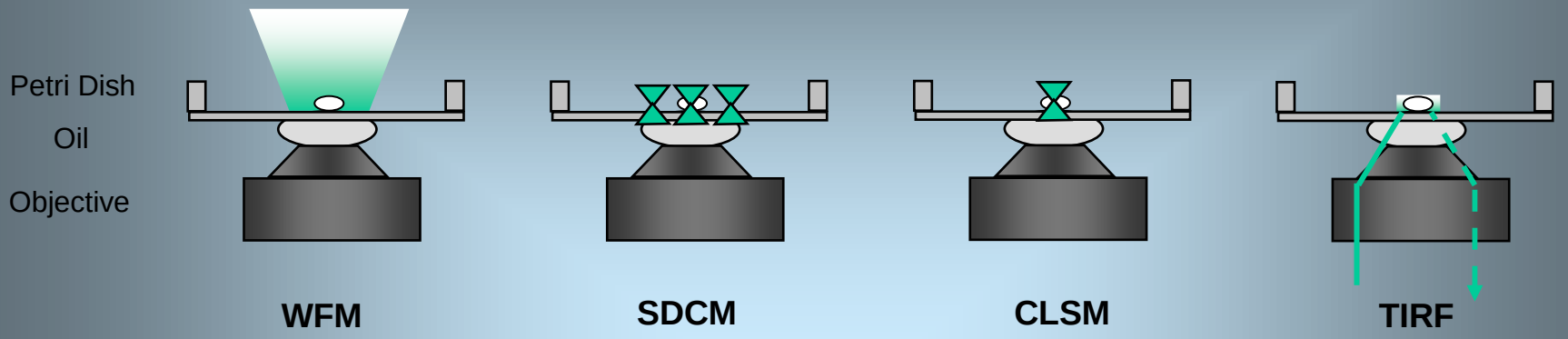

	WFM	SDCM	CLSM	TIRF
Z resolution measured	widefield: ~ 1.13 µm	SD6000: ~ 0.84 µm	SP5: ~ 0.50 µm	**TIRF: 0.1 – 0.3 µm**

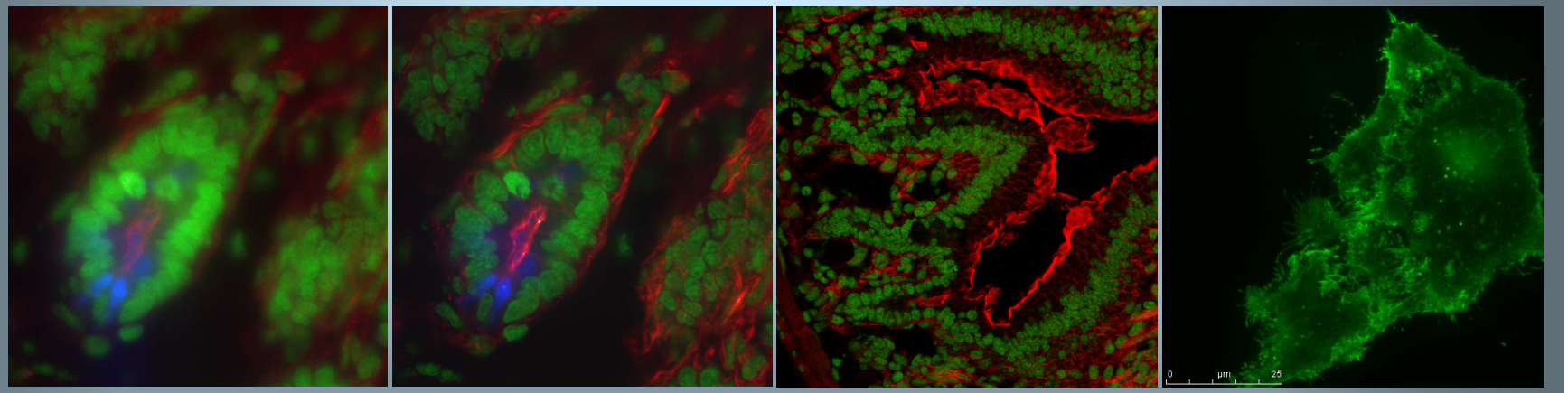

samples	**thin samples < 5 µm moderately thick + deconvolution**	**moderately thick 5 µm – 30 µm**	**thick > 30 µm 4PI: 0.1 – 0.12 µm!**	**! does not matter ! Only evanescent waves**

Confocal Laser Scanning Microscopy – advanced systems

Leica TCS SP5 – universal system for everything!

FRAP
FRET AB, SE
Live Data Mode
ROI spectrophotometer
APD
SMD – FCS, FLIM, FCCS
Spectral FLIM
High Content Screening Auto
2-photon, 3-photon

Leica DM6000 CFS – Confocal Fixed Stage

Leica TCS SP5-X WLL

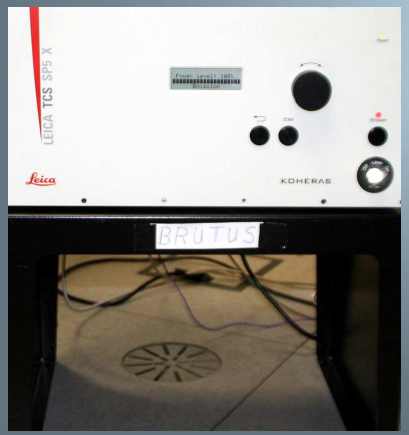

Leica TCS SP5 STED

Leica TCS 4PI

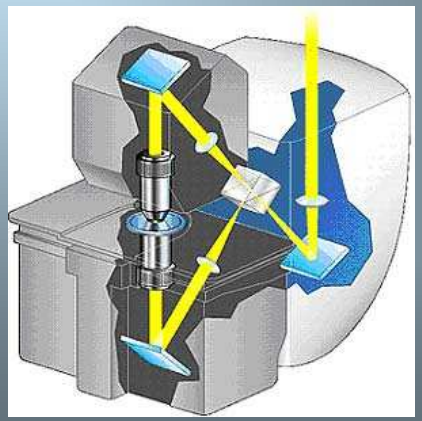

Leica TCS SP5: the only broadband confocal

Leica TCS SP5 basic features

- full range of lasers: 355, 405, VIS, IR up to 1300 nm
- conventional scanner up to 8192x8192 pxls
- resonant scanner up to 29 f/s for 512x512pxls
- AOBS – Acousto-Optical Beam Splitter
- Up to 5 confocal spectral detectors
- SuperZ Galvo and Pifoc

Wide range of UNIQUE upgrades:

- **White Light Laser**
- Spectral FLIM
- online ROI spectrometer
- STED – super-resolution in xy plane

Unique

Separate UNIQUE systems

- Leica DM6000 B CFS - electrophysiology
- Leica 4PI – high resolution in z axis

Unique

White Light Laser – set of lasers or just one tuneable source?

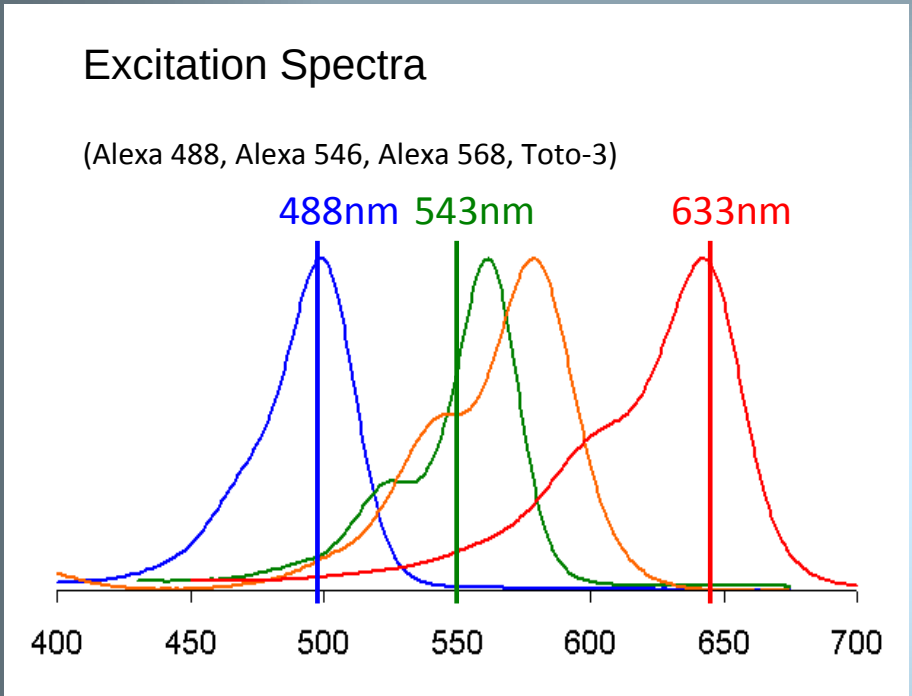

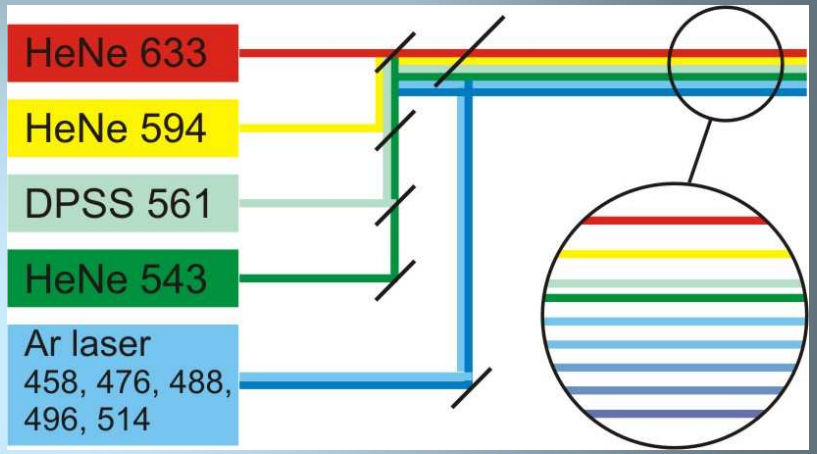

- No tunability
- Sub-optimal excitation
- Cross-excitation fixed

- Set of gas, DPSS or DL lasers
- Sophisticated merge module
- Expensive solution
- Only several combinations of wavelengths

White Light Laser – new lambda scan, new wavelengths

- setting of excitation wavelength and intensity in software or at Panel Box „Smart Wavelength“ and „Smart Intensity“
- Lambda Square Scan: lambda excitation and emission over whole visible spectra

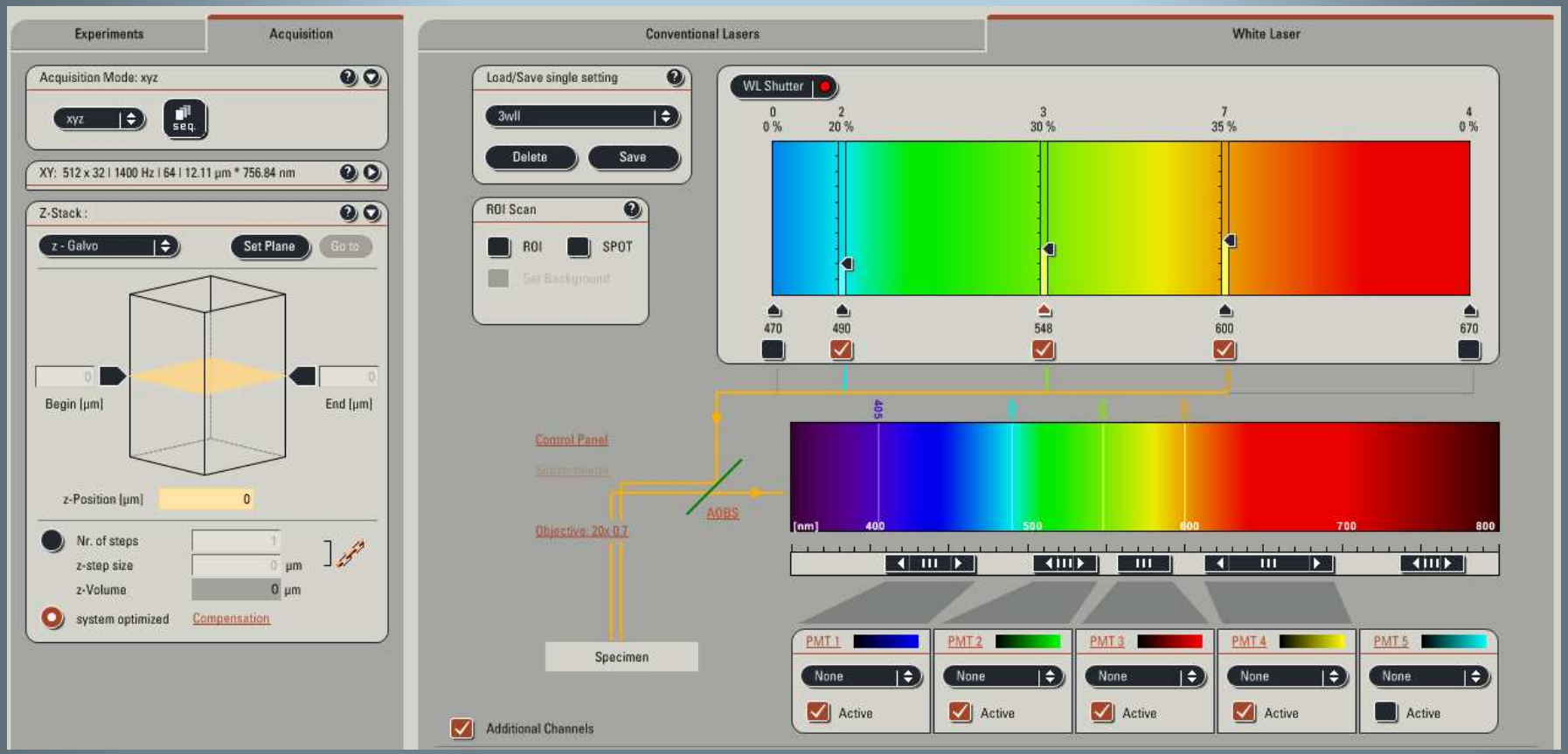

Quantify Life! – The Challenge

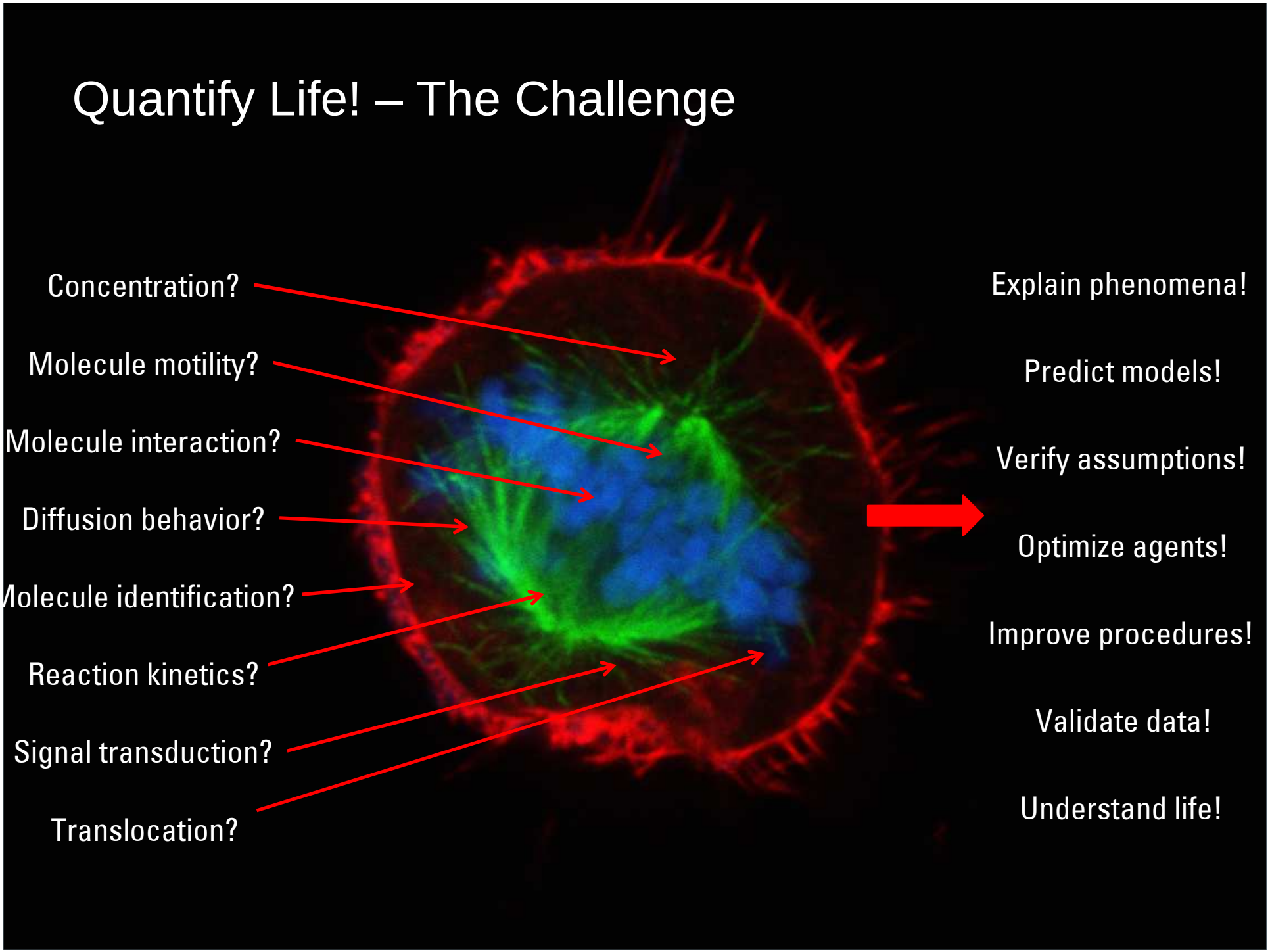

Eva Bártová, Gabriela Šustáčková, Lenka Stixová, Soňa Legartová, Darya Orlova, Veronika Foltánková, Pavel Matula, Petra Sehnalová

Institute of Biophysics, the Academy of Sciences of the Czech Republic, v.v.i., Brno

Projects: Ministry of Education Youth and Sports of the Czech Republic; COST-CZ project LC11020. Grant Agency of the Czech Republic by grants Nos. P302/10/1022 and P302/12/G157. European Union project COST TD09/05 and EU-Marie Curie project PIRSES-GA-2010-269156.